



Search for heavy Majorana or Dirac neutrinos and right-handed W gauge bosons in final states with charged leptons and jets in pp collisions at $\sqrt{s} = 13$ TeV with the ATLAS detector

The ATLAS Collaboration

A search for heavy right-handed Majorana or Dirac neutrinos N_R and heavy right-handed gauge bosons W_R is performed in events with energetic electrons or muons, with the same or opposite electric charge, and energetic jets. The search is carried out separately for topologies of clearly separated final-state products (“resolved” channel) and topologies with boosted final states with hadronic and/or leptonic products partially overlapping and reconstructed as a large-radius jet (“boosted” channel). The events are selected from pp collision data at the LHC with an integrated luminosity of 139 fb^{-1} collected by the ATLAS detector at $\sqrt{s} = 13$ TeV. No significant deviations from the Standard Model predictions are observed. The results are interpreted within the theoretical framework of a left-right symmetric model, and lower limits are set on masses in the heavy right-handed W_R boson and N_R plane. The excluded region extends to about $m(W_R) = 6.4$ TeV for both Majorana and Dirac N_R neutrinos at $m(N_R) < 1$ TeV. N_R with masses of less than 3.5 (3.6) TeV are excluded in the electron (muon) channel at $m(W_R) = 4.8$ TeV for the Majorana neutrinos, and limits of $m(N_R)$ up to 3.6 TeV for $m(W_R) = 5.2$ (5.0) TeV in the electron (muon) channel are set for the Dirac neutrinos. These constitute the most stringent exclusion limits to date for the model considered.

1 Introduction

The very small mass of neutrinos is one of the biggest puzzles in the Standard Model (SM) of particle physics. The seesaw mechanism [1–3] is a proposed solution, in which the light neutrinos acquire their Majorana masses through heavy right-handed neutrinos. From the effective field theory point of view, this is equivalent to dimension-5 operators [4] through electroweak symmetry breaking. Several types of the seesaw mechanism are proposed; for example, Type-I with right-handed neutrinos [1–3], Type-II with a scalar triplet [5–7] and Type-III with at least two fermion triplets [5, 8] scenarios. Type-I and Type-II models can further be embedded into the Left-Right Symmetric Model (LRSM) [9–11]. The LRSM attempts to explain the broken parity symmetry of the weak interaction in the SM and can introduce, depending on the form of the model, right-handed counterparts to the W and Z bosons (W_R and Z_R), and right-handed heavy neutrinos N_R as the parity gauge partners of the corresponding left-handed neutrino fields.

In this analysis, a search for W_R bosons decaying to N_R and a charged lepton ℓ^\pm in proton-proton (pp) collisions at a centre-of-mass energy $\sqrt{s} = 13$ TeV with the ATLAS detector is presented, where ℓ^\pm denotes an electron/positron (e^\pm) or a muon (μ^\pm). The exact process of interest is the Keung-Senjanović (KS) process [11]. In the case where the mass of W_R is larger than the N_R mass, $m(W_R) > m(N_R)$, N_R decays into a charged lepton and an off-shell W_R (W_R^*). In the case of $m(W_R) < m(N_R)$, a W_R produced off-shell decays into a pair of N_R and ℓ , and the N_R subsequently decays via the W_R resonant state. The charge of the final state leptons is a key feature of the analysis, as it determines the Dirac or Majorana nature of N_R . The focus of the search is on hadronic decays of the final-state $W_R^{(*)}$ because of their high branching fractions. The leading-order Feynman diagrams for the KS process targeted by this analysis are shown in Figure 1. Depending on the target mass range, two types of analyses are performed; one requiring that the two quarks in the final state are clearly separated geometrically and are reconstructed as two separate jets (hereafter labelled as the “resolved” channel), with the second one targeting the $m(W_R) \gg m(N_R)$ region where particles from the N_R decay are merged due to the Lorentz boost, and are reconstructed as a single large-radius (large- R) jet (the “boosted” channel) [12, 13].

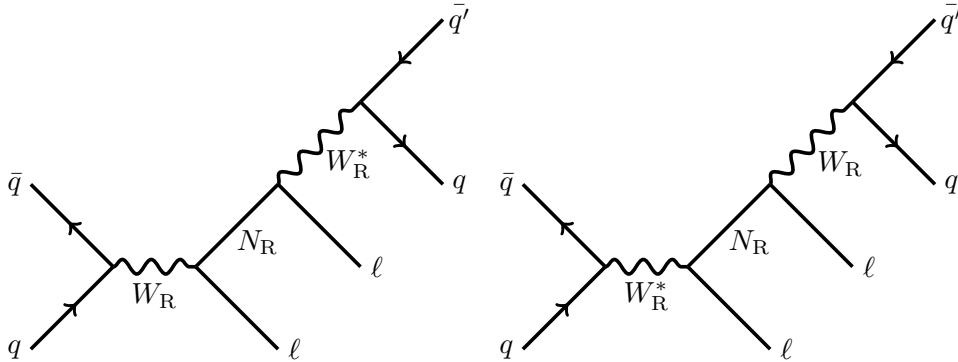


Figure 1: The Keung-Senjanović process for the $m(W_R) > m(N_R)$ (left) and the $m(N_R) > m(W_R)$ (right) cases. The asterisk (*) on the W_R denotes an off-shell particle. In the case of Majorana N_R , the final state appears with two same-sign charged leptons 50% of the time, violating the lepton number conservation.

Multiple experimental results can give constraints on the target signal of this analysis [14, 15]. The LRSM can enhance some low-energy processes, such as $K-\bar{K}$ and $B_{d,s}-\bar{B}_{d,s}$ oscillations, via W_R contributions in the box diagram. The lower limit on $m(W_R)$ from the latest mixing results is about 3 TeV [16, 17],

assuming equal mixing matrices for left- and right-handed quarks. A Majorana right-handed electron neutrino and W_R boson can contribute to the neutrinoless double beta decay ($0\nu\beta\beta$) diagram. Assuming purely right-handed contributions to the $0\nu\beta\beta$ decay, the non-observation of this lepton number violating process can be used to set limits on the W_R and N_R masses in the LRSM. As an example, at $m(W_R) = 3$ TeV (5 TeV), the upper limit on the N_R mass is about 180 GeV (20 GeV) [18, 19].

The pp collisions at the Large Hadron Collider (LHC) offer a window into a unique phase space for this search, allowing the exploration of $m(N_R)$ in a range from $O(100)$ GeV to a few TeV. Searches by the ATLAS [20–22] and CMS [23–27] collaborations have excluded signals in the LRSM with $m(W_R)$ up to about 4.7 TeV and 5 TeV in the electron and muon final states, respectively, for a $m(N_R)$ range from 100 GeV to 3 TeV.

2 Signal model

The theoretical framework of LRSM offers the prediction of a right-handed charged current and a mass-generating mechanism for light and heavy neutrinos. The small left-handed neutrino masses are naturally explained via right-handed neutrinos in the Type-I seesaw mechanism, or via SU(2)-triplet scalars in the Type-II seesaw model. Both Type-I and Type-II contributions can coexist in the LRSM.

In the minimal LRSM, the left-handed (i.e. SM-like) neutrinos as well as the right-handed neutrinos are predicted to be Majorana particles. The model thus features the violation of the global lepton number symmetry. In the target KS process, same- and opposite-sign lepton pairs would be equally observed in a 50%-50% admixture of signal events. In the LRSM variants that include the inverse seesaw mechanism [28–31], the N_R neutrinos are pseudo-Dirac particles formed by two Majorana particles with identical masses [32]. For simple versions of LRSMs incorporating the inverse seesaw mechanism, lepton-number-violating processes are not expected [33]. In this paper we explore both “Dirac” and “Majorana” interpretations of the LRSM.

3 ATLAS detector

The ATLAS experiment [34] at the LHC is a multipurpose particle detector with a forward–backward symmetric cylindrical geometry and a near 4π coverage in solid angle.¹ It consists of an inner tracking detector surrounded by a thin superconducting solenoid providing a 2 T axial magnetic field, electromagnetic and hadron calorimeters, and a muon spectrometer (MS). The inner tracking detector covers the pseudorapidity range $|\eta| < 2.5$. It consists of silicon pixel, silicon microstrip, and transition radiation tracking detectors. Lead/liquid-argon (LAr) sampling calorimeters provide electromagnetic (EM) energy measurements with high granularity. A steel/scintillator-tile hadron calorimeter covers the central pseudorapidity range ($|\eta| < 1.7$). The endcap and forward regions are instrumented with LAr calorimeters for both the EM and hadronic energy measurements up to $|\eta| = 4.9$. The MS surrounds the calorimeters and is based on three large superconducting air-core toroidal magnets with eight coils each. The field integral of the

¹ ATLAS uses a right-handed coordinate system with its origin at the nominal interaction point (IP) in the centre of the detector and the z -axis along the beam pipe. The x -axis points from the IP to the centre of the LHC ring, and the y -axis points upwards. Cylindrical coordinates (r, ϕ) are used in the transverse plane, ϕ being the azimuthal angle around the z -axis. The pseudorapidity is defined in terms of the polar angle θ as $\eta = -\ln \tan(\theta/2)$. Angular distance is measured in units of $\Delta R \equiv \sqrt{(\Delta\eta)^2 + (\Delta\phi)^2}$.

toroids ranges between 2.0 and 6.0 T m across most of the detector. The MS includes a system of precision tracking chambers and fast detectors for triggering. A two-level trigger system is used to select events. The first-level trigger (L1) is implemented in hardware and uses a subset of the detector information to accept events at a rate below 100 kHz. This is followed by a software-based high-level trigger (HLT) that reduces the accepted event rate to 1 kHz on average depending on the data-taking conditions. An extensive software suite [35] is used in the reconstruction and analysis of real and simulated data, in detector operations, and in the trigger and data acquisition systems of the experiment.

4 Dataset and simulated event samples

The data used in this analysis were collected with the ATLAS detector between 2015 and 2018, and correspond to an integrated luminosity of 139 fb^{-1} . The average number of pp interactions per bunch crossing (“pile-up”) in the dataset is 33.7. Only high-quality data, collected when the LHC has declared the beams to be stable and all of the ATLAS subdetectors are reported to be operating well, are analysed [36, 37]. All events are required to have a vertex with at least two associated ID tracks with $p_T > 500 \text{ MeV}$ [38, 39]. The one with the highest $\sum p_T^2$ of the associated tracks is selected as the primary vertex.

The dataset was collected by single or dilepton triggers with a variety of transverse momentum (p_T) and isolation requirements, which depend on the data-taking period. In both resolved and boosted channels, only events in the region of trigger efficiency plateau [40, 41] are used. Trigger thresholds are no higher than (24 GeV, 24 GeV) for dielectrons and (22 GeV, 8 GeV) for dimuons in the resolved channel, and 140 GeV for electrons and 50 GeV for muons in the boosted channel. The trigger efficiency for most signal points for both resolved and boosted channels ranges from 90 to 95%, dropping to 85% in the $m(W_R) \sim m(N_R)$ region where the compressed phase space affects the charged lepton kinematics. For the resolved analysis, the $e\mu$ trigger is used for the $t\bar{t}$ background estimation. In addition, for the study of mis-identified leptons in the resolved analysis (Section 6) some non-isolated, heavily-prescaled single lepton triggers were also used.

Monte-Carlo (MC) simulated events are used to optimise the event selections, and to estimate the background contribution and the systematic uncertainties. For all MC events, the response of the ATLAS detector is simulated using the GEANT4 toolkit [42]. The same reconstruction and trigger algorithms are applied for data and simulated events, using the default ATLAS software [43]. Multiple overlaid pp collisions are simulated with the soft QCD processes of Pythia 8.230 [44] using the A3 set of tuned parameters [45] and the NNPDF2.3LO parton distribution function (PDF) set [46]. MC events are reweighted so that the distribution of the average number of interactions per bunch crossing agrees with the data (“pile-up reweighting”).

Table 1 summarises the simulation packages used for the SM background processes. More details are found in other recent ATLAS publications, for example Refs. [47–50]. The multijet and γ +jets samples are used only in the boosted channel.

The signal events for $pp \rightarrow W_R^{(*)} \rightarrow \ell\ell qq'$ in the LRSM are generated at leading-order (LO) using FeynRules [51] implemented in MadGraph5_aMC@NLO [52] and further modified as described in Ref. [53], where ℓ includes the tau lepton. The generated events are interfaced with Pythia 8.230 [44] for parton showering and hadronisation. The A14 parameter set is used for tuning the shower [54]. The NNPDF3.1NLO [55] PDF set enters in the matrix element calculation and the NNPDF2.3LO is used in the parton shower.

Lepton flavour mixing, albeit possible in principle in the LRSM, is not considered in this analysis. The branching fractions for the electron, muon and tau channels for W_R decays to N_R of equal masses are assumed to be exactly one-third for each flavour due to lepton universality. For sufficiently heavy W_R masses, $m(W_R) > m_t$, the hadronic final state also includes the $W_R \rightarrow tb$ channel. However, b -jets are vetoed in this search to reduce the top background contamination, effectively limiting the phase space to hadronic W_R decays excluding b -quarks. At very low N_R masses of less than 50 GeV, the decay length of N_R is greater than 1 mm [53]. This mass range can be explored by dedicated ATLAS and CMS analyses requiring a displaced vertex, and is beyond the scope of this paper. The $m(W_R)$ and $m(N_R)$ are sampled from 1 TeV to 7 TeV and from 50 GeV to 4 TeV, respectively, at intervals of about 500 GeV. In the $m(W_R) > 10 \times m(N_R)$ region, which is the focus of the boosted channel, the N_R mass is further sampled in steps of 100 GeV. The simulation assumes a Majorana N_R , giving a 50% mixture of same-sign and opposite-sign lepton pairs. For the Dirac neutrino case, only the opposite-sign events are used in the analysis as no other differences are expected, and the production cross section is adjusted appropriately.

Table 1: Summary of the simulated background events used in this analysis, including name of the event generator, accuracy in QCD when the matrix element is calculated, parton shower algorithm, underlying event (UE) tune, and accuracy in QCD when the cross section is calculated. NLO, NNLO and NNLL denote the next-to-leading order, next-to-next-to-leading order, and next-to-next-to-leading logarithm, respectively, and n_{parton} is the number of partons in the matrix-element calculation. V denotes a W or Z boson.

Sample	Generator	Matrix Element	Parton shower	UE tune	cross section
$Z \rightarrow \ell\ell + \text{jets}$ and $W \rightarrow \ell\nu + \text{jets}$	Sherpa 2.2.11 [56]	NLO@ $n_{\text{parton}} \leq 2$ LO@ $n_{\text{parton}} = 3,4,5$	Sherpa default [57]	Sherpa default	NNLO [58]
$t\bar{t}$ and single- t	Powheg-Box v2 [59–62]	NLO	Pythia 8.230	A14 tune [54]	NNLO+NNLL [63–69]
VV and VVV	Sherpa 2.2.1 or 2.2.2 [56]	NLO@ $n_{\text{parton}} \leq 1$ LO@ $n_{\text{parton}} = 2,3$	Sherpa default	Sherpa default	NLO (VV) [70] / NNLO (VVV) [71]
$\gamma + \text{jets}$	Sherpa 2.1 [56]	LO@ $n_{\text{parton}} \leq 3$	Sherpa default	Sherpa default	LO
Multijet	Pythia 8.230 [44]	LO for dijet events	Pythia 8.230	A14 tune [54]	LO

5 Object reconstruction

The definitions of the physics objects used in this analysis are summarised in Table 2. Physics objects in the events (electrons, muons, jets, and missing transverse momentum) are separately defined for the resolved and boosted analyses. The orthogonality between the two channels is not enforced: the same event can be used in both analyses, which are not statistically combined.

Electrons are reconstructed as ID tracks, matched to energy clusters in the EM calorimeter within $|\eta| < 2.47$ [72]. The electron candidates in the crack region of the EM calorimeter ($1.37 < |\eta| < 1.52$) are discarded. The electron identification utilises a multivariate likelihood-based discriminant that exploits the shower shapes in the EM calorimeter and the associated track properties. There are ‘Loose’, ‘Medium’ and ‘Tight’ identification working points described in Ref. [72]. To further suppress the mis-identified electrons, an isolation criterion can be applied to the electron candidates. Several isolation working points are defined in Ref. [72] e.g. ‘Loose’ and ‘HighPtCaLoOnly’. Slightly different p_T thresholds are used across the resolved and boosted channels to ensure the operation at a region of constant trigger efficiency. For the resolved analysis, electrons are required to have $p_T > 25$ GeV and to satisfy Tight identification

Table 2: Definitions of the electrons, muons, small- R and large- R jets, used in this analysis. Optimisations of the object selections are performed separately for the resolved and boosted analyses. See text about the definitions of ‘Baseline’ and ‘Leading’ leptons as well as leptons for ‘Fake estimation’.

	Resolved			Boosted		
	Baseline	Fake estimation		Baseline	Leading	Fake estimation
Electrons	$ \eta $		(0, 1.37] or [1.52, 2.47]			
	p_T (GeV)	> 25		> 25	> 200	
	Quality	Tight	Loose	Medium	Tight	
	Isolation	Loose	Fail Loose or Tight	Loose	HighPtCaloOnly	Loose but fail HighPtCaloOnly
Muons		Baseline	Fake estimation	Baseline	Leading	
	p_T (GeV)	> 25		> 28	> 200	—
	$ \eta $	< 2.5			< 2.5	—
	Quality	High- p_T if $p_T > 300$ GeV else Medium		Medium	Tight	—
Isolation	FixedCutTightTrackOnly	fail FixedCutTightTrackOnly	—	Tight	—	
Small-R jet	p_T (GeV)		> 20			
	$ \eta $		< 2.5			
Large-R jet	p_T (GeV)	—			> 200	
	$ \eta $	—			< 2	

and Loose isolation criteria. For the boosted analysis, electrons must have $p_T > 25$ GeV, and satisfy Medium identification and Loose isolation criteria. Additional cuts are applied for the highest- p_T electron candidate in the boosted channel (Section 7.1), to ensure that $p_T > 200$ GeV, and to satisfy the Tight identification and HighPtCaloOnly isolation criteria. Tighter isolation criteria are required in the boosted channel because the multijet process with a mis-identified electron is a major source of background.

Muons are reconstructed from MS tracks matching ID tracks in the $|\eta| < 2.5$ region. There are several muon identification working points described in Ref. [73], namely ‘Loose’, ‘Medium’, ‘Tight’ and ‘High- p_T ’. The resolved channel uses muons with $p_T > 25$ GeV satisfying the Medium identification working point. For muons with $p_T > 300$ GeV, the High- p_T working point requirements must be met. For the boosted channel, muons with $p_T > 28$ GeV satisfying the Medium working point are used. As with electrons, several muon isolation working points are defined in Ref. [73], e.g. ‘FixedCutTightTrackOnly’ and ‘Tight’. The resolved channel requires muons to satisfy the FixedCutTightTrackOnly working point. In the boosted channel, no isolation criterion is required on the muon from the $N_R \rightarrow \mu q q'$ decay, as it is not expected to be clearly isolated from the hadrons. Further selection cuts are applied for the highest- p_T muon candidate in the event, namely to have $p_T > 200$ GeV and satisfy the Tight identification and Tight isolation criteria (Section 7.1).

For both electrons and muons, track-to-vertex association requirements are employed by using the impact parameter observables. The longitudinal impact parameter of the lepton track, z_0 , is required to satisfy $|z_0 \sin \theta| < 0.5$ mm, where θ is the polar angle of the track. In addition, the transverse impact parameter divided by its uncertainty, $|d_0|/\sigma(d_0)$, is required to be less than 5 (3) for electrons (muons). The leptons’ reconstruction, identification, isolation and trigger efficiencies differ slightly between simulation and data. The simulation is corrected with scale factors to match the data efficiencies [72, 73].

Apart from the baseline leptons described above, leptons with modified requirements are employed for control samples for the estimation of jets misidentified as leptons or non-prompt leptons from decays of hadrons. In the resolved channel, the isolation requirement is inverted and the Loose identification is employed. In the boosted channel, the fraction of events containing fake muons surviving the $p_T > 200$ GeV requirement for the leading lepton is negligibly small. To estimate the hadrons mis-identified as electrons, electron candidates satisfying the Loose but failing the HighPtCaloOnly isolation criterion are used.

Jets are reconstructed from particle-flow objects [74] using the anti- k_t algorithm [75, 76] with radius parameter $R = 0.4$. They are referred to as ‘small- R jets’ hereafter. A detailed description of the calibration of these jets is found in Ref. [77]. Only small- R jets with $p_T > 20$ GeV and $|\eta| < 2.5$ are considered. small- R jets with $p_T < 60$ GeV and $|\eta| < 2.4$ from pile-up interactions are suppressed using a jet-vertex tagging (JVT) discriminant [78]. small- R jets containing b -flavoured hadrons (b -jets) are identified with the DL1r multivariate b -tagging algorithms [79, 80]. A working point to achieve 77% efficiency for b -jets is employed, which has a rejection factor of 5 for c -jets and 169 for light jets. It is only used to veto events containing jets identified as b -jets.

The missing transverse momentum, with magnitude E_T^{miss} , is calculated using the baseline electrons and the small- R jets in each event as described in Refs. [81, 82] using the Tight working point. The particle-flow track-based soft term, built from tracks that are matched to the primary vertex but not associated with any other objects, is also used in the calculation. The E_T^{miss} is used only in the electron channel, and muons are not considered in the calculation, since the muon momentum resolution is significantly degraded in the high- p_T region and affects the E_T^{miss} calculation.

To avoid cases where the detector response to a single physical object is reconstructed as two different final-state objects, e.g. an electron reconstructed as both an electron and a jet, several steps are followed, as summarised in Table 3. To improve the efficiency for muons from N_R decays in the boosted analysis, the last step of muon-jet overlap removal is considered only for the highest- p_T muon in the event.

Table 3: The order of overlap removal used in this analysis. ΔR is defined as $\Delta R = \sqrt{\Delta y^2 + \Delta\phi^2}$, where Δy and $\Delta\phi$ are the rapidity and azimuthal-angle differences between two objects. The variables $p_T(e)$, $p_T(\mu)$, $p_T(j)$ and $p_T(\text{trk})$ are the transverse momenta of the corresponding electron, muon, small- R jets, and all tracks associated with the small- R jet. The baseline definitions of electrons and muons are used. In the boosted channel, the last step of muon-jet overlap removal is considered only for the highest- p_T muon in the event. Large- R jets are reclustered from small- R jets after the overlap removal.

Order	Object discarded	Object kept	Matching condition
1.	Electron	Electron	If two electrons share a track, discard the softer electron
2.	Muon	Electron	If they share a track and the muon type is calorimeter-tagged [73]
3.	Electron	Muon	If they share a track with the remaining muon
4.	Small- R jet	Electron	$\Delta R < 0.2$, but step is skipped if jet is b -tagged and $p_T(e) < 100$ GeV
5.	Electron	Small- R jet	$\Delta R < 0.4$
6.	Small- R jet	Muon	$\Delta R < 0.2$, number of tracks associated to the jet < 3 , $p_T(\mu)/p_T(j) > 0.5$ and $p_T(\mu)/\sum p_T(\text{trk}) > 0.7$
7.	Muon	Small- R jet	$\Delta R < 0.4$

In the boosted analysis, the hadronic jets from the N_R decay are reconstructed as a single large- R jet. The large- R jet is reconstructed from the small- R jets described above, using the anti- k_t algorithm with $R = 1.0$. For such large- R jets, ‘re-clustered’ from small- R jets, the small- R jet calibration can be propagated. Large- R jets with $p_T > 200$ GeV and $|\eta| < 2.0$ are considered.

6 Resolved channel: event selection and background estimate

6.1 Event reconstruction and selection

The resolved channel targets signals with a mass splitting between W_R and N_R , i.e. $\Delta m \equiv m(W_R) - m(N_R)$, up to 4 TeV. Events passing the following requirements are filtered into datasets comprising signal regions (SRs), namely regions where the presence of signal is hypothesised by the theoretical models and the analysis is expected to have high sensitivity. The definitions of the SRs are summarised in Table 4. Events are required to have exactly two baseline, same-flavour charged leptons, with $p_T > 40$ GeV for the leading lepton, and at least two small- R jets with $p_T > 100$ GeV. To suppress the Z +jets background, the dilepton invariant mass must satisfy $m_{\ell\ell} > 400$ GeV. Since the focus of this search is the high W_R mass region, the following requirements are imposed on the dijet invariant mass (m_{jj}), and the scalar sum of the transverse momentum of the leptons and the two leading small- R jets (h_T): $m_{jj} > 110$ GeV and $h_T > 400$ GeV. Events are further separated into two categories based on the charge product of the two leptons: same- (rSRSS) or opposite-sign (rSROS) lepton pairs, where **r** denotes the resolved channel and SR the classification as signal region. The relatively small SM background in rSRSS increases the search sensitivity for Majorana N_R signals where half of the events are expected to appear with same-sign lepton pairs. The ΔR between the two leptons is required to be less than 3.9 in rSRSS to reduce some mismodelling of the simulated diboson background without a signal efficiency loss. Finally, the SRs are separated into electron and muon channels. The four resulting SRs (rSROS2e, rSROS2mu, rSRSS2e and rSRSS2mu) are orthogonal to each other and combined for a statistical analysis in the Majorana N_R interpretation. For the Dirac N_R interpretation, only rSROS2e and rSROS2mu are considered.

Table 4: Definition of signal regions in the resolved channel. The baseline definitions of electrons and muons are used.

Variable	rSRSS2e	rSRSS2mu	rSROS2e	rSROS2mu
Number of electrons	2	0	2	0
Number of muons	0	2	0	2
Lepton charge	same sign		opposite sign	
Leading lepton p_T [GeV]	> 40			
Dilepton mass $m_{\ell\ell}$ [GeV]	> 400			
$\Delta R_{\ell\ell}$	< 3.9		—	
Number of small- R jets with $p_T > 100$ GeV	≥ 2			
Number of b -tagged jets	0			
Dijet mass m_{jj} [GeV]	> 110			
$h_T \equiv p_T(\ell_1) + p_T(\ell_2) + p_T(j_1) + p_T(j_2)$ [GeV]	> 400			

In rSROS, the W_R mass is reconstructed by combining the two charged leptons and the two leading small- R jets ($m_{\ell\ell jj}$), and used as the final discriminant for signal points in the $m(W_R) > m(N_R)$ region. The $0 < m_{\ell\ell jj} < 5$ TeV region is scanned with a step size of 500 GeV, with one additional overflow bin that includes all events with $m_{\ell\ell jj} > 5$ TeV. For signals with $m(W_R) < m(N_R)$, the m_{jj} is used instead as a discriminant, with a similar 500 GeV binning in $0 < m_{jj} < 3$ TeV, and one additional overflow bin for $m_{jj} > 3$ TeV. The significance of yields is checked in every bin for both discriminants ($m_{\ell\ell jj}$ and m_{jj}) and the appropriate one is used for each ($m(W_R)$, $m(N_R)$) hypothesis for the interpretation. In the smaller-background rSRSS subset, the variable h_T offers slightly better sensitivity and is used instead as the final discriminant. This variable is segmented into five bins: 400–600 GeV, 600–1000 GeV,

1–1.5 TeV, 1.5–2.2 TeV, and > 2.2 TeV, which take into consideration the signal resolution and MC statistical uncertainty in each bin.

6.2 Background estimation

The composition of the SM background is substantially different between rSROS and rSRSS, requiring different estimation techniques in the two categories. SM backgrounds containing two prompt leptons are estimated using simulations in both cases. An overall normalisation correction obtained from the observed data in control regions (CRs) is used for the main background sources: Z +jets, diboson, and $t\bar{t}$ processes. CRs are kinematically similar to SRs, and enriched in the process for which the normalisation correction is applied. Signal contamination is very low (typically 1-2%). A different normalisation correction factor is assigned to each process, and typically treated as a free parameter in the fit discussed in Section 9. The validity of the normalisation correction factor is confirmed in validation regions (VRs). The component containing non-prompt or mis-identified leptons is estimated separately by employing a data-driven method. The definitions of SRs, CRs and VRs for the resolved channel are visualised in Figure 2.

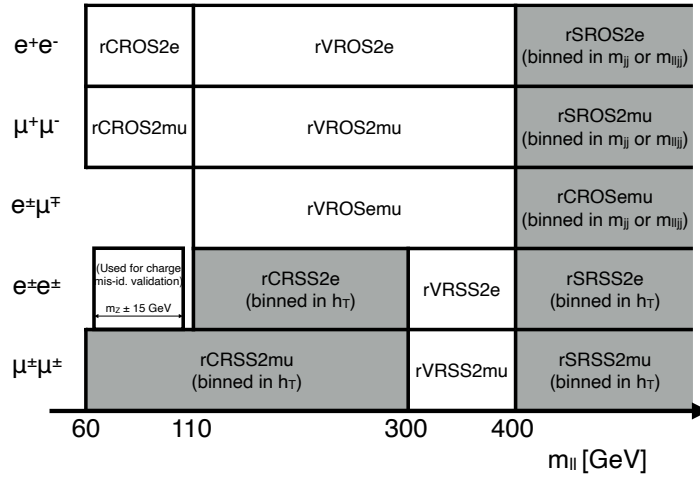


Figure 2: Resolved channel: Schematic view of SR/CR/VRs definitions. The grey coloured regions are contributing simultaneously to the final fit in the electron or muons channels. The remaining regions are used to verify the background estimations (see text for details).

6.2.1 Opposite-sign category

The main SM backgrounds contributing to rSROS are events with top quarks (mainly $t\bar{t}$) and Z +jets production, with contributions of 41% and 45% respectively in rSROS2e and 41% and 48% in rSROS2mu. Minor contributions arise from diboson processes (mainly $ZW \rightarrow \ell\ell jj$ and $ZZ \rightarrow \ell\ell jj$).

The normalisation factor for Z +jets is estimated in a control region defined by the same selection as rSROS with a modification in the dilepton mass selection: $60 < m_{\ell\ell} < 110$ GeV (rCROS). There is a known issue in the jet multiplicity description of the Z +jets MC sample observed in a previous analysis [21], leading to the mis-modelling of the dijet invariant mass m_{jj} . Following the prescription described therein,

a data-driven method is employed to correct for this effect. Electron and muon channels are combined and used to derive the m_{jj} -dependent correction factor. The rCROS data is used after subtracting the top-quark (3%) and other minor prompt-lepton (2%) background contributions evaluated with MC simulation, leaving a distribution with a size of about 94% of the original dataset. The normalisation of the Z+jets MC sample is then scaled to match the resulting rCROS distribution. The data-to-Z+jets MC ratio, r , reaches a maximum value of about 1.05 at $m_{jj} = 300$ GeV, and decreases at the higher-mass region to reach a value of ~ 0.7 at $m_{jj} = 3$ TeV. The ratio r is parameterised by the Novosibirsk function, as discussed in Ref. [21]. The r is used to apply an event-by-event correction to the Z+jets simulated sample in the OS channel. The method corrects not only the m_{jj} shape but also the normalisation of Z+jets in the simulation. Therefore, rCROS is not used in the final distribution fit discussed in Section 9.

The $t\bar{t}$ background is estimated with the same selection as rSROS, but by requiring a different flavour for the two charged leptons i.e. $m_{e\mu} > 400$ GeV (rCROSemu). The normalisation factor is treated as a free parameter in the final fit, but determined mainly in rCROSemu due to its high purity in $t\bar{t}$ ($\sim 80\%$), with dibosons being the other main component ($\sim 19\%$).

The validity of the background estimations described above is checked in the validation region rVROS, defined in an intermediate $m_{\ell\ell}$ region between SR and CR, i.e. $110 < m_{\ell\ell} < 400$ GeV. An additional validation region is defined with the same selection as rSROS but with an $e\mu$ pair instead of two same-flavour charged leptons (rVROSemu). Validation results are presented in Sec. 9.1.

6.2.2 Same-sign category

Diboson processes (mainly $WZ \rightarrow \ell\ell$ and same-sign $W^\pm W^\pm \rightarrow \ell^\pm \nu \ell^\pm \nu$) are the main background source in rSRSS. In particular, about 83% of the background in rSRSS2mu can be attributed to dibosons. In addition, there are non-negligible contributions from $Z(\rightarrow ee)$ +jets and top-quark events with charge mis-identification in rSRSS2e. The background contributions from diboson and charge mis-identified processes in rSRSS2e are 29% and 39%.

The diboson background is estimated with the same selection as rSRSS, but by requiring $110 < m_{ee} < 300$ GeV or $60 < m_{\mu\mu} < 300$ GeV (rCRSS). To increase the CR dataset size, no selection is applied on h_T or m_{jj} . The validity of the background estimation technique is confirmed in the $300 < m_{\ell\ell} < 400$ GeV validation region (rVRSS), with validation results shown in Sec. 9.1.

The charge-mis-identified background consists of events with two opposite-sign electrons, one of which has its charge sign mis-measured. The most frequent cause of electron charge flip is the bremsstrahlung effect. The probability of an electron undergoing charge mis-identification is measured in the data [83] and compared to the MC prediction. A correction factor is then derived for the charge flip probability and applied to simulated events featuring same-sign electron pairs. The method is validated in a same-sign dielectron region with $|m_{ee} - m_Z| < 15$ GeV, which does not overlap with the rCRSS region ($110 < m_{ee} < 300$ GeV). The data agrees well with the corrected prediction within uncertainties. This result confirms the validity of the correction factor for the charge-flip probability in a limited m_{ee} range, but does not cover a possible mis-modelling of the extended m_{ee} distribution. Unlike opposite-sign Z+jets, the normalisation of the same-sign Z+jet sample is therefore free to float and determined mainly in rCRSS2e.

Another smaller background contribution comes from mis-identified leptons originating from non-isolated, non-prompt electrons and muons produced by secondary decays of light- or heavy-flavour hadrons. Another significant component of fake electrons arises from photon conversions, as well as from jets that are

misreconstructed as electrons. The contribution of events with mis-identified leptons is estimated by a data-driven technique, known as the “fake-factor” method. The fake factor F is defined as the ratio of mis-identified leptons satisfying the baseline lepton criteria (labelled as `Tight` in this section) to those satisfying the selection criteria for fake estimation (`Loose`). The factors are estimated separately for electrons and muons. The fake factors calculated in Ref. [84] are used in this analysis, as common object definitions are employed. Fake factors are measured in data as a function of lepton p_T and η in control samples that are orthogonal to the SR, VR, and CRs used in this analysis.

The contribution of mis-identified leptons in SR, VR, and CRs is estimated as follows. The calculated F is applied to events satisfying the same selection criteria as in SR, VR, and CRs but by lowering the lepton ID requirement from `Tight` to `Loose` for at least one lepton. The signal contamination in these regions is found to be small (typically 1-2%) and ignored here. Three categories are considered separately, depending on the identification criteria satisfied by the leading and sub-leading leptons: they are the LT (`Loose - Tight`), TL (`Tight - Loose`) and LL (`Loose - Loose`) categories. Data events are weighted with fake factors according to the loose-lepton multiplicity of the region:

$$N^{\text{fake}} = [F(N_{TL} + N_{LT}) - F^2 N_{LL}]_{\text{data}} - [F(N_{TL} + N_{LT}) - F^2 N_{LL}]_{\text{MC}}^{\text{prompt } \ell \text{ only}} \quad (1)$$

with N_{TL} , N_{LT} , N_{LL} denoting the number of events in the corresponding category. The prompt lepton contribution in the events with `Loose` leptons is subtracted using the MC simulation to account for the prompt-lepton contamination in the given category.

The composition of rCRSS is dibosons (32%), charge mis-identified background (45%) and fakes (20%) in the electron channel, and dibosons (65%), fakes (27%) and charge mis-identified background (8%) in the muon channel.

7 Boosted channel: event selection and background estimate

7.1 Event reconstruction and selection

The boosted analysis is designed for signals in the $\Delta m > 4$ TeV region by using the large- R jet to reconstruct the hadrons from the N_R decay. The signal events have a very energetic charged lepton and N_R from the W_R decay produced back-to-back in the x - y plane. In the highest Δm region, the large- R jet overlaps with the lepton from the N_R decay. In the muon channel, such a muon inside the jet can be identified, and a single SR (`bSR2mu`) with two baseline muons is used to cover the full Δm range. On the other hand, in the electron channel, calorimeter clusters from the electron from the N_R decay overlap with other hadron activities, making its identification challenging. Two signal regions, `bSR1e` and `bSR2e`, are thus defined requiring exactly one and two baseline electrons in the event, respectively, to cover the higher and lower Δm ranges. The W_R mass is reconstructed from the large- R jet and the electron (m_{eJ}) in `bSR1e`, and from the large- R jet and the two charged leptons (m_{eeJ} and $m_{\mu\mu J}$, or collectively $m_{\ell\ell J}$) in `bSR2e` and `bSR2mu`. Due to the relatively small background after the event selections, the sensitivity gain by separating SR into same- and opposite-sign events is marginal, hence the lepton charge is not considered in the boosted analysis.

For all three SRs, the requirement that only one large- R jet is reconstructed in the event is imposed, which is expected to cover about 90% of signal events. This selection cut is useful in suppressing the multijet background, and improving the fake-lepton, multijet and γ +jets modelling by the LO simulation with the

exception of an overall normalisation factor. Assuming well-isolated and highly-boosted leptons from the prompt W_R decay, tighter identification and isolation criteria (as detailed in Section 5) are required for the lepton with the highest- p_T in the event. The azimuthal difference between the large- R jet and the highest- p_T lepton is required to be greater than 2. In addition, to suppress the top-quark backgrounds, the number of b -tagged small- R jets is required to be zero.

7.1.1 One-electron category (bSR1e)

Region bSR1e requires exactly one electron from the W_R decay, with the large- R jet encapsulating all decay products of the heavy neutrino $N_R \rightarrow e q q'$. A $E_T^{\text{miss}} < 200$ GeV selection is applied to suppress the main background process, $W(\rightarrow e\nu) + \text{jets}$. The high- p_T electron and low E_T^{miss} requirements bias the W +jets events towards higher helicity angles, $|\cos \theta| \sim 1.0$, where θ is the polar angle of the electron from the W boson decay in the rest frame of the W^2 . The $|\cos \theta| > 0.7$ region is used for the signal search. The $|\cos \theta| < 0.7$ region is used for the normalisation of the W +jets contribution. To further reduce the γ +jets and dijet contributions, a selection on the η difference between the large- R jet and the electron candidate, $\Delta\eta = |\eta(J) - \eta(e)| < 2$ is applied. The bSR1e definition is summarised in Table 5.

7.1.2 Two-electrons category (bSR2e)

Region bSR2e covers the intermediate Δm region between bSR1e and the resolved analysis. The events are selected if they contain exactly two electrons and one large- R jet. The $E_T^{\text{miss}} < 200$ GeV selection is applied to further reduce the $t\bar{t}$ background. The dominant background source is $Z(\rightarrow ee) + \text{jets}$. To remove contributions from the pole mass of the Z boson, a $m_{ee} > 200$ GeV selection is applied. The bSR2e definition is summarised in Table 5. bSR1e and bSR2e are orthogonal to each other and are statistically combined to obtain the final results.

Table 5: Definition of the signal regions in the boosted analysis. The baseline definitions of electrons and muons are used. Two regions in the electron channel cover higher- and lower- Δm regions, where Δm denotes the mass difference between W_R and N_R .

Region	bSR1e (higher Δm)	bSR2e (lower Δm)	bSR2mu
Number of large- R jets		1	
Number of electrons	1	2	0
Number of muons	0	0	2
Leading lepton p_T [GeV]		> 200	
E_T^{miss} [GeV]		< 200	—
$ \cos \theta $	> 0.7	—	—
$\Delta\phi_{J,\ell_1}$		> 2.0	
$\Delta\eta_{J,\ell_1}$	< 2.0	—	—
Dilepton p_T (GeV)	—	—	> 200
Dilepton mass $m_{\ell\ell}$ [GeV]	—		> 200
Number of b -tagged small- R jets		0	

² The W boson rest frame is calculated from the E_T^{miss} and the reconstructed electron by solving the kinematic equation for the neutrino momentum in the z -axis direction ($p_{z,\nu}$) and by assuming a W boson mass of 80.4 GeV.

7.1.3 Two-muons category (bSR2mu)

Events are selected in bSR2mu if they contain exactly two muons and one large- R jet. A $m_{\mu\mu} > 200$ GeV selection is applied. The upper cut on E_T^{miss} is not useful in this channel due to the deteriorated momentum resolution for very high- p_T muons. Instead, the dimuon system's p_T is required to be greater than 200 GeV to suppress the $t\bar{t}$ background. The bSR2mu definition is also summarised in Table 5.

7.1.4 Event categorisation for the background estimation

The normalisations of the main background sources, $W(\rightarrow e\nu)+\text{jets}$ and $Z(\rightarrow \ell\ell)+\text{jets}$, as well as for the processes with less reliable yield predictions, $\gamma+\text{jets}$ and multijet, are estimated from data in control regions and adjusted by using the SR-to-CR ratio in the simulation.

In each category, the reconstructed W_R mass distribution is segmented into four bins; 1–2 TeV, 2–3 TeV, 3–4 TeV, and > 4 TeV, having considered the search sensitivity for signals with various W_R masses and the stability of the background estimation. High-mass W_R signals are expected to be observed in the third and fourth bins, which are designated bins 1 and 2 of the SR for each channel (for example, bins 1 and 2 of bSR2mu for the two-muon case). The first bin of the W_R mass histogram is used for the SM background determination in a region where the presence of lower-mass W_R signals is negligibly small, given exclusion limits obtained in previous ATLAS analyses [22]. For the two-electron and two-muon categories, the first bin is used to estimate the $Z+\text{jets}$ background normalisation in designated bCRZ2e and bCRZ2mu, respectively. In the one-electron case, the 1–2 TeV $m(W_R)$ bin is used to distinguish between $\gamma+\text{jets}$ and $W+\text{jets}$ events. If there is an additional ID track with opposite charge within $\Delta R < 0.3$ and $|\Delta z_0 \sin \theta| < 0.5$ from the electron candidate track, the electron is possibly coming from a photon conversion and the events are categorised into bCR γ 1e. The remaining events are categorised into bCRLow1e. The fractions of $W+\text{jets}$, $Z+\text{jets}$, multijet and $\gamma+\text{jets}$ are about 33%, 10%, 24% and 30%, respectively, in bCR γ 1e, and approximately 73%, 17%, 3% and 1% in bCRLow1e.

The normalisation for $W(\rightarrow e\nu)+\text{jets}$ and multijet events is estimated in the dedicated control regions, bCRW1e and bCRFake1e, requiring $|\cos \theta| < 0.7$ and the inverted electron isolation cut, respectively, with the remaining selection identical to that of bCRLow1e. The purity of the $W+\text{jets}$ and multijet events in bCRW1e and bCRFake1e is about 83% and 91%. One should note that the $\gamma+\text{jets}$ contribution in bCRFake1e is not large since mis-identified electrons from photon conversions can satisfy the tight isolation requirement.

The estimated CR normalisation factors are extrapolated to higher-mass bins. The validity of the method is first checked in the second bin ($m(W_R) = [2, 3]$ TeV) in each channel: bVR2e, bVR2mu and bVR1e, for bSR2e, bSR2mu and bSR1e, before the third and fourth bins are tested. In addition, the regions with $|\cos \theta| < 0.7$ and the inverted electron isolation in the one-electron channel are used to check the extrapolation of $W+\text{jets}$ and multijet normalisations from the lower to the higher W_R mass bins. The regions are segmented into 2–3 TeV and > 3 TeV and labelled as bVRW1e and bVRFake1e, respectively.

To check the extrapolation of the $Z+\text{jets}$ normalisation from the lower to the higher W_R mass bins, additional validation regions are defined (bVRZ2e and bVRZ2mu), but which are not used in the final fit. They require $120 < m_{\ell\ell} < 200$ GeV instead of > 200 GeV.

The definitions of SRs, CRs and VRs for the boosted channel are visualised in Figure 3. Validation results are presented in Sec. 9.2.

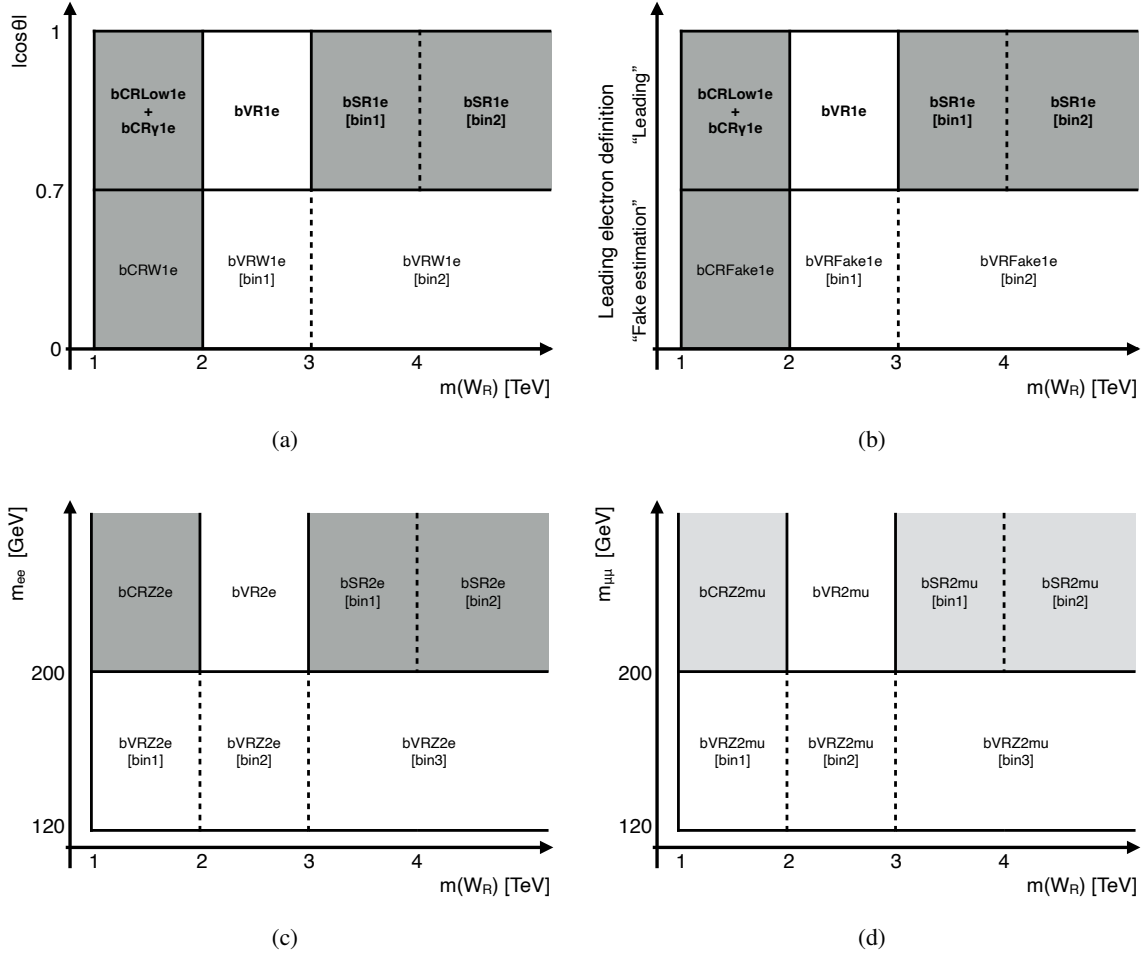


Figure 3: Boosted channel: Schematic view of SR/CR/VRs definitions for $bSR1e$ (a)–(b), $bSR2e$ (c) and $bSR2\mu$ (d). (a) and (b) show the regions for the estimation of W +jets and multijet backgrounds, respectively. The labels $bSR1e$, $bVR1e$, $bCRLow1e$ and $bCR\gamma1e$ shown in bold in the two figures correspond to the same regions. The dark-grey coloured regions in (a), (b) and (c) are contributing simultaneously to the final fit in the electron channel, while the light-grey coloured regions in (d) are used for the muon channel, separately. The remaining regions are used to verify the background estimations (see text for details).

7.2 Background estimation

For the W +jets and Z +jets estimation in the boosted analysis, since the number of jets is forced to be one, the correction for jet multiplicity mis-modelling used in the resolved analysis is not required. The simulated W_R mass distributions for W +jets in $bVRW1e$ (with $|\cos\theta| < 0.7$) and those for Z +jets $bVRZ2e$ and $bVRZ2\mu$ agree well with the observed data. The W_R mass distributions in these regions are only used to confirm the normalisation methodology for each process and these are within the considered uncertainties.

The fake lepton contribution is negligibly small in $bSR2e$ and $bSR2\mu$ after the requirement of a high- p_T selection on the leading lepton. It is, however, not negligible at the higher W_R mass tail in $bSR1e$. MC simulation is used to estimate the non-prompt electron contribution with a data-driven correction factor

obtained in the CR. The simulated W_R mass in `bVRFake1e` agrees well with the multijet sample within the uncertainties considered. In the final fits the normalisation is mainly constrained by `bCRFake1e` and its validity in the SR relies on the good simulation of the isolation efficiency for fake electrons. To check the validity of this approach, two additional regions beyond those shown in Figure 3 are defined, corresponding to `bSR1e` and `bCRFake1e`: the electron candidate is forced to satisfy the `Medium` identification but fail the `Tight` identification criterion in order to be orthogonal to the SR, CRs and VR. The remaining selection is the same as in `bSR1e` (`bCRFake1e`), with the requirement to satisfy (fail) the `HighPtCaloOnly` isolation criterion. In both regions, the purity of the multijet process is greater than 90%. By comparing data to MC in both regions, it is found that the simulated isolation efficiency for fake electrons agrees with the data within the considered uncertainties. A small data/MC disagreement on $m(W_R)$ distribution is considered as an additional uncertainty on the multijet estimation in `bSR1e`.

The γ +jets contribution with isolated electrons from photon conversions is also estimated by MC simulation with a normalisation factor determined in a data-driven way. Additional validation regions are defined requiring exactly one reconstructed photon instead of an electron, with the remaining selection the same as in `bSR1e`. The purity of γ +jets sample in this region is about 70%, and the fraction of multijet events is 30%. The reconstructed W_R mass with the photon (in the place of the electron) and the large- R jet agrees between data and MC within the considered uncertainties. The p_T - and η -dependent photon conversion rate may change the reconstructed W_R mass distribution for the γ +jets process, but this rate mainly depends on the detector geometry and it is well modelled in the simulation. The normalisation of the γ +jets contribution is estimated mainly from `bCR γ 1e`, by requiring an additional ID track close to the electron. The modelling of the fraction of events with an ID track close to the electron in simulated W +jets and multijets can affect the γ +jets estimation, so a comparison is carried out with data in `bCRW1e` and `bCRFake1e`. For the γ +jets contribution, the same check is performed in the $\Delta\eta > 2.0$ region. The purity of γ +jets in this region is about 50%, and a conservative uncertainty on the other background subtraction is included in the study.

8 Systematic uncertainties

Several experimental and theoretical systematic uncertainties are considered, affecting both the background and signal predictions as well as the total event yield. In addition, the statistical uncertainty of the MC simulated events is also considered. These uncertainties also affect the shape of the variables used in the fit, with the exception of the luminosity and cross-section uncertainties.

The uncertainty on the integrated luminosity is 1.7% [85]. It is obtained using the LUCID-2 detector [86] for the primary luminosity measurements. The uncertainty due to the pile-up reweighting procedure is estimated by varying the amount of pile-up in the simulation to cover the uncertainty in the ratio of the predicted and measured inelastic cross section [87].

A set of experimental systematic uncertainties arise from the energy and momentum calibrations of leptons and jets, the lepton reconstruction, isolation and trigger efficiencies, and the jet vertex tagger and flavour-tagging efficiencies. The largest uncertainty in the total SM yield arises from the energy calibration and smearing of jets, derived in Ref. [77], and is between 1 and 6% in the SS and about 4% in the OS in the resolved channel, and between 5 and 12% in the boosted channel, depending on the signal region. Uncertainties associated with lepton reconstruction, identification, isolation and trigger efficiencies, as well as energy or momentum calibration [41, 72, 88] and b -jet tagging [79, 89], vary between 5% (OS) and 13% (SS) of the total SM yield in the resolved analysis, and between 2% and 5% in the boosted. These uncertainties are propagated to the E_T^{miss} calculation. In addition, uncertainties on the scale and resolution

of the ‘soft term’ of the E_T^{miss} are taken into account [81]. In bSR2mu, the muon p_T is further smeared by taking into account the impact of MS outliers on the muon resolution not described by the simulation. This additional effect is considered as the high- p_T muon uncertainty.

There are three additional sources of systematic uncertainty associated with the background estimation techniques. In rSRSS, the uncertainty related to the charge mis-identification probability of electrons arises from the statistical uncertainty of the data and simulated samples of Z+jets events used in this measurement. The uncertainty is around 6.8% with a mild dependence on the electron E_T and η [90]. The uncertainty on the fake estimation arises from the limited knowledge in the composition of fakes, as well as from the statistical uncertainty and prompt lepton subtraction used to derive F in the fake-enriched regions. The uncertainty due to the composition of fakes is estimated by varying the nominal criteria defining the selection sample used in the fake-factor measurement [84]. The effect on the SM yields is 3.8% (electrons) and 0.8% (muons). In rSROS, an additional uncertainty is associated with the m_{jj} reweighting of the Z+jets process. This is evaluated by comparing the shape difference between the reweighted simulated m_{jj} distribution and the one measured in data, using rVROS: the uncertainty in the reweighting factor is found to vary between 0.4% and 0.8%, as a function of the dijet invariant mass. This observed difference covers all possible mismodellings of the Z+jets shape, hence additional theoretical uncertainties for the Z+jets process are not considered in the resolved channel.

In the boosted channel, the theory uncertainties estimated for the W+jets, Z+jets, diboson, multijet and γ +jets background processes are considered, which include the choice of QCD renormalisation (μ_r) and factorisation (μ_f) scales, choice of the PDF set and α_S , as well as CKKW matching scale and the resummation scale. The QCD scale uncertainty is estimated by varying μ_r and μ_f to half and twice their nominal values. The PDF uncertainty is estimated using the envelope of the NNPDF3.0 PDF set, as recommended in Ref. [91]. In addition, the MMHT2014 [92] and CT14NNLO [93] PDF sets are used to estimate the uncertainty due to the PDF choice. Moreover, the uncertainty due to α_S is evaluated by varying its nominal value of 0.118 by ± 0.001 . The CKKW matching scale is the parameter to remove the overlap between jets from the matrix element calculation and the parton shower algorithm. The nominal value is 20 GeV, and the uncertainty is estimated by varying it to 30 GeV and 15 GeV. The uncertainty on the resummation scale of soft gluon emission is estimated by varying the parameter to half and twice the nominal value. The largest theory uncertainties generally originate from the CKKW matching and Sherpa resummation scales ($\sim 20\%$), and QCD scales variations which range between 10% and 20%, depending on the simulated process and the mass of the target signal.

The theory uncertainties associated with $t\bar{t}$ processes are as follows. The uncertainty from hard scatter generation is evaluated by comparing the Powheg-Box and MG5_aMC@NLO generators, both interfaced to the Pythia 8.186 [94] parton shower model. The uncertainty due to the hadronisation and fragmentation model is determined by comparing the nominal Powheg-Box + Pythia 8.186 generated sample with the one generated by Powheg-Box interfaced to Herwig [95] (version 7.13). The uncertainty related to the amount of initial- and final-state radiation (ISR and FSR) is assessed by varying parton shower settings. The largest theory uncertainty generally originates from the amount of initial- and final-state radiation and is between 0.4% – 0.5% (ISR) and 0.6% (FSR) of the $t\bar{t}$ process yield.

In the boosted analysis, additional uncertainties are considered by comparing different MC samples on the possible variations of the reconstructed $m(W_R)$, $\cos\theta$ and the isolation efficiency for the fake electrons. For W/Z+jets, the nominal Sherpa 2.2.11 samples are compared with the samples generated with MadGraph5_aMC@NLO+Pythia 8.186. For γ +jets, the nominal Sherpa 2.1 sample is compared with the alternative sample generated with Pythia 8.235 [44]. The nominal Pythia 8.230 multijet MC sample is compared with the sample generated with Sherpa 2.2.5. For the multijet sample, an additional

uncertainty on the $m(W_R)$ shape is considered by taking the residual non-closure in studies employing different electron identification discussed in Section 7.2. The possible mis-modelling of the $bCR\gamma 1e$ to $bCRLow 1e$ ratio is evaluated by considering the observed discrepancy in the CRs.

The theory uncertainty of the signal efficiency times acceptance amounts to 20%. It is evaluated by varying renormalisation and factorisation scales as described above and by using alternative PDF sets, CTEQ6 [96] and MSTW [97]. The α_S emission scale factor is also varied to half and twice the nominal value. The uncertainty is dominated by the variation in factorisation scale. The variations are performed using SysCalc [98].

The systematic uncertainties in each SR are summarised in Figure 4. Individual uncertainties can be correlated with others, and do not necessarily add in quadrature towards the total background uncertainty.

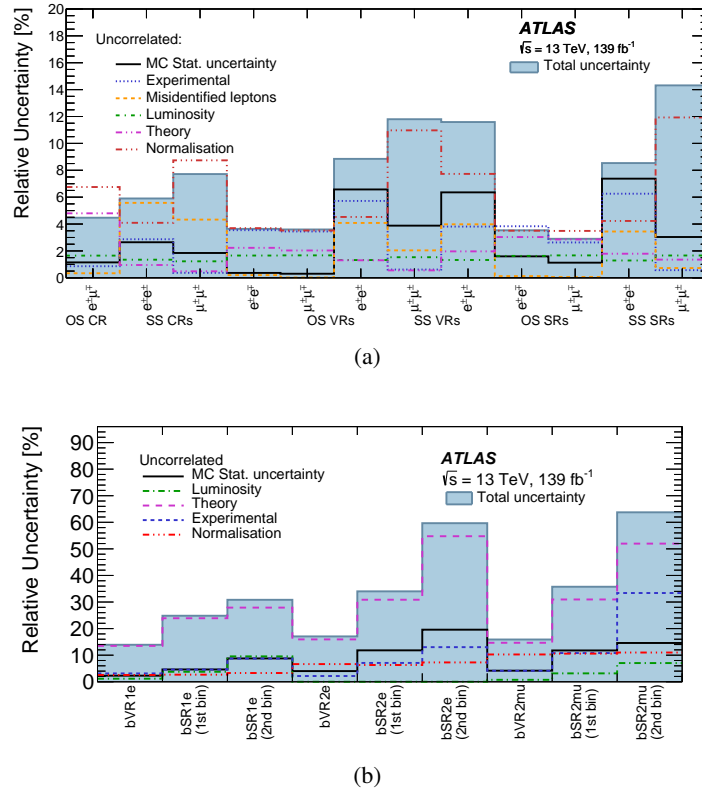


Figure 4: Relative uncertainties in the total background yield post-fit estimates for the (a) resolved and (b) boosted channels. “Theory” indicates the theoretical uncertainty associated with the simulated physics processes (e.g. cross sections). “Normalisation” is the uncertainty associated with the yield variations of the dominant backgrounds in the fit. “Experimental” corresponds to the combined uncertainty on physics object efficiencies (such as trigger, identification or isolation) and uncertainties associated with E_T^{miss} and pile-up. The total uncertainty takes into account any correlations among nuisance parameters.

9 Statistical analysis and results

The search for a W_R and N_R signal is carried out using the theoretical model described in Section 2. The statistical treatment is done separately for samples containing electrons and muons since there is

no theoretical motivation that the N_R should have the same mass across different flavours. The resolved and boosted channels are analysed independently. The statistical interpretation is performed by carrying out binned maximum-likelihood fits using the HistFitter [99] framework. The likelihood is a product of Poisson probability density functions, describing the observed number of events in each bin of regions involved in the fit, and Gaussian distributions that describe the nuisance parameters associated with each of the systematic uncertainties. Systematic uncertainties that are correlated between different samples and different regions are accounted for via a common nuisance parameter.

A “background-only” fit is carried out first by using the observed event yield in CRs assuming that no signal contributes in these regions, and by applying the resulting normalisation factor to the number of background events predicted by simulation for the equivalent process in the validation regions. The normalisation factors of the background processes are allowed to vary freely. The VRs are only employed to confirm the validity of the background modelling in the background-only CR fits, and do not contribute to the search results presented here.

A non-zero signal contribution for each $m(W_R)$ and $m(N_R)$ mass point is then allowed involving both SR and CRs in the fit, as summarised in Figures 2 and 3. The normalisation factors of the various (signal or background) processes are allowed to vary freely. Upper limits at 95% C.L. on the signal strength of the KS process are calculated using the CL_s method [100] and the profile likelihood-ratio as the test statistic. The asymptotic method [101] was used, but similar results were obtained with toy MC tests.

9.1 Resolved channel

In the resolved channel, the $m_{\ell\ell jj}$ distribution is used in the rSROS fit when $m(W_R) > m(N_R)$. In the $m(W_R) < m(N_R)$ case, the fit results are obtained by employing the m_{jj} distribution. The h_T distribution is used in the rSRSS fit. For the scenario in which the N_R neutrino is a Majorana particle, the OS and SS channels are fitted simultaneously, whereas for the Dirac neutrino scenario, only the OS channel is used in the fit.

A combined “background-only” fit is first carried out in the rCROSemu, rCRSS2e and rCRSS2mu regions. The free normalisation factors for the $t\bar{t}$ and diboson processes are estimated mainly from rCROSemu and rCRSS2mu. The validity of the evaluated normalisation factors for same-sign Z +jets, $t\bar{t}$ and diboson samples is confirmed by applying them in the rVROS2e, rVROS2mu, rVRSSemu, rVRSS2e, and rVRSS2mu regions. All systematic uncertainties described in Section 8 are considered as nuisance parameters. Figure 5 shows an example of the post-fit $m_{\ell\ell jj}$ distribution in rVROS2mu and h_T distribution in rVRSS2e, showing a good agreement between the observed data and the expected background.

The integrated event counts for the observed data and the estimated background for the CR, VR and SR regions are shown in Figure 6. The post-fit $m_{\ell\ell jj}$ and m_{jj} distributions in rSROS and h_T distributions in rSRSS are shown in Figure 7. In all cases, no significant deviation above the expected background is observed in the data. The largest excess is observed in rSRSS2e around $h_T \sim 1.0$ TeV (Figure 7e): 39 events are observed in a region where 24.0 ± 2.4 background events are expected. The observed deviation is in a background-rich region and is not consistent with the shape of the signal.

Exclusion limits at 95% CL on the signal strength of the KS process as a function of $m(W_R)$ and $m(N_R)$ are calculated. The results are shown in Figure 9. For electron Majorana neutrinos, the excluded region extends to a W_R mass of 5.6 TeV and to a N_R mass of 3.5 TeV. For muon Majorana neutrinos, W_R masses of up to 5.7 TeV were excluded, and N_R masses of up to 3.6 TeV. For electron Dirac neutrinos, the excluded

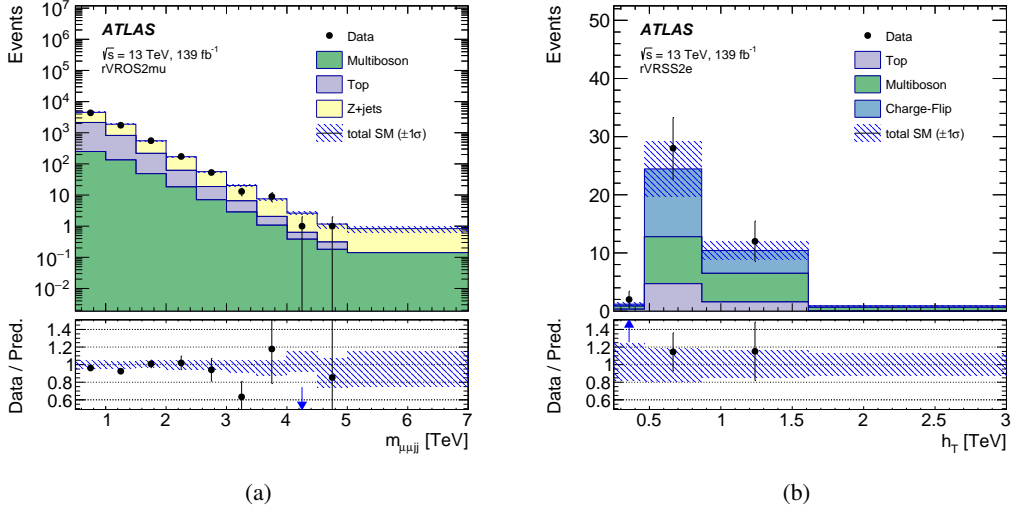


Figure 5: VR fits in the resolved channel: (a) $m_{\ell\ell jj}$ in rVROS2mu and (b) h_T distribution in rVRS2e. ‘Top’ refers to all processes containing at least one top quark. ‘Multiboson’ refers to VV and VVV processes, where $V = W$ or Z . The expected background is determined via a fit on the CR data. The hatched band (‘total SM’) includes all post-fit systematic uncertainties, having taken into account all correlations among various sources. A blue arrow indicates an out-of-range data point for a given bin.

region extends to a W_R mass of 5.9 TeV and to a N_R mass of 3.6 TeV. For muon Dirac neutrinos, W_R masses of up to 5.8 TeV were excluded, and N_R masses of up to 3.8 TeV. Compared to the previous ATLAS analysis in the resolved channel [21], the exclusion limits on the W_R masses are extended by 0.8–1.2 TeV in the case of $m(W_R) > m(N_R)$.

9.2 Boosted channel

In the boosted channel, the reconstructed $m(W_R)$ distribution (m_{eJ} or $m_{\ell\ell J}$) is used exclusively since $m(W_R) \gg m(N_R)$. In the electron channel, the normalisations of W +jets, Z +jets, γ +jets and multijet samples are simultaneously estimated by the fit in the CRs and SRs. In the muon channel, only the Z +jet contribution is estimated by the fit.

A combined “background-only” fit is performed separately in the electron and muon channels in the bCRW1e, bCRFake1e, bCR γ 1e, bCRLow1e and bCRZ2e, and bCRZ2mu regions, respectively. The normalisation factors for W +jets, Z +jets, γ +jets and multijet are free to float in the electron channel, while only the Z +jets normalisation is treated as a free parameter in the muon channel. The validity of the method is confirmed by applying the normalisation factors obtained with the fit in the bVR1e and bVR2e regions in the electron channel, and the bVR2mu region in the muon channel. As shown in Figure 8, a good agreement between data and the estimated SM background is found in all CRs and VRs.

The post-fit $m(W_R)$ distributions for 1e, 2e and 2mu categories are found in Figure 8. The first bin in the 1e category shows the sum of bCRLow1e and bCR γ 1e. Again, no significant deviation above the expected background is observed in the data.

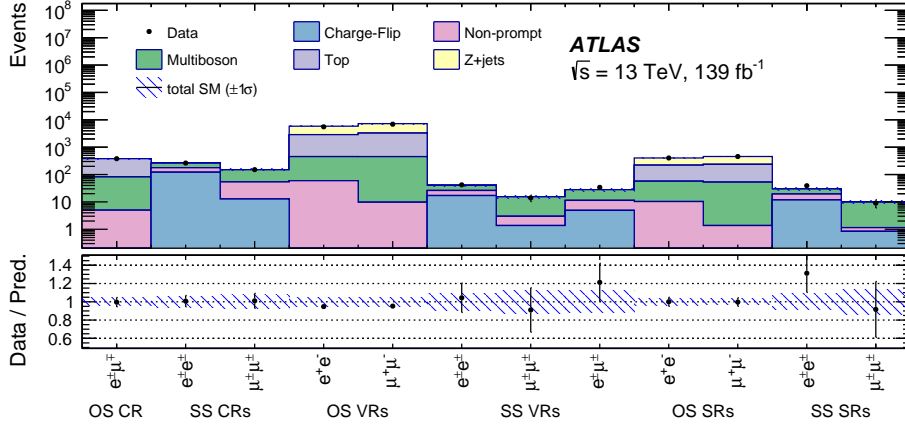


Figure 6: CR/VR/SR fits in the resolved channel: Integrated number of events for observed data and expected background in $e\mu$ (OS), and ee and $\mu\mu$ (SS) CR, ee and $\mu\mu$ (OS), and ee , $\mu\mu$ and $e\mu$ VR and ee and $\mu\mu$ (both OS and SS) SRs. ‘Top’ refers to all processes containing at least one top quark. ‘Multiboson’ refers to VV and VVV processes, where $V = W$ or Z . The expected background is determined via a fit on the CR data. The hatched bands (‘total SM’) include all post-fit systematic uncertainties, having taken into account all correlations among various sources.

Exclusion limits at 95% CL on the signal strength of the KS process as a function of $m(W_R)$ and $m(N_R)$ are calculated again, with the results shown in Figure 9. For Majorana neutrinos, the most stringent lower limit on the W_R mass is 6.4 TeV, observed in both electron and muon channels at $m(N_R) < 1$ TeV. This result is an improvement over previous ATLAS searches, and extends the exclusion limits on $m(W_R)$ by about 1.5 TeV. There is a particular improvement in the $m(N_R) < 100$ GeV region via the incorporation of the new bSR1e region and the optimisation of bSR2mu. The observed limit on $m(W_R)$ is 6.2 (6.1) TeV in the electron (muon) channel at $m(N_R) = 50$ GeV.

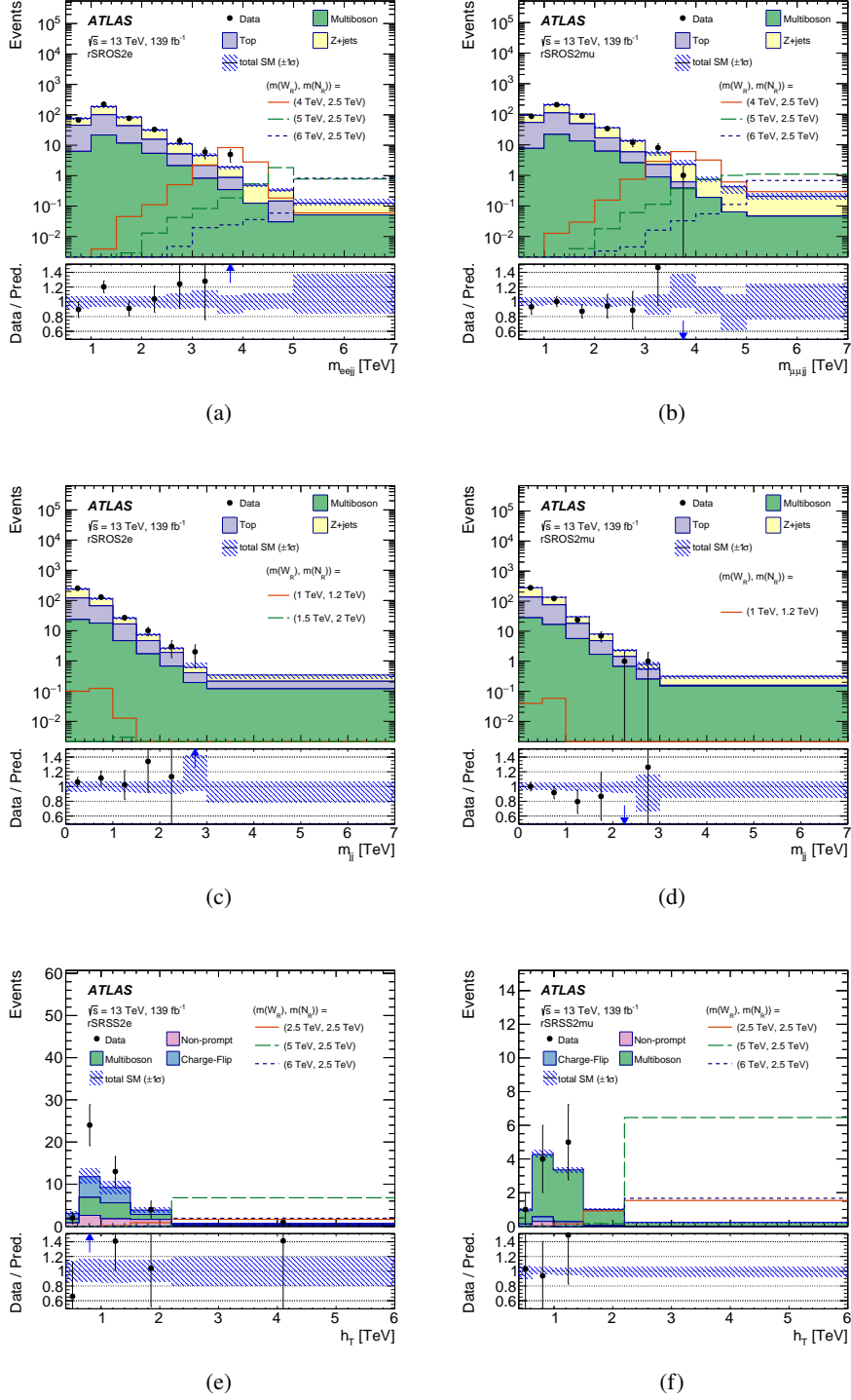


Figure 7: SR fits in the resolved channel: The $m_{\ell\ell jj}$ distributions in (a) rSRSS2e and (b) rSRSS2mu, the m_{jj} distributions in (c) rSRSS2e and (d) rSRSS2mu, and the h_T distributions in (e) rSRSS2e and (f) rSRSS2mu. ‘Top’ refers to all processes containing at least one top quark. ‘Multiboson’ refers to VV and VVV processes, where $V = W$ or Z . ‘Non-prompt’ and ‘Charge-Flip’ refer to processes containing a mis-identified electron and Z+jets with charge mis-identification. The background expectation is the result of the fit to the CR data. The hatched bands (‘total SM’) include all systematic uncertainties post-fit with the correlation between various sources taken into account. A blue arrow indicates an out-of-range data point for a given bin.

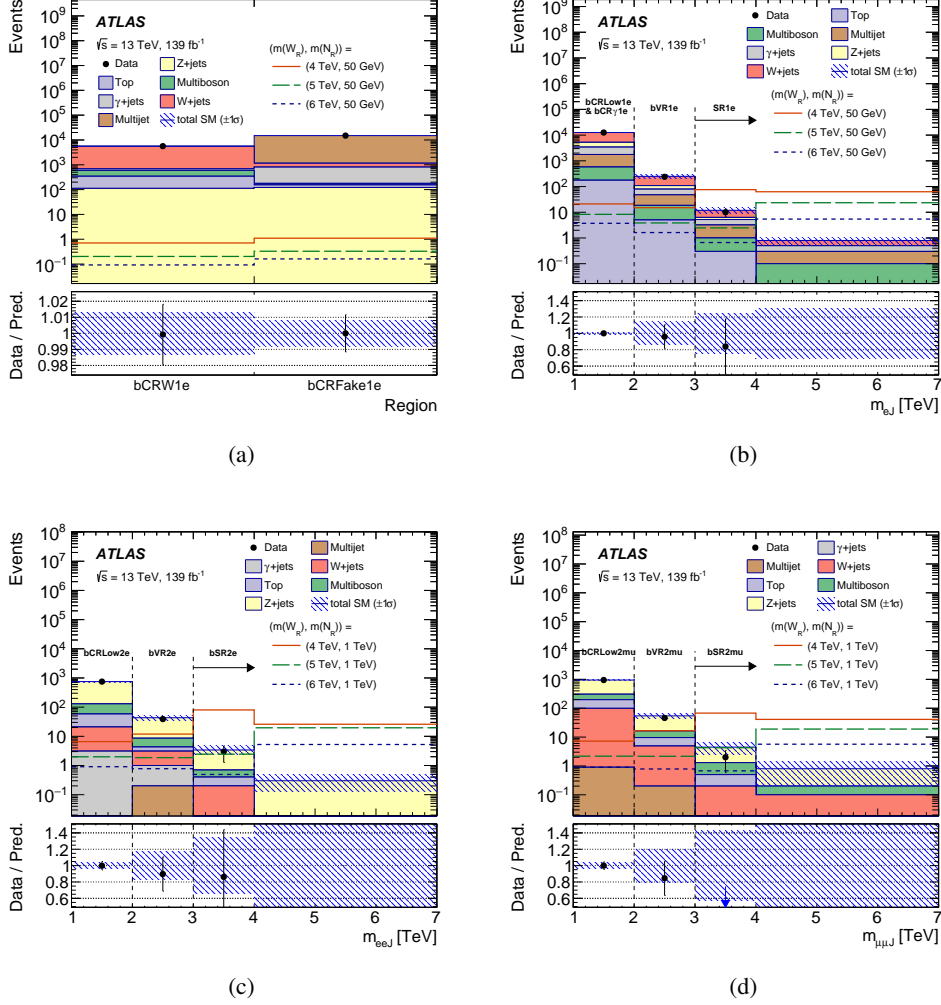


Figure 8: CR/VR/SR fits in the boosted channel: Integrated number of events for observed data and expected background in $bCRW1e$ and $bCRFake1e$ (a), and observed $m(W_R)$ distributions in $1e$ (b), $2e$ (c) and 2μ (d) categories. For (b)–(d), the first and second bins are used as CR and VR, and the third and fourth bins correspond to the SR. ‘Top’ refers to all processes containing at least one top quark. ‘Multiboson’ refers to VV and VVV processes, where $V = W$ or Z . The expected background is determined via a fit on the CR data. The hatched bands (‘total SM’) include all post-fit systematic uncertainties, having taken into account all correlations among various sources. A blue arrow indicates an out-of-range data point for a given bin.

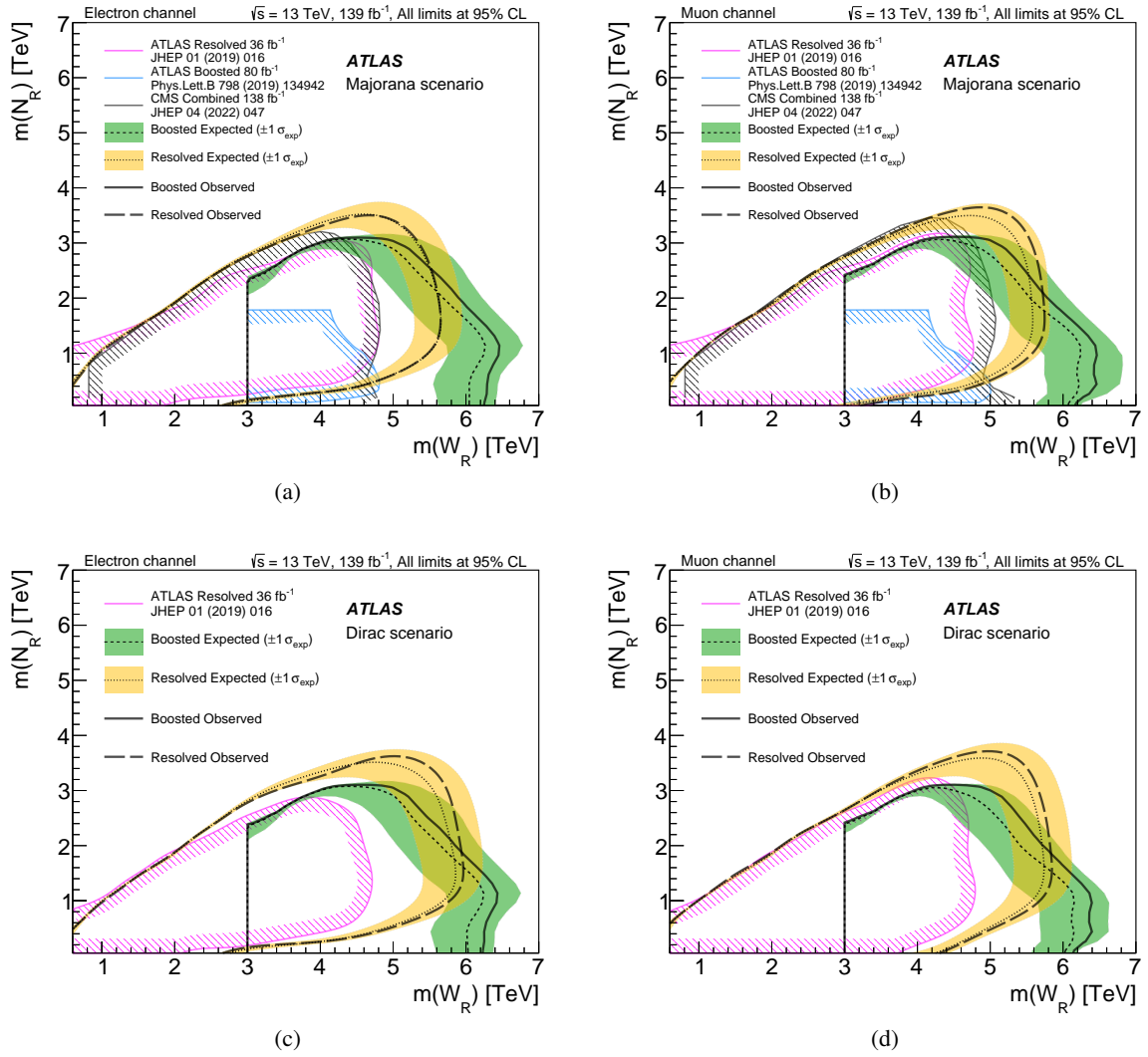


Figure 9: Expected and observed 95% CL upper limits for the Majorana (top) and Dirac (bottom) neutrino interpretations in the electron (left) and muon (right) channels. Exclusion limits from previous ATLAS [21, 22] and CMS [27] searches are overlaid for comparison.

10 Conclusion

A search for right-handed W_R bosons and heavy right-handed Majorana or Dirac neutrinos N_R is presented. The analysis uses various final states depending on the mass difference between W_R and N_R : two jets and a pair of charged leptons ($\ell\ell jj$), one large- R jet and two charged leptons ($\ell\ell J$), or one large- R jet and one electron (eJ), with $\ell = e, \mu$. It is performed with a 139 fb^{-1} sample of pp collisions at $\sqrt{s} = 13 \text{ TeV}$ recorded by the ATLAS detector at LHC. No evidence of W_R bosons or Majorana or Dirac heavy neutrinos is found assuming the KS process, and lower limits are set on $m(W_R)$ and $m(N_R)$, assuming equality of left- and right-handed weak couplings ($g_L = g_R$). The excluded region for the Majorana neutrinos extends to about $m(W_R) = 6.4 \text{ TeV}$ for $m(N_R) = 1 \text{ TeV}$ in both electron and muon channels. The $m(N_R)$ limits reach about 3.5 TeV in the electron channel and 3.6 TeV in the muon channel (for $m(W_R) = 4.8 \text{ TeV}$). For Dirac neutrinos, limits reach about $m(W_R) = 6.4 \text{ TeV}$ for $m(N_R) = 1 \text{ TeV}$ in both electron and muon channels. Limits of $m(N_R)$ up to 3.6 TeV in the electron channel and 3.8 TeV in the muon channel for $m(W_R) = 5.0 \text{ TeV}$ are set. The new results constitute the most stringent limits to date for the KS process.

Acknowledgements

We thank CERN for the very successful operation of the LHC, as well as the support staff from our institutions without whom ATLAS could not be operated efficiently.

We acknowledge the support of ANPCyT, Argentina; YerPhI, Armenia; ARC, Australia; BMWFW and FWF, Austria; ANAS, Azerbaijan; CNPq and FAPESP, Brazil; NSERC, NRC and CFI, Canada; CERN; ANID, Chile; CAS, MOST and NSFC, China; Minciencias, Colombia; MEYS CR, Czech Republic; DNRf and DNSRC, Denmark; IN2P3-CNRS and CEA-DRF/IRFU, France; SRNSFG, Georgia; BMBF, HGF and MPG, Germany; GSRI, Greece; RGC and Hong Kong SAR, China; ISF and Benoziyo Center, Israel; INFN, Italy; MEXT and JSPS, Japan; CNRST, Morocco; NWO, Netherlands; RCN, Norway; MEiN, Poland; FCT, Portugal; MNE/IFA, Romania; MESTD, Serbia; MSSR, Slovakia; ARRS and MIZŠ, Slovenia; DSI/NRF, South Africa; MICINN, Spain; SRC and Wallenberg Foundation, Sweden; SERI, SNSF and Cantons of Bern and Geneva, Switzerland; MOST, Taipei; TENMAK, Türkiye; STFC, United Kingdom; DOE and NSF, United States of America. In addition, individual groups and members have received support from BCKDF, CANARIE, CRC and DRAC, Canada; PRIMUS 21/SCI/017 and UNCE SCI/013, Czech Republic; COST, ERC, ERDF, Horizon 2020, ICSC-NextGenerationEU and Marie Skłodowska-Curie Actions, European Union; Investissements d’Avenir Labex, Investissements d’Avenir IDEX and ANR, France; DFG and AvH Foundation, Germany; Herakleitos, Thales and Aristeia programmes co-financed by EU-ESF and the Greek NSRF, Greece; BSF-NSF and MINERVA, Israel; Norwegian Financial Mechanism 2014-2021, Norway; NCN and NAWA, Poland; La Caixa Banking Foundation, CERCA Programme Generalitat de Catalunya and PROMETEO and GenT Programmes Generalitat Valenciana, Spain; Göran Gustafssons Stiftelse, Sweden; The Royal Society and Leverhulme Trust, United Kingdom.

The crucial computing support from all WLCG partners is acknowledged gratefully, in particular from CERN, the ATLAS Tier-1 facilities at TRIUMF/SFU (Canada), NDGF (Denmark, Norway, Sweden), CC-IN2P3 (France), KIT/GridKA (Germany), INFN-CNAF (Italy), NL-T1 (Netherlands), PIC (Spain), RAL (UK) and BNL (USA), the Tier-2 facilities worldwide and large non-WLCG resource providers. Major contributors of computing resources are listed in Ref. [102].

References

- [1] P. Minkowski, $\mu \rightarrow e\gamma$ at a Rate of One Out of 10^9 Muon Decays?, *Phys. Lett. B* **67** (1977) 421.
- [2] T. Yanagida, *Horizontal Symmetry and Masses of Neutrinos*, Conf. Proc. **C7902131** (1979) 95.
- [3] M. Gell-Mann, P. Ramond and R. Slansky, *Complex Spinors and Unified Theories*, Conf. Proc. **C790927** (1979) 315, arXiv: [1306.4669](https://arxiv.org/abs/1306.4669) [hep-th].
- [4] S. Weinberg, *Baryon- and Lepton-Nonconserving Processes*, *Phys. Rev. Lett.* **43** (1979) 1566.
- [5] M. Magg and C. Wetterich, *Neutrino Mass Problem and Gauge Hierarchy*, *Phys. Lett. B* **94** (1980) 61.
- [6] T. P. Cheng and L.-F. Li, *Neutrino masses, mixings, and oscillations in $SU(2)\times U(1)$ models of electroweak interactions*, *Phys. Rev. D* **22** (1980) 2860.
- [7] R. N. Mohapatra and G. Senjanović, *Neutrino masses and mixings in gauge models with spontaneous parity violation*, *Phys. Rev. D* **23** (1981) 165.
- [8] R. Foot, H. Lew, X. G. He and G. C. Joshi, *See-saw neutrino masses induced by a triplet of leptons*, *Z. Phys. C* **44** (1989) 441.
- [9] J. C. Pati and A. Salam, *Lepton number as the fourth "color"*, *Phys. Rev. D* **10** (1974) 275, [Erratum: *Phys. Rev. D* **11** (1975) 703].
- [10] R. N. Mohapatra and J. C. Pati, *"Natural" left-right symmetry*, *Phys. Rev. D* **11** (1975) 2558.
- [11] G. Senjanović and R. N. Mohapatra, *Exact left-right symmetry and spontaneous violation of parity*, *Phys. Rev. D* **12** (1975) 1502.
- [12] M. Mitra, R. Ruiz, D. J. Scott and M. Spannowsky, *Neutrino jets from high-mass W_R gauge bosons in TeV-scale left-right symmetric models*, *Physical Review D* **94** (2016), URL: <https://doi.org/10.1103/PhysRevD.94.095016>.
- [13] A. Ferrari et al., *Sensitivity study for new gauge bosons and right-handed Majorana neutrinos in pp collisions at $\sqrt{s} = 14\text{TeV}$* , *Phys. Rev. D* **62** (1 2000) 013001, URL: <https://link.aps.org/doi/10.1103/PhysRevD.62.013001>.
- [14] M. Lindner, F. S. Queiroz, W. Rodejohann and C. E. Yaguna, *Left-Right Symmetry and Lepton Number Violation at the Large Hadron Electron Collider*, *JHEP* **06** (2016) 140, arXiv: [1604.08596](https://arxiv.org/abs/1604.08596) [hep-ph].
- [15] S. S. Biswal and P. S. B. Dev, *Probing left-right seesaw models using beam polarization at an e^+e^- collider*, *Phys. Rev. D* **95** (2017) 115031, arXiv: [1701.08751](https://arxiv.org/abs/1701.08751) [hep-ph].
- [16] S. Bertolini, A. Maiezza and F. Nesti, *Present and Future K and B Meson Mixing Constraints on TeV Scale Left-Right Symmetry*, *Phys. Rev. D* **89** (2014) 095028, arXiv: [1403.7112](https://arxiv.org/abs/1403.7112) [hep-ph].
- [17] A. Maiezza and M. Nemevšek, *Strong P invariance, neutron electric dipole moment, and minimal left-right parity at LHC*, *Phys. Rev. D* **90** (2014) 095002, arXiv: [1407.3678](https://arxiv.org/abs/1407.3678) [hep-ph].
- [18] M. Agostini et al., *Final Results of GERDA on the Search for Neutrinoless Double- β Decay*, *Phys. Rev. Lett.* **125** (2020) 252502, arXiv: [2009.06079](https://arxiv.org/abs/2009.06079) [nucl-ex].

- [19] S. Abe et al., *Search for the Majorana Nature of Neutrinos in the Inverted Mass Ordering Region with KamLAND-Zen*, *Phys. Rev. Lett.* **130** (2023) 051801, arXiv: 2203.02139 [hep-ex].
- [20] ATLAS Collaboration, *Search for heavy Majorana neutrinos with the ATLAS detector in pp collisions at $\sqrt{s} = 8$ TeV*, *JHEP* **07** (2015) 162, arXiv: 1506.06020 [hep-ex].
- [21] ATLAS Collaboration, *Search for heavy Majorana or Dirac neutrinos and right-handed W gauge bosons in final states with two charged leptons and two jets at $\sqrt{s} = 13$ TeV with the ATLAS detector*, *JHEP* **01** (2019) 016, arXiv: 1809.11105 [hep-ex].
- [22] ATLAS Collaboration, *Search for a right-handed gauge boson decaying into a high-momentum heavy neutrino and a charged lepton in pp collisions with the ATLAS detector at $\sqrt{s} = 13$ TeV*, *Phys. Lett. B* **798** (2019) 134942, arXiv: 1904.12679 [hep-ex].
- [23] CMS Collaboration, *Search for heavy neutrinos and W_R bosons with right-handed couplings in a left-right symmetric model in pp collisions at $\sqrt{s} = 7$ TeV*, *Phys. Rev. Lett.* **109** (2012) 261802, arXiv: 1210.2402 [hep-ex].
- [24] CMS Collaboration, *Search for a heavy right-handed W boson and a heavy neutrino in events with two same-flavor leptons and two jets at $\sqrt{s} = 13$ TeV*, *JHEP* **05** (2018) 148, arXiv: 1803.11116 [hep-ex].
- [25] CMS Collaboration, *Search for heavy neutrinos and third-generation leptoquarks in hadronic states of two τ leptons and two jets in proton–proton collisions at $\sqrt{s} = 13$ TeV*, *JHEP* **03** (2019) 170, arXiv: 1811.00806 [hep-ex].
- [26] CMS Collaboration, *Search for heavy Majorana neutrinos in same-sign dilepton channels in proton–proton collisions at $\sqrt{s} = 13$ TeV*, *JHEP* **01** (2019) 122, arXiv: 1806.10905 [hep-ex].
- [27] CMS Collaboration, *Search for a right-handed W boson and a heavy neutrino in proton–proton collisions at $\sqrt{s} = 13$ TeV*, *JHEP* **04** (2022) 047, arXiv: 2112.03949 [hep-ex].
- [28] R. N. Mohapatra, *Mechanism for understanding small neutrino mass in superstring theories*, *Phys. Rev. Lett.* **56** (1986) 561.
- [29] R. N. Mohapatra and J. W. F. Valle, *Neutrino mass and baryon-number nonconservation in superstring models*, *Phys. Rev. D* **34** (1986) 1642.
- [30] C.-Y. Chen and P. S. B. Dev, *Multilepton collider signatures of heavy Dirac and Majorana neutrinos*, *Phys. Rev. D* **85** (2012) 093018, arXiv: 1112.6419 [hep-ph].
- [31] P. S. Bhupal Dev and R. N. Mohapatra, *Unified Explanation of the $eejj$, Diboson and Dijet Resonances at the LHC*, *Phys. Rev. Lett.* **115** (2015) 181803, arXiv: 1508.02277 [hep-ph].
- [32] L. Wolfenstein, *Different Varieties of Massive Dirac Neutrinos*, *Nucl. Phys. B* **186** (1981) 147.
- [33] A. Das, P. S. B. Dev and R. N. Mohapatra, *Same Sign versus Opposite Sign Dileptons as a Probe of Low Scale Seesaw Mechanisms*, *Phys. Rev. D* **97** (2018) 015018, arXiv: 1709.06553 [hep-ph].
- [34] ATLAS Collaboration, *The ATLAS Experiment at the CERN Large Hadron Collider*, *JINST* **3** (2008) S08003.

- [35] ATLAS Collaboration, *The ATLAS Collaboration Software and Firmware*, ATL-SOFT-PUB-2021-001, 2021, URL: <https://cds.cern.ch/record/2767187>.
- [36] ATLAS Collaboration, *ATLAS data quality operations and performance for 2015–2018 data-taking*, *JINST* **15** (2020) P04003, arXiv: 1911.04632 [physics.ins-det].
- [37] ATLAS Collaboration, *Selection of jets produced in 13 TeV proton–proton collisions with the ATLAS detector*, ATL-CONF-2015-029, 2015, URL: <https://cds.cern.ch/record/2037702>.
- [38] ATLAS Collaboration, *Vertex Reconstruction Performance of the ATLAS Detector at $\sqrt{s} = 13$ TeV*, ATL-PHYS-PUB-2015-026, 2015, URL: <https://cds.cern.ch/record/2037717>.
- [39] ATLAS Collaboration, *Reconstruction of primary vertices at the ATLAS experiment in Run 1 proton–proton collisions at the LHC*, *Eur. Phys. J. C* **77** (2017) 332, arXiv: 1611.10235 [hep-ex].
- [40] ATLAS Collaboration, *Performance of the ATLAS muon triggers in Run 2*, *JINST* **15** (2020) P09015, arXiv: 2004.13447 [physics.ins-det].
- [41] ATLAS Collaboration, *Performance of electron and photon triggers in ATLAS during LHC Run 2*, *Eur. Phys. J. C* **80** (2020) 47, arXiv: 1909.00761 [hep-ex].
- [42] S. Agostinelli et al., *Geant4—a simulation toolkit*, *Nuclear Instruments and Methods in Physics Research Section A: Accelerators, Spectrometers, Detectors and Associated Equipment* **506** (2003) 250, ISSN: 0168-9002.
- [43] ATLAS Collaboration, *The ATLAS Simulation Infrastructure*, *Eur. Phys. J. C* **70** (2010) 823, arXiv: 1005.4568 [physics.ins-det].
- [44] T. Sjöstrand et al., *An introduction to PYTHIA 8.2*, *Comput. Phys. Commun.* **191** (2015) 159, arXiv: 1410.3012 [hep-ph].
- [45] ATLAS Collaboration, *The Pythia 8 A3 tune description of ATLAS minimum bias and inelastic measurements incorporating the Donnachie–Landshoff diffractive model*, ATL-PHYS-PUB-2016-017, 2016, URL: <https://cds.cern.ch/record/2206965>.
- [46] NNPDF Collaboration, R. D. Ball et al., *Parton distributions with LHC data*, *Nucl. Phys. B* **867** (2013) 244, arXiv: 1207.1303 [hep-ph].
- [47] ATLAS Collaboration, *Measurement of the production of a W boson in association with a charmed hadron in pp collisions at $\sqrt{s} = 13$ TeV with the ATLAS detector*, (2023), arXiv: 2302.00336 [hep-ex].
- [48] *Modelling and computational improvements to the simulation of single vector-boson plus jet processes for the ATLAS experiment*, *JHEP* **2208** (2022) 089, arXiv: 2112.09588, URL: <https://cds.cern.ch/record/2798348>.
- [49] ATLAS Collaboration, *Studies on top-quark Monte Carlo modelling with Sherpa and MG5_aMC@NLO*, ATL-PHYS-PUB-2017-007, 2017, URL: <https://cds.cern.ch/record/2261938>.
- [50] *Prospects for the $\mathcal{B}(B_{(s)}^0 \rightarrow \mu^+ \mu^-)$ measurements with the ATLAS detector in the Run 2 and HL-LHC data campaigns*, tech. rep., All figures including auxiliary figures are available at <https://atlas.web.cern.ch/Atlas/GROUPS/PHYSICS/PUBNOTES/ATL-PHYS-PUB-2018-005>: CERN, 2018, URL: <https://cds.cern.ch/record/2317211>.

- [51] A. Alloul, N. D. Christensen, C. Degrande, C. Duhr and B. Fuks, *FeynRules 2.0 — A complete toolbox for tree-level phenomenology*, *Comput. Phys. Commun.* **185** (2014) 2250, arXiv: [1310.1921 \[hep-ph\]](#).
- [52] J. Alwall et al., *The automated computation of tree-level and next-to-leading order differential cross sections, and their matching to parton shower simulations*, *JHEP* **2014** (2014), arXiv: [1405.0301 \[hep-ph\]](#).
- [53] M. Nemevšek, F. Nesti and G. Popara, *Keung-Senjanović process at the LHC: From lepton number violation to displaced vertices to invisible decays*, *Phys. Rev. D* **97** (2018) 115018, arXiv: [1801.05813 \[hep-ph\]](#).
- [54] ATLAS Collaboration, *ATLAS Pythia 8 tunes to 7 TeV data*, ATL-PHYS-PUB-2014-021, 2014, URL: <https://cds.cern.ch/record/1966419>.
- [55] NNPDF Collaboration, R. D. Ball et al., *Parton distributions for the LHC run II*, *JHEP* **04** (2015) 040, arXiv: [1410.8849 \[hep-ph\]](#).
- [56] E. Bothmann et al., *Event generation with Sherpa 2.2*, *SciPost Phys.* **7** (2019) 034, arXiv: [1905.09127 \[hep-ph\]](#).
- [57] S. Schumann and F. Krauss, *A parton shower algorithm based on Catani–Seymour dipole factorisation*, *JHEP* **03** (2008) 038, arXiv: [0709.1027 \[hep-ph\]](#).
- [58] C. Anastasiou, L. Dixon, K. Melnikov and F. Petriello, *High-precision QCD at hadron colliders: Electroweak gauge boson rapidity distributions at next-to-next-to leading order*, *Phys. Rev. D* **69** (2004) 094008, arXiv: [hep-ph/0312266](#).
- [59] S. Frixione, G. Ridolfi and P. Nason, *A positive-weight next-to-leading-order Monte Carlo for heavy flavour hadroproduction*, *JHEP* **09** (2007) 126, arXiv: [0707.3088 \[hep-ph\]](#).
- [60] P. Nason, *A new method for combining NLO QCD with shower Monte Carlo algorithms*, *JHEP* **11** (2004) 040, arXiv: [hep-ph/0409146](#).
- [61] S. Frixione, P. Nason and C. Oleari, *Matching NLO QCD computations with parton shower simulations: the POWHEG method*, *JHEP* **11** (2007) 070, arXiv: [0709.2092 \[hep-ph\]](#).
- [62] S. Alioli, P. Nason, C. Oleari and E. Re, *A general framework for implementing NLO calculations in shower Monte Carlo programs: the POWHEG BOX*, *JHEP* **06** (2010) 043, arXiv: [1002.2581 \[hep-ph\]](#).
- [63] M. Beneke, P. Falgari, S. Klein and C. Schwinn, *Hadronic top-quark pair production with NNLL threshold resummation*, *Nucl. Phys. B* **855** (2012) 695, arXiv: [1109.1536 \[hep-ph\]](#).
- [64] M. Cacciari, M. Czakon, M. Mangano, A. Mitov and P. Nason, *Top-pair production at hadron colliders with next-to-next-to-leading logarithmic soft-gluon resummation*, *Phys. Lett. B* **710** (2012) 612, arXiv: [1111.5869 \[hep-ph\]](#).
- [65] P. Bärnreuther, M. Czakon and A. Mitov, *Percent-Level-Precision Physics at the Tevatron: Next-to-Next-to-Leading Order QCD Corrections to $q\bar{q} \rightarrow t\bar{t} + X$* , *Phys. Rev. Lett.* **109** (2012) 132001, arXiv: [1204.5201 \[hep-ph\]](#).

- [66] M. Czakon and A. Mitov, *NNLO corrections to top-pair production at hadron colliders: the all-fermionic scattering channels*, *JHEP* **12** (2012) 054, arXiv: [1207.0236 \[hep-ph\]](#).
- [67] M. Czakon and A. Mitov, *NNLO corrections to top pair production at hadron colliders: the quark-gluon reaction*, *JHEP* **01** (2013) 080, arXiv: [1210.6832 \[hep-ph\]](#).
- [68] M. Czakon, P. Fiedler and A. Mitov, *Total Top-Quark Pair-Production Cross Section at Hadron Colliders Through $O(\alpha_S^4)$* , *Phys. Rev. Lett.* **110** (2013) 252004, arXiv: [1303.6254 \[hep-ph\]](#).
- [69] M. Czakon and A. Mitov, *Top++: A program for the calculation of the top-pair cross-section at hadron colliders*, *Comput. Phys. Commun.* **185** (2014) 2930, arXiv: [1112.5675 \[hep-ph\]](#).
- [70] M. Chiesa, C. Oleari and E. Re, *NLO QCD+NLO EW corrections to diboson production matched to parton shower*, *The European Physical Journal C* **80** (2020), URL: <https://doi.org/10.1140%2Fepjc%2Fs10052-020-8419-3>.
- [71] S. Kallweit, V. Sotnikov and M. Wiesemann, *Triphoton production at hadron colliders in NNLO QCD*, *Physics Letters B* **812** (2021) 136013, ISSN: 0370-2693, URL: <https://www.sciencedirect.com/science/article/pii/S0370269320308169>.
- [72] ATLAS Collaboration, *Electron and photon performance measurements with the ATLAS detector using the 2015–2017 LHC proton–proton collision data*, *JINST* **14** (2019) P12006, arXiv: [1908.00005 \[hep-ex\]](#).
- [73] ATLAS Collaboration, *Muon reconstruction performance of the ATLAS detector in proton–proton collision data at $\sqrt{s} = 13$ TeV*, *Eur. Phys. J. C* **76** (2016) 292, arXiv: [1603.05598 \[hep-ex\]](#).
- [74] ATLAS Collaboration, *Jet reconstruction and performance using particle flow with the ATLAS Detector*, *Eur. Phys. J. C* **77** (2017) 466, arXiv: [1703.10485 \[hep-ex\]](#).
- [75] M. Cacciari, G. P. Salam and G. Soyez, *The anti- k_t jet clustering algorithm*, *JHEP* **04** (2008) 063, arXiv: [0802.1189 \[hep-ph\]](#).
- [76] M. Cacciari, G. P. Salam and G. Soyez, *FastJet user manual*, *Eur. Phys. J. C* **72** (2012) 1896, arXiv: [1111.6097 \[hep-ph\]](#).
- [77] ATLAS Collaboration, *Jet energy scale and resolution measured in proton–proton collisions at $\sqrt{s} = 13$ TeV with the ATLAS detector*, *Eur. Phys. J. C* **81** (2021) 689, arXiv: [2007.02645 \[hep-ex\]](#).
- [78] ATLAS Collaboration, *Performance of pile-up mitigation techniques for jets in pp collisions at $\sqrt{s} = 8$ TeV using the ATLAS detector*, *Eur. Phys. J. C* **76** (2016) 581, arXiv: [1510.03823 \[hep-ex\]](#).
- [79] ATLAS Collaboration, *ATLAS b-jet identification performance and efficiency measurement with $t\bar{t}$ events in pp collisions at $\sqrt{s} = 13$ TeV*, *Eur. Phys. J. C* **79** (2019) 970, arXiv: [1907.05120 \[hep-ex\]](#).
- [80] ATLAS Collaboration, *Optimisation and performance studies of the ATLAS b-tagging algorithms for the 2017-18 LHC run*, ATL-PHYS-PUB-2017-013, 2017, URL: <https://cds.cern.ch/record/2273281>.

- [81] ATLAS Collaboration, *Performance of missing transverse momentum reconstruction with the ATLAS detector using proton–proton collisions at $\sqrt{s} = 13$ TeV*, *Eur. Phys. J. C* **78** (2018) 903, arXiv: 1802.08168 [hep-ex].
- [82] ATLAS Collaboration, *E_T^{miss} performance in the ATLAS detector using 2015–2016 LHC pp collisions*, ATLAS-CONF-2018-023, 2018, URL: <https://cds.cern.ch/record/2625233>.
- [83] ATLAS Collaboration, *Electron reconstruction and identification in the ATLAS experiment using the 2015 and 2016 LHC proton–proton collision data at $\sqrt{s} = 13$ TeV*, *Eur. Phys. J. C* **79** (2019) 639, arXiv: 1902.04655 [physics.ins-det].
- [84] ATLAS Collaboration, *Search for type-III seesaw heavy leptons in dilepton final states in pp collisions at $\sqrt{s} = 13$ TeV with the ATLAS detector*, *Eur. Phys. J. C* **81** (2021) 218, arXiv: 2008.07949 [hep-ex].
- [85] ATLAS Collaboration, *Luminosity determination in pp collisions at $\sqrt{s} = 13$ TeV using the ATLAS detector at the LHC*, ATLAS-CONF-2019-021, 2019, URL: <https://cds.cern.ch/record/2677054>.
- [86] G. Avoni et al., *The new LUCID-2 detector for luminosity measurement and monitoring in ATLAS*, *JINST* **13** (2018) P07017.
- [87] ATLAS Collaboration, *Measurement of the Inelastic Proton–Proton Cross Section at $\sqrt{s} = 13$ TeV with the ATLAS Detector at the LHC*, *Phys. Rev. Lett.* **117** (2016) 182002, arXiv: 1606.02625 [hep-ex].
- [88] ATLAS Collaboration, *Muon reconstruction and identification efficiency in ATLAS using the full Run 2 pp collision data set at $\sqrt{s} = 13$ TeV*, *Eur. Phys. J. C* **81** (2021) 578, arXiv: 2012.00578 [hep-ex].
- [89] ATLAS Collaboration, *Measurement of the c -jet mistagging efficiency in $t\bar{t}$ events using pp collision data at $\sqrt{s} = 13$ TeV collected with the ATLAS detector*, *Eur. Phys. J. C* **82** (2022) 95, arXiv: 2109.10627 [hep-ex].
- [90] ATLAS Collaboration, *Electron reconstruction and identification in the ATLAS experiment using the 2015 and 2016 LHC proton–proton collision data at $\sqrt{s} = 13$ TeV*, *The European Physical Journal C* **79** (2019), URL: <https://doi.org/10.1140%2Fepjc%2Fs10052-019-7140-6>.
- [91] J. Butterworth et al., *PDF4LHC recommendations for LHC Run II*, *J. Phys. G* **43** (2016) 023001, arXiv: 1510.03865 [hep-ph].
- [92] L. A. Harland-Lang, A. D. Martin, P. Motylinski and R. S. Thorne, *Parton distributions in the LHC era: MMHT 2014 PDFs*, *Eur. Phys. J. C* **75** (2015), arXiv: 1412.3989 [hep-ph].
- [93] S. Dulat et al., *New parton distribution functions from a global analysis of quantum chromodynamics*, *Phys. Rev. D* **93** (2016) 033006, arXiv: 1506.07443 [hep-ph].
- [94] T. Sjöstrand, S. Mrenna and P. Skands, *A brief introduction to PYTHIA 8.1*, *Computer Physics Communications* **178** (2008) 852, URL: <https://doi.org/10.1016%2Fj.cpc.2008.01.036>.
- [95] M. Bähr et al., *Herwig++ physics and manual*, *Eur. Phys. J. C* **58** (2008) 639, arXiv: 0803.0883 [hep-ph].

- [96] J. Pumplin et al.,
New Generation of Parton Distributions with Uncertainties from Global QCD Analysis,
[JHEP **2002** \(2002\) 012](#), arXiv: [0201195 \[hep-ph\]](#).
- [97] A. D. Martin, W. J. Stirling, R. S. Thorne and G. Watt, *Parton distributions for the LHC*,
[Eur. Phys. J. C **63** \(2009\) 189](#), arXiv: [0901.0002 \[hep-ph\]](#).
- [98] A. Kalogeropoulos and J. Alwall,
The SysCalc code: A tool to derive theoretical systematic uncertainties, (2018),
arXiv: [1801.08401 \[hep-ph\]](#).
- [99] M. Baak et al., *HistFitter software framework for statistical data analysis*,
[Eur. Phys. J. C **75** \(2015\) 153](#), arXiv: [1410.1280 \[hep-ex\]](#).
- [100] A. L. Read, *Presentation of search results: the CLs technique*, [J. Phys. G **28** \(2002\) 2693](#).
- [101] G. Cowan, K. Cranmer, E. Gross and O. Vitells,
Asymptotic formulae for likelihood-based tests of new physics, [Eur. Phys. J. C **71** \(2011\) 1554](#),
arXiv: [1007.1727 \[physics.data-an\]](#).
- [102] ATLAS Collaboration, *ATLAS Computing Acknowledgements*, ATL-SOFT-PUB-2023-001, 2023,
URL: <https://cds.cern.ch/record/2869272>.

The ATLAS Collaboration

G. Aad ¹⁰², B. Abbott ¹²⁰, K. Abeling ⁵⁵, N.J. Abicht ⁴⁹, S.H. Abidi ²⁹, A. Aboulhorma ^{35e}, H. Abramowicz ¹⁵¹, H. Abreu ¹⁵⁰, Y. Abulaiti ¹¹⁷, A.C. Abusleme Hoffman ^{137a}, B.S. Acharya ^{69a,69b,n}, C. Adam Bourdarios ⁴, L. Adamczyk ^{85a}, L. Adamek ¹⁵⁵, S.V. Addepalli ²⁶, M.J. Addison ¹⁰¹, J. Adelman ¹¹⁵, A. Adiguzel ^{21c}, T. Abye ¹³⁴, A.A. Affolder ¹³⁶, Y. Afik ³⁶, M.N. Agaras ¹³, J. Agarwala ^{73a,73b}, A. Aggarwal ¹⁰⁰, C. Agheorghiesei ^{27c}, A. Ahmad ³⁶, F. Ahmadov ^{38,z}, W.S. Ahmed ¹⁰⁴, S. Ahuja ⁹⁵, X. Ai ^{62a}, G. Aielli ^{76a,76b}, M. Ait Tamliah ^{35e}, B. Aitbenkikh ^{35a}, I. Aizenberg ¹⁶⁹, M. Akbiyik ¹⁰⁰, T.P.A. Åkesson ⁹⁸, A.V. Akimov ³⁷, D. Akiyama ¹⁶⁸, N.N. Akolkar ²⁴, K. Al Houry ⁴¹, G.L. Alberghi ^{23b}, J. Albert ¹⁶⁵, P. Albicocco ⁵³, G.L. Albouy ⁶⁰, S. Alderweireldt ⁵², M. Aleksa ³⁶, I.N. Aleksandrov ³⁸, C. Alexa ^{27b}, T. Alexopoulos ¹⁰, A. Alfonsi ¹¹⁴, F. Alfonsi ^{23b}, M. Algren ⁵⁶, M. Alhroob ¹²⁰, B. Ali ¹³², H.M.J. Ali ⁹¹, S. Ali ¹⁴⁸, S.W. Alibocus ⁹², M. Aliev ³⁷, G. Alimonti ^{71a}, W. Alkahi ⁵⁵, C. Allaire ⁶⁶, B.M.M. Allbrooke ¹⁴⁶, J.F. Allen ⁵², C.A. Allendes Flores ^{137f}, P.P. Allport ²⁰, A. Aloisio ^{72a,72b}, F. Alonso ⁹⁰, C. Alpigiani ¹³⁸, M. Alvarez Estevez ⁹⁹, A. Alvarez Fernandez ¹⁰⁰, M.G. Alvigi ^{72a,72b}, M. Aly ¹⁰¹, Y. Amaral Coutinho ^{82b}, A. Ambler ¹⁰⁴, C. Amelung ³⁶, M. Amerl ¹⁰¹, C.G. Ames ¹⁰⁹, D. Amidei ¹⁰⁶, S.P. Amor Dos Santos ^{130a}, K.R. Amos ¹⁶³, V. Ananiev ¹²⁵, C. Anastopoulos ¹³⁹, T. Andeen ¹¹, J.K. Anders ³⁶, S.Y. Andrean ^{47a,47b}, A. Andreazza ^{71a,71b}, S. Angelidakis ⁹, A. Angerami ^{41,ac}, A.V. Anisenkov ³⁷, A. Annovi ^{74a}, C. Antel ⁵⁶, M.T. Anthony ¹³⁹, E. Antipov ¹⁴⁵, M. Antonelli ⁵³, D.J.A. Antrim ^{17a}, F. Anulli ^{75a}, M. Aoki ⁸³, T. Aoki ¹⁵³, J.A. Aparisi Pozo ¹⁶³, M.A. Aparo ¹⁴⁶, L. Aperio Bella ⁴⁸, C. Appelt ¹⁸, N. Aranzabal ³⁶, C. Arcangeletti ⁵³, A.T.H. Arce ⁵¹, E. Arena ⁹², J-F. Arguin ¹⁰⁸, S. Argyropoulos ⁵⁴, J.-H. Arling ⁴⁸, A.J. Armbruster ³⁶, O. Arnaez ⁴, H. Arnold ¹¹⁴, Z.P. Arrubarrena Tame ¹⁰⁹, G. Artoni ^{75a,75b}, H. Asada ¹¹¹, K. Asai ¹¹⁸, S. Asai ¹⁵³, N.A. Asbah ⁶¹, J. Assahsah ^{35d}, K. Assamagan ²⁹, R. Astalos ^{28a}, S. Atashi ¹⁶⁰, R.J. Atkin ^{33a}, M. Atkinson ¹⁶², N.B. Atlay ¹⁸, H. Atmani ^{62b}, P.A. Atmasiddha ¹⁰⁶, K. Augsten ¹³², S. Auricchio ^{72a,72b}, A.D. Auriol ²⁰, V.A. Austrup ¹⁰¹, G. Avolio ³⁶, K. Axiotis ⁵⁶, G. Azuelos ^{108,ag}, D. Babal ^{28b}, H. Bachacou ¹³⁵, K. Bachas ^{152,q}, A. Bachi ³⁴, F. Backman ^{47a,47b}, A. Badea ⁶¹, P. Bagnaia ^{75a,75b}, M. Bahmani ¹⁸, A.J. Bailey ¹⁶³, V.R. Bailey ¹⁶², J.T. Baines ¹³⁴, L. Baines ⁹⁴, C. Bakalis ¹⁰, O.K. Baker ¹⁷², E. Bakos ¹⁵, D. Bakshi Gupta ⁸, R. Balasubramanian ¹¹⁴, E.M. Baldin ³⁷, P. Balek ^{85a}, E. Ballabene ^{23b,23a}, F. Balli ¹³⁵, L.M. Baltes ^{63a}, W.K. Balunas ³², J. Balz ¹⁰⁰, E. Banas ⁸⁶, M. Bandieramonte ¹²⁹, A. Bandyopadhyay ²⁴, S. Bansal ²⁴, L. Barak ¹⁵¹, M. Barakat ⁴⁸, E.L. Barberio ¹⁰⁵, D. Barberis ^{57b,57a}, M. Barbero ¹⁰², G. Barbour ⁹⁶, K.N. Barends ^{33a}, T. Barillari ¹¹⁰, M-S. Barisits ³⁶, T. Barklow ¹⁴³, P. Baron ¹²², D.A. Baron Moreno ¹⁰¹, A. Baroncelli ^{62a}, G. Barone ²⁹, A.J. Barr ¹²⁶, J.D. Barr ⁹⁶, L. Barranco Navarro ^{47a,47b}, F. Barreiro ⁹⁹, J. Barreiro Guimarães da Costa ^{14a}, U. Barron ¹⁵¹, M.G. Barros Teixeira ^{130a}, S. Barsov ³⁷, F. Bartels ^{63a}, R. Bartoldus ¹⁴³, A.E. Barton ⁹¹, P. Bartos ^{28a}, A. Basan ¹⁰⁰, M. Baselga ⁴⁹, A. Bassalat ^{66,b}, M.J. Basso ^{156a}, C.R. Basson ¹⁰¹, R.L. Bates ⁵⁹, S. Batlamous ^{35e}, J.R. Batley ³², B. Batool ¹⁴¹, M. Battaglia ¹³⁶, D. Battulga ¹⁸, M. Baucé ^{75a,75b}, M. Bauer ³⁶, P. Bauer ²⁴, L.T. Bazzano Hurrell ³⁰, J.B. Beacham ⁵¹, T. Beau ¹²⁷, P.H. Beauchemin ¹⁵⁸, F. Becherer ⁵⁴, P. Bechtel ²⁴, H.P. Beck ^{19,p}, K. Becker ¹⁶⁷, A.J. Beddall ^{21d}, V.A. Bednyakov ³⁸, C.P. Bee ¹⁴⁵, L.J. Beemster ¹⁵, T.A. Beermann ³⁶, M. Begalli ^{82d}, M. Beger ²⁹, A. Behera ¹⁴⁵, J.K. Behr ⁴⁸, J.F. Beirer ⁵⁵, F. Beisiegel ²⁴, M. Belfkir ¹⁵⁹, G. Bella ¹⁵¹, L. Bellagamba ^{23b}, A. Bellerive ³⁴, P. Bellos ²⁰, K. Beloborodov ³⁷, N.L. Belyaev ³⁷, D. Benchekroun ^{35a}, F. Bendebba ^{35a},

Y. Benhammou [ID151](#), M. Benoit [ID29](#), J.R. Bensingler [ID26](#), S. Bentvelsen [ID114](#), L. Beresford [ID48](#),
 M. Beretta [ID53](#), E. Bergeaas Kuutmann [ID161](#), N. Berger [ID4](#), B. Bergmann [ID132](#), J. Beringer [ID17a](#),
 G. Bernardi [ID5](#), C. Bernius [ID143](#), F.U. Bernlochner [ID24](#), F. Bernon [ID36,102](#), T. Berry [ID95](#), P. Berta [ID133](#),
 A. Berthold [ID50](#), I.A. Bertram [ID91](#), S. Bethke [ID110](#), A. Betti [ID75a,75b](#), A.J. Bevan [ID94](#), M. Bhamjee [ID33c](#),
 S. Bhatta [ID145](#), D.S. Bhattacharya [ID166](#), P. Bhattarai [ID26](#), V.S. Bhopatkar [ID121](#), R. Bi [ID29,ai](#),
 R.M. Bianchi [ID129](#), G. Bianco [ID23b,23a](#), O. Biebel [ID109](#), R. Bielski [ID123](#), M. Biglietti [ID77a](#),
 T.R.V. Billoud [ID132](#), M. Bindi [ID55](#), A. Bingul [ID21b](#), C. Bini [ID75a,75b](#), A. Biondini [ID92](#),
 C.J. Birch-sykes [ID101](#), G.A. Bird [ID20,134](#), M. Birman [ID169](#), M. Biros [ID133](#), T. Bisanz [ID49](#),
 E. Bisceglie [ID43b,43a](#), D. Biswas [ID141](#), A. Bitadze [ID101](#), K. Bjørke [ID125](#), I. Bloch [ID48](#), C. Blocker [ID26](#),
 A. Blue [ID59](#), U. Blumenschein [ID94](#), J. Blumenthal [ID100](#), G.J. Bobbink [ID114](#), V.S. Bobrovnikov [ID37](#),
 M. Boehler [ID54](#), B. Boehm [ID166](#), D. Bogavac [ID36](#), A.G. Bogdanchikov [ID37](#), C. Bohm [ID47a](#),
 V. Boisvert [ID95](#), P. Bokan [ID48](#), T. Bold [ID85a](#), M. Bomben [ID5](#), M. Bona [ID94](#), M. Boonekamp [ID135](#),
 C.D. Booth [ID95](#), A.G. Borbély [ID59](#), I.S. Bordulev [ID37](#), H.M. Borecka-Bielska [ID108](#), L.S. Borgna [ID96](#),
 G. Borissov [ID91](#), D. Bortoletto [ID126](#), D. Boscherini [ID23b](#), M. Bosman [ID13](#), J.D. Bossio Sola [ID36](#),
 K. Bouaouda [ID35a](#), N. Bouchhar [ID163](#), J. Boudreau [ID129](#), E.V. Bouhova-Thacker [ID91](#), D. Boumediene [ID40](#),
 R. Bouquet [ID5](#), A. Boveia [ID119](#), J. Boyd [ID36](#), D. Boye [ID29](#), I.R. Boyko [ID38](#), J. Bracinik [ID20](#),
 N. Brahim [ID62d](#), G. Brandt [ID171](#), O. Brandt [ID32](#), F. Braren [ID48](#), B. Brau [ID103](#), J.E. Brau [ID123](#),
 R. Brenner [ID169](#), L. Brenner [ID114](#), R. Brenner [ID161](#), S. Bressler [ID169](#), D. Britton [ID59](#), D. Britzger [ID110](#),
 I. Brock [ID24](#), G. Brooijmans [ID41](#), W.K. Brooks [ID137f](#), E. Brost [ID29](#), L.M. Brown [ID165](#), L.E. Bruce [ID61](#),
 T.L. Bruckler [ID126](#), P.A. Bruckman de Renstrom [ID86](#), B. Brüers [ID48](#), D. Bruncko [ID28b,*](#), A. Bruni [ID23b](#),
 G. Bruni [ID23b](#), M. Bruschi [ID23b](#), N. Bruscano [ID75a,75b](#), T. Buanes [ID16](#), Q. Buat [ID138](#), D. Buchin [ID110](#),
 A.G. Buckley [ID59](#), M.K. Bugge [ID125](#), O. Bulekov [ID37](#), B.A. Bullard [ID143](#), S. Burdin [ID92](#),
 C.D. Burgard [ID49](#), A.M. Burger [ID40](#), B. Burghgrave [ID8](#), O. Burlayenko [ID54](#), J.T.P. Burr [ID32](#),
 C.D. Burton [ID11](#), J.C. Burzynski [ID142](#), E.L. Busch [ID41](#), V. Büscher [ID100](#), P.J. Bussey [ID59](#),
 J.M. Butler [ID25](#), C.M. Buttar [ID59](#), J.M. Butterworth [ID96](#), W. Buttinger [ID134](#), C.J. Buxo Vazquez [ID107](#),
 A.R. Buzykaev [ID37](#), G. Cabras [ID23b](#), S. Cabrera Urbán [ID163](#), D. Caforio [ID58](#), H. Cai [ID129](#), Y. Cai [ID14a,14e](#),
 V.M.M. Cairo [ID36](#), O. Cakir [ID3a](#), N. Calace [ID36](#), P. Calafiura [ID17a](#), G. Calderini [ID127](#), P. Calfayan [ID68](#),
 G. Callea [ID59](#), L.P. Caloba [ID82b](#), D. Calvet [ID40](#), S. Calvet [ID40](#), T.P. Calvet [ID102](#), M. Calvetti [ID74a,74b](#),
 R. Camacho Toro [ID127](#), S. Camarda [ID36](#), D. Camarero Munoz [ID26](#), P. Camarri [ID76a,76b](#),
 M.T. Camerlingo [ID72a,72b](#), D. Cameron [ID125](#), C. Camincher [ID165](#), M. Campanelli [ID96](#), A. Camplani [ID42](#),
 V. Canale [ID72a,72b](#), A. Canesse [ID104](#), M. Cano Bret [ID80](#), J. Cantero [ID163](#), Y. Cao [ID162](#), F. Capocasa [ID26](#),
 M. Capua [ID43b,43a](#), A. Carbone [ID71a,71b](#), R. Cardarelli [ID76a](#), J.C.J. Cardenas [ID8](#), F. Cardillo [ID163](#),
 T. Carli [ID36](#), G. Carlino [ID72a](#), J.I. Carlotto [ID13](#), B.T. Carlson [ID129,r](#), E.M. Carlson [ID165,156a](#),
 L. Carminati [ID71a,71b](#), A. Carnelli [ID135](#), M. Carnesale [ID75a,75b](#), S. Caron [ID113](#), E. Carquin [ID137f](#),
 S. Carrá [ID71a,71b](#), G. Carratta [ID23b,23a](#), F. Carrio Argos [ID33g](#), J.W.S. Carter [ID155](#), T.M. Carter [ID52](#),
 M.P. Casado [ID13,i](#), M. Caspar [ID48](#), E.G. Castiglia [ID172](#), F.L. Castillo [ID4](#), L. Castillo Garcia [ID13](#),
 V. Castillo Gimenez [ID163](#), N.F. Castro [ID130a,130e](#), A. Catinaccio [ID36](#), J.R. Catmore [ID125](#), V. Cavaliere [ID29](#),
 N. Cavalli [ID23b,23a](#), V. Cavalanni [ID74a,74b](#), Y.C. Cekmecelioglu [ID48](#), E. Celebi [ID21a](#), F. Celli [ID126](#),
 M.S. Centonze [ID70a,70b](#), K. Cerny [ID122](#), A.S. Cerqueira [ID82a](#), A. Cerri [ID146](#), L. Cerrito [ID76a,76b](#),
 F. Cerutti [ID17a](#), B. Cervato [ID141](#), A. Cervelli [ID23b](#), G. Cesarini [ID53](#), S.A. Cetin [ID21d](#), Z. Chadi [ID35a](#),
 D. Chakraborty [ID115](#), M. Chala [ID130f](#), J. Chan [ID170](#), W.Y. Chan [ID153](#), J.D. Chapman [ID32](#),
 E. Chapon [ID135](#), B. Chargeishvili [ID149b](#), D.G. Charlton [ID20](#), T.P. Charman [ID94](#), M. Chatterjee [ID19](#),
 C. Chauhan [ID133](#), S. Chekanov [ID6](#), S.V. Chekulaev [ID156a](#), G.A. Chelkov [ID38,a](#), A. Chen [ID106](#),
 B. Chen [ID151](#), B. Chen [ID165](#), H. Chen [ID14c](#), H. Chen [ID29](#), J. Chen [ID62c](#), J. Chen [ID142](#), M. Chen [ID126](#),
 S. Chen [ID153](#), S.J. Chen [ID14c](#), X. Chen [ID62c](#), X. Chen [ID14b,af](#), Y. Chen [ID62a](#), C.L. Cheng [ID170](#),
 H.C. Cheng [ID64a](#), S. Cheong [ID143](#), A. Cheplakov [ID38](#), E. Cheremushkina [ID48](#), E. Cherepanova [ID114](#),
 R. Cherkaoui El Moursli [ID35e](#), E. Cheu [ID7](#), K. Cheung [ID65](#), L. Chevalier [ID135](#), V. Chiarella [ID53](#),

G. Chiarelli ^{74a}, N. Chiedde ¹⁰², G. Chiodini ^{70a}, A.S. Chisholm ²⁰, A. Chitan ^{27b}, M. Chitishvili ¹⁶³, M.V. Chizhov ³⁸, K. Choi ¹¹, A.R. Chomont ^{75a,75b}, Y. Chou ¹⁰³, E.Y.S. Chow ¹¹⁴, T. Chowdhury ^{33g}, K.L. Chu ¹⁶⁹, M.C. Chu ^{64a}, X. Chu ^{14a,14e}, J. Chudoba ¹³¹, J.J. Chwastowski ⁸⁶, D. Cieri ¹¹⁰, K.M. Ciesla ^{85a}, V. Cindro ⁹³, A. Ciocio ^{17a}, F. Ciroto ^{72a,72b}, Z.H. Citron ^{169,1}, M. Citterio ^{71a}, D.A. Ciubotaru ^{27b}, B.M. Ciungu ¹⁵⁵, A. Clark ⁵⁶, P.J. Clark ⁵², J.M. Clavijo Columbie ⁴⁸, S.E. Clawson ⁴⁸, C. Clement ^{47a,47b}, J. Clercx ⁴⁸, L. Clissa ^{23b,23a}, Y. Coadou ¹⁰², M. Cobal ^{69a,69c}, A. Coccaro ^{57b}, R.F. Coelho Barrue ^{130a}, R. Coelho Lopes De Sa ¹⁰³, S. Coelli ^{71a}, H. Cohen ¹⁵¹, A.E.C. Coimbra ^{71a,71b}, B. Cole ⁴¹, J. Collot ⁶⁰, P. Conde Muiño ^{130a,130g}, M.P. Connell ^{33c}, S.H. Connell ^{33c}, I.A. Connelly ⁵⁹, E.I. Conroy ¹²⁶, F. Conventi ^{72a,ah}, H.G. Cooke ²⁰, A.M. Cooper-Sarkar ¹²⁶, A. Cordeiro Oudot Choi ¹²⁷, F. Cormier ¹⁶⁴, L.D. Corpe ⁴⁰, M. Corradi ^{75a,75b}, F. Corriveau ^{104,x}, A. Cortes-Gonzalez ¹⁸, M.J. Costa ¹⁶³, F. Costanza ⁴, D. Costanzo ¹³⁹, B.M. Cote ¹¹⁹, G. Cowan ⁹⁵, K. Cranmer ¹⁷⁰, D. Cremonini ^{23b,23a}, S. Crépe-Renaudin ⁶⁰, F. Crescioli ¹²⁷, M. Cristinziani ¹⁴¹, M. Cristoforetti ^{78a,78b}, V. Croft ¹¹⁴, J.E. Crosby ¹²¹, G. Crosetti ^{43b,43a}, A. Cueto ⁹⁹, T. Cuhadar Donszelmann ¹⁶⁰, H. Cui ^{14a,14e}, Z. Cui ⁷, W.R. Cunningham ⁵⁹, F. Curcio ^{43b,43a}, P. Czodrowski ³⁶, M.M. Czurylo ^{63b}, M.J. Da Cunha Sargedas De Sousa ^{62a}, J.V. Da Fonseca Pinto ^{82b}, C. Da Via ¹⁰¹, W. Dabrowski ^{85a}, T. Dado ⁴⁹, S. Dahbi ^{33g}, T. Dai ¹⁰⁶, C. Dallapiccola ¹⁰³, M. Dam ⁴², G. D'amen ²⁹, V. D'Amico ¹⁰⁹, J. Damp ¹⁰⁰, J.R. Dandoy ¹²⁸, M.F. Daneri ³⁰, M. Danninger ¹⁴², V. Dao ³⁶, G. Darbo ^{57b}, S. Darmora ⁶, S.J. Das ^{29,ai}, S. D'Auria ^{71a,71b}, C. David ^{156b}, T. Davidek ¹³³, B. Davis-Purcell ³⁴, I. Dawson ⁹⁴, H.A. Day-hall ¹³², K. De ⁸, R. De Asmundis ^{72a}, N. De Biase ⁴⁸, S. De Castro ^{23b,23a}, N. De Groot ¹¹³, P. de Jong ¹¹⁴, H. De la Torre ¹⁰⁷, A. De Maria ^{14c}, A. De Salvo ^{75a}, U. De Sanctis ^{76a,76b}, A. De Santo ¹⁴⁶, J.B. De Vivie De Regie ⁶⁰, D.V. Dedovich ³⁸, J. Degens ¹¹⁴, A.M. Deiana ⁴⁴, F. Del Corso ^{23b,23a}, J. Del Peso ⁹⁹, F. Del Rio ^{63a}, F. Deliot ¹³⁵, C.M. Delitzsch ⁴⁹, M. Della Pietra ^{72a,72b}, D. Della Volpe ⁵⁶, A. Dell'Acqua ³⁶, L. Dell'Asta ^{71a,71b}, M. Delmastro ⁴, P.A. Delsart ⁶⁰, S. Demers ¹⁷², M. Demichev ³⁸, S.P. Denisov ³⁷, L. D'Eramo ⁴⁰, D. Derendarz ⁸⁶, F. Derue ¹²⁷, P. Dervan ⁹², K. Desch ²⁴, C. Deutsch ²⁴, F.A. Di Bello ^{57b,57a}, A. Di Ciaccio ^{76a,76b}, L. Di Ciaccio ⁴, A. Di Domenico ^{75a,75b}, C. Di Donato ^{72a,72b}, A. Di Girolamo ³⁶, G. Di Gregorio ⁵, A. Di Luca ^{78a,78b}, B. Di Micco ^{77a,77b}, R. Di Nardo ^{77a,77b}, C. Diaconu ¹⁰², F.A. Dias ¹¹⁴, T. Dias Do Vale ¹⁴², M.A. Diaz ^{137a,137b}, F.G. Diaz Capriles ²⁴, M. Didenko ¹⁶³, E.B. Diehl ¹⁰⁶, L. Diehl ⁵⁴, S. Díez Cornell ⁴⁸, C. Diez Pardos ¹⁴¹, C. Dimitriadi ^{24,161}, A. Dimitrievska ^{17a}, J. Dingfelder ²⁴, I-M. Dinu ^{27b}, S.J. Dittmeier ^{63b}, F. Dittus ³⁶, F. Djama ¹⁰², T. Djobava ^{149b}, J.I. Djuvsland ¹⁶, C. Doglioni ^{101,98}, J. Dolejsi ¹³³, Z. Dolezal ¹³³, M. Donadelli ^{82c}, B. Dong ¹⁰⁷, J. Donini ⁴⁰, A. D'Onofrio ^{77a,77b}, M. D'Onofrio ⁹², J. Dopke ¹³⁴, A. Doria ^{72a}, N. Dos Santos Fernandes ^{130a}, M.T. Dova ⁹⁰, A.T. Doyle ⁵⁹, M.A. Draguet ¹²⁶, E. Dreyer ¹⁶⁹, I. Drivas-koulouris ¹⁰, A.S. Drobac ¹⁵⁸, M. Drozdova ⁵⁶, D. Du ^{62a}, T.A. du Pree ¹¹⁴, F. Dubinin ³⁷, M. Dubovsky ^{28a}, E. Duchovni ¹⁶⁹, G. Duckeck ¹⁰⁹, O.A. Ducu ^{27b}, D. Duda ⁵², A. Dudarev ³⁶, E.R. Duden ²⁶, M. D'uffizi ¹⁰¹, L. Duflot ⁶⁶, M. Dührssen ³⁶, C. Dülsen ¹⁷¹, A.E. Dumitriu ^{27b}, M. Dunford ^{63a}, S. Dungs ⁴⁹, K. Dunne ^{47a,47b}, A. Duperrin ¹⁰², H. Duran Yildiz ^{3a}, M. Düren ⁵⁸, A. Durglishvili ^{149b}, B.L. Dwyer ¹¹⁵, G.I. Dyckes ^{17a}, M. Dyndal ^{85a}, S. Dysch ¹⁰¹, B.S. Dziedzic ⁸⁶, Z.O. Earnshaw ¹⁴⁶, G.H. Eberwein ¹²⁶, B. Eckerova ^{28a}, S. Eggebrecht ⁵⁵, M.G. Eggleston ⁵¹, E. Egidio Purcino De Souza ¹²⁷, L.F. Ehrke ⁵⁶, G. Eigen ¹⁶, K. Einsweiler ^{17a}, T. Ekelof ¹⁶¹, P.A. Ekman ⁹⁸, S. El Farkh ^{35b}, Y. El Ghazali ^{35b}, H. El Jarrari ^{35e,148}, A. El Moussaouy ^{35a}, V. Ellajosyula ¹⁶¹, M. Ellert ¹⁶¹, F. Ellinghaus ¹⁷¹, A.A. Elliot ⁹⁴, N. Ellis ³⁶, J. Elmsheuser ²⁹, M. Elsing ³⁶, D. Emelianov ¹³⁴, Y. Enari ¹⁵³, I. Ene ^{17a}, S. Epari ¹³, J. Erdmann ⁴⁹, P.A. Erland ⁸⁶, M. Errenst ¹⁷¹,

M. Escalier ⁶⁶, C. Escobar ¹⁶³, E. Etzion ¹⁵¹, G. Evans ^{130a}, H. Evans ⁶⁸, L.S. Evans ⁹⁵,
M.O. Evans ¹⁴⁶, A. Ezhilov ³⁷, S. Ezzarqouni ^{35a}, F. Fabbri ⁵⁹, L. Fabbri ^{23b,23a}, G. Facini ⁹⁶,
V. Fadeyev ¹³⁶, R.M. Fakhruddinov ³⁷, S. Falciano ^{75a}, L.F. Falda Ulhoa Coelho ³⁶, P.J. Falke ²⁴,
J. Faltova ¹³³, C. Fan ¹⁶², Y. Fan ^{14a}, Y. Fang ^{14a,14e}, M. Fanti ^{71a,71b}, M. Faraj ^{69a,69b},
Z. Farazpay ⁹⁷, A. Farbin ⁸, A. Farilla ^{77a}, T. Faroouque ¹⁰⁷, S.M. Farrington ⁵², F. Fassi ^{35e},
D. Fassouliotis ⁹, M. Faucci Giannelli ^{76a,76b}, W.J. Fawcett ³², L. Fayard ⁶⁶, P. Federic ¹³³,
P. Federicova ¹³¹, O.L. Fedin ^{37,a}, G. Fedotov ³⁷, M. Feickert ¹⁷⁰, L. Feligioni ¹⁰², A. Fell ¹³⁹,
D.E. Fellers ¹²³, C. Feng ^{62b}, M. Feng ^{14b}, Z. Feng ¹¹⁴, M.J. Fenton ¹⁶⁰, A.B. Fenyuk ³⁷,
L. Ferencz ⁴⁸, R.A.M. Ferguson ⁹¹, S.I. Fernandez Luengo ^{137f}, M.J.V. Fernoux ¹⁰²,
J. Ferrando ⁴⁸, A. Ferrari ¹⁶¹, P. Ferrari ^{114,113}, R. Ferrari ^{73a}, D. Ferrere ⁵⁶, C. Ferretti ¹⁰⁶,
F. Fiedler ¹⁰⁰, A. Filipčič ⁹³, E.K. Filmer ¹, F. Filthaut ¹¹³, M.C.N. Fiolhais ^{130a,130c,c},
L. Fiorini ¹⁶³, W.C. Fisher ¹⁰⁷, T. Fitschen ¹⁰¹, P.M. Fitzhugh ¹³⁵, I. Fleck ¹⁴¹, P. Fleischmann ¹⁰⁶,
T. Flick ¹⁷¹, L. Flores ¹²⁸, M. Flores ^{33d,ad}, L.R. Flores Castillo ^{64a}, L. Flores Sanz De Acedo ³⁶,
F.M. Follega ^{78a,78b}, N. Fomin ¹⁶, J.H. Foo ¹⁵⁵, B.C. Forland ⁶⁸, A. Formica ¹³⁵, A.C. Forti ¹⁰¹,
E. Fortin ³⁶, A.W. Fortman ⁶¹, M.G. Foti ^{17a}, L. Fountas ^{9j}, D. Fournier ⁶⁶, H. Fox ⁹¹,
P. Francavilla ^{74a,74b}, S. Francescato ⁶¹, S. Franchellucci ⁵⁶, M. Franchini ^{23b,23a},
S. Franchino ^{63a}, D. Francis ³⁶, L. Franco ¹¹³, L. Franconi ⁴⁸, M. Franklin ⁶¹, G. Frattari ²⁶,
A.C. Freegard ⁹⁴, W.S. Freund ^{82b}, Y.Y. Frid ¹⁵¹, N. Fritzsche ⁵⁰, A. Froch ⁵⁴, D. Froidevaux ³⁶,
J.A. Frost ¹²⁶, Y. Fu ^{62a}, M. Fujimoto ¹¹⁸, E. Fullana Torregrosa ^{163,*}, K.Y. Fung ^{64a},
E. Furtado De Simas Filho ^{82b}, M. Furukawa ¹⁵³, J. Fuster ¹⁶³, A. Gabrielli ^{23b,23a},
A. Gabrielli ¹⁵⁵, P. Gadow ⁴⁸, G. Gagliardi ^{57b,57a}, L.G. Gagnon ^{17a}, E.J. Gallas ¹²⁶,
B.J. Gallop ¹³⁴, K.K. Gan ¹¹⁹, S. Ganguly ¹⁵³, J. Gao ^{62a}, Y. Gao ⁵², F.M. Garay Walls ^{137a,137b},
B. Garcia ^{29,ai}, C. García ¹⁶³, A. Garcia Alonso ¹¹⁴, A.G. Garcia Caffaro ¹⁷²,
J.E. García Navarro ¹⁶³, M. Garcia-Sciveres ^{17a}, G.L. Gardner ¹²⁸, R.W. Gardner ³⁹,
N. Garelli ¹⁵⁸, D. Garg ⁸⁰, R.B. Garg ^{143,o}, J.M. Gargan ⁵², C.A. Garner ¹⁵⁵, S.J. Gasiorowski ¹³⁸,
P. Gaspar ^{82b}, G. Gaudio ^{73a}, V. Gautam ¹³, P. Gauzzi ^{75a,75b}, I.L. Gavrilenko ³⁷, A. Gavrilyuk ³⁷,
C. Gay ¹⁶⁴, G. Gaycken ⁴⁸, E.N. Gazis ¹⁰, A.A. Geanta ^{27b}, C.M. Gee ¹³⁶, C. Gemme ^{57b},
M.H. Genest ⁶⁰, S. Gentile ^{75a,75b}, S. George ⁹⁵, W.F. George ²⁰, T. Geralis ⁴⁶,
P. Gessinger-Befurt ³⁶, M.E. Geyik ¹⁷¹, M. Ghneimat ¹⁴¹, K. Ghorbanian ⁹⁴, A. Ghosal ¹⁴¹,
A. Ghosh ¹⁶⁰, A. Ghosh ⁷, B. Giacobbe ^{23b}, S. Giagu ^{75a,75b}, P. Giannetti ^{74a}, A. Giannini ^{62a},
S.M. Gibson ⁹⁵, M. Gignac ¹³⁶, D.T. Gil ^{85b}, A.K. Gilbert ^{85a}, B.J. Gilbert ⁴¹, D. Gillberg ³⁴,
G. Gilles ¹¹⁴, N.E.K. Gillwald ⁴⁸, L. Ginabat ¹²⁷, D.M. Gingrich ^{2,ag}, M.P. Giordani ^{69a,69c},
P.F. Giraud ¹³⁵, G. Giugliarelli ^{69a,69c}, D. Giugni ^{71a}, F. Giuli ³⁶, I. Gkialas ^{9j}, L.K. Gladilin ³⁷,
C. Glasman ⁹⁹, G.R. Gledhill ¹²³, M. Glisic ¹²³, I. Gnesi ^{43b,f}, Y. Go ^{29,ai}, M. Goblirsch-Kolb ³⁶,
B. Gocke ⁴⁹, D. Godin ¹⁰⁸, B. Gokturk ^{21a}, S. Goldfarb ¹⁰⁵, T. Golling ⁵⁶, M.G.D. Gololo ^{33g},
D. Golubkov ³⁷, J.P. Gombas ¹⁰⁷, A. Gomes ^{130a,130b}, G. Gomes Da Silva ¹⁴¹,
A.J. Gomez Delegido ¹⁶³, R. Gonçalo ^{130a,130c}, G. Gonella ¹²³, L. Gonella ²⁰, A. Gongadze ³⁸,
F. Gonnella ²⁰, J.L. Gonski ⁴¹, R.Y. González Andana ⁵², S. González de la Hoz ¹⁶³,
S. Gonzalez Fernandez ¹³, R. Gonzalez Lopez ⁹², C. Gonzalez Renteria ^{17a},
R. Gonzalez Suarez ¹⁶¹, S. Gonzalez-Sevilla ⁵⁶, G.R. Gonzalvo Rodriguez ¹⁶³, L. Goossens ³⁶,
P.A. Gorbounov ³⁷, B. Gorini ³⁶, E. Gorini ^{70a,70b}, A. Gorišek ⁹³, T.C. Gosart ¹²⁸,
A.T. Goshaw ⁵¹, M.I. Gostkin ³⁸, S. Goswami ¹²¹, C.A. Gottardo ³⁶, M. Gouighri ^{35b},
V. Goumarre ⁴⁸, A.G. Goussiou ¹³⁸, N. Govender ^{33c}, I. Grabowska-Bold ^{85a}, K. Graham ³⁴,
E. Gramstad ¹²⁵, S. Grancagnolo ^{70a,70b}, M. Grandi ¹⁴⁶, V. Gratchev ^{37,*}, P.M. Gravila ^{27f},
F.G. Gravili ^{70a,70b}, H.M. Gray ^{17a}, M. Greco ^{70a,70b}, C. Grefe ²⁴, I.M. Gregor ⁴⁸, P. Grenier ¹⁴³,
C. Grieco ¹³, A.A. Grillo ¹³⁶, K. Grimm ³¹, S. Grinstein ^{13,t}, J.-F. Grivaz ⁶⁶, E. Gross ¹⁶⁹,
J. Grosse-Knetter ⁵⁵, C. Grud ¹⁰⁶, J.C. Grundy ¹²⁶, L. Guan ¹⁰⁶, W. Guan ²⁹, C. Gubbels ¹⁶⁴,

J.G.R. Guerrero Rojas ¹⁶³, G. Guerrieri ^{69a,69b}, F. Guescini ¹¹⁰, R. Gugel ¹⁰⁰, J.A.M. Guhit ¹⁰⁶, A. Guida ¹⁸, T. Guillemain ⁴, E. Guilloton ^{167,134}, S. Guindon ³⁶, F. Guo ^{14a,14e}, J. Guo ^{62c}, L. Guo ⁴⁸, Y. Guo ¹⁰⁶, R. Gupta ⁴⁸, S. Gurbuz ²⁴, S.S. Gurdasani ⁵⁴, G. Gustavino ³⁶, M. Guth ⁵⁶, P. Gutierrez ¹²⁰, L.F. Gutierrez Zagazeta ¹²⁸, C. Gutschow ⁹⁶, C. Gwenlan ¹²⁶, C.B. Gwilliam ⁹², E.S. Haaland ¹²⁵, A. Haas ¹¹⁷, M. Habedank ⁴⁸, C. Haber ^{17a}, H.K. Hadavand ⁸, A. Hadeef ¹⁰⁰, S. Hadzic ¹¹⁰, J.J. Hahn ¹⁴¹, E.H. Haines ⁹⁶, M. Haleem ¹⁶⁶, J. Haley ¹²¹, J.J. Hall ¹³⁹, G.D. Hallewell ¹⁰², L. Halser ¹⁹, K. Hamano ¹⁶⁵, H. Hamdaoui ^{35e}, M. Hamer ²⁴, G.N. Hamity ⁵², E.J. Hampshire ⁹⁵, J. Han ^{62b}, K. Han ^{62a}, L. Han ^{14c}, L. Han ^{62a}, S. Han ^{17a}, Y.F. Han ¹⁵⁵, K. Hanagaki ⁸³, M. Hance ¹³⁶, D.A. Hangal ^{41,ac}, H. Hanif ¹⁴², M.D. Hank ¹²⁸, R. Hankache ¹⁰¹, J.B. Hansen ⁴², J.D. Hansen ⁴², P.H. Hansen ⁴², K. Hara ¹⁵⁷, D. Harada ⁵⁶, T. Harenberg ¹⁷¹, S. Harkusha ³⁷, M.L. Harris ¹⁰³, Y.T. Harris ¹²⁶, J. Harrison ¹³, N.M. Harrison ¹¹⁹, P.F. Harrison ¹⁶⁷, N.M. Hartman ¹¹⁰, N.M. Hartmann ¹⁰⁹, Y. Hasegawa ¹⁴⁰, A. Hasib ⁵², S. Haug ¹⁹, R. Hauser ¹⁰⁷, C.M. Hawkes ²⁰, R.J. Hawkins ³⁶, Y. Hayashi ¹⁵³, S. Hayashida ¹¹¹, D. Hayden ¹⁰⁷, C. Hayes ¹⁰⁶, R.L. Hayes ¹¹⁴, C.P. Hays ¹²⁶, J.M. Hays ⁹⁴, H.S. Hayward ⁹², F. He ^{62a}, M. He ^{14a,14e}, Y. He ¹⁵⁴, Y. He ¹²⁷, N.B. Heatley ⁹⁴, V. Hedberg ⁹⁸, A.L. Heggelund ¹²⁵, N.D. Hehir ⁹⁴, C. Heidegger ⁵⁴, K.K. Heidegger ⁵⁴, W.D. Heidorn ⁸¹, J. Heilman ³⁴, S. Heim ⁴⁸, T. Heim ^{17a}, J.G. Heinlein ¹²⁸, J.J. Heinrich ¹²³, L. Heinrich ^{110,ae}, J. Hejbal ¹³¹, L. Helary ⁴⁸, A. Held ¹⁷⁰, S. Hellesund ¹⁶, C.M. Helling ¹⁶⁴, S. Hellman ^{47a,47b}, C. Helsen ³⁶, R.C.W. Henderson ⁹¹, L. Henkelmann ³², A.M. Henriques Correia ³⁶, H. Herde ⁹⁸, Y. Hernández Jiménez ¹⁴⁵, L.M. Herrmann ²⁴, T. Herrmann ⁵⁰, G. Herten ⁵⁴, R. Hertenberger ¹⁰⁹, L. Hervas ³⁶, M.E. Hespig ¹⁰⁰, N.P. Hessey ^{156a}, H. Hibi ⁸⁴, S.J. Hillier ²⁰, J.R. Hinds ¹⁰⁷, F. Hinterkeuser ²⁴, M. Hirose ¹²⁴, S. Hirose ¹⁵⁷, D. Hirschbuehl ¹⁷¹, T.G. Hitchings ¹⁰¹, B. Hiti ⁹³, J. Hobbs ¹⁴⁵, R. Hobincu ^{27e}, N. Hod ¹⁶⁹, M.C. Hodgkinson ¹³⁹, B.H. Hodgkinson ³², A. Hoecker ³⁶, J. Hofer ⁴⁸, T. Holm ²⁴, M. Holzbock ¹¹⁰, L.B.A.H. Hommels ³², B.P. Honan ¹⁰¹, J. Hong ^{62c}, T.M. Hong ¹²⁹, B.H. Hooberman ¹⁶², W.H. Hopkins ⁶, Y. Horii ¹¹¹, S. Hou ¹⁴⁸, A.S. Howard ⁹³, J. Howarth ⁵⁹, J. Hoya ⁶, M. Hrabovsky ¹²², A. Hrynevich ⁴⁸, T. Hryn'ova ⁴, P.J. Hsu ⁶⁵, S.-C. Hsu ¹³⁸, Q. Hu ⁴¹, Y.F. Hu ^{14a,14e}, S. Huang ^{64b}, X. Huang ^{14c}, Y. Huang ^{62a}, Y. Huang ^{14a}, Z. Huang ¹⁰¹, Z. Hubacek ¹³², M. Huebner ²⁴, F. Huegging ²⁴, T.B. Huffman ¹²⁶, C.A. Hugli ⁴⁸, M. Huhtinen ³⁶, S.K. Huiberts ¹⁶, R. Hulsken ¹⁰⁴, N. Huseynov ^{12,a}, J. Huston ¹⁰⁷, J. Huth ⁶¹, R. Hyneman ¹⁴³, G. Iacobucci ⁵⁶, G. Iakovidis ²⁹, I. Ibragimov ¹⁴¹, L. Iconomidou-Fayard ⁶⁶, P. Iengo ^{72a,72b}, R. Iguchi ¹⁵³, T. Iizawa ⁸³, Y. Ikegami ⁸³, N. Ilic ¹⁵⁵, H. Imam ^{35a}, M. Ince Lezki ⁵⁶, T. Ingebretsen Carlson ^{47a,47b}, G. Introzzi ^{73a,73b}, M. Iodice ^{77a}, V. Ippolito ^{75a,75b}, R.K. Irwin ⁹², M. Ishino ¹⁵³, W. Islam ¹⁷⁰, C. Issever ^{18,48}, S. Istin ^{21a,ak}, H. Ito ¹⁶⁸, J.M. Iturbe Ponce ^{64a}, R. Iuppa ^{78a,78b}, A. Ivina ¹⁶⁹, J.M. Izen ⁴⁵, V. Izzo ^{72a}, P. Jacka ^{131,132}, P. Jackson ¹, R.M. Jacobs ⁴⁸, B.P. Jaeger ¹⁴², C.S. Jagfeld ¹⁰⁹, P. Jain ⁵⁴, G. Jäkel ¹⁷¹, K. Jakobs ⁵⁴, T. Jakoubek ¹⁶⁹, J. Jamieson ⁵⁹, K.W. Janas ^{85a}, A.E. Jaspán ⁹², M. Javurkova ¹⁰³, F. Jeanneau ¹³⁵, L. Jeanty ¹²³, J. Jejelava ^{149a,aa}, P. Jenni ^{54,g}, C.E. Jessiman ³⁴, S. Jézéquel ⁴, C. Jia ^{62b}, J. Jia ¹⁴⁵, X. Jia ⁶¹, X. Jia ^{14a,14e}, Z. Jia ^{14c}, Y. Jiang ^{62a}, S. Jiggins ⁴⁸, J. Jimenez Pena ¹³, S. Jin ^{14c}, A. Jinaru ^{27b}, O. Jinnouchi ¹⁵⁴, P. Johansson ¹³⁹, K.A. Johns ⁷, J.W. Johnson ¹³⁶, D.M. Jones ³², E. Jones ⁴⁸, P. Jones ³², R.W.L. Jones ⁹¹, T.J. Jones ⁹², R. Joshi ¹¹⁹, J. Jovicevic ¹⁵, X. Ju ^{17a}, J.J. Junggeburth ³⁶, T. Junkermann ^{63a}, A. Juste Rozas ^{13,t}, M.K. Juzek ⁸⁶, S. Kabana ^{137e}, A. Kaczmarska ⁸⁶, M. Kado ¹¹⁰, H. Kagan ¹¹⁹, M. Kagan ¹⁴³, A. Kahn ⁴¹, A. Kahn ¹²⁸, C. Kahra ¹⁰⁰, T. Kaji ¹⁶⁸, E. Kajomovitz ¹⁵⁰, N. Kakati ¹⁶⁹, I. Kalaitzidou ⁵⁴, C.W. Kalderon ²⁹, A. Kamenshchikov ¹⁵⁵, S. Kanayama ¹⁵⁴, N.J. Kang ¹³⁶, D. Kar ^{33g}, K. Karava ¹²⁶, M.J. Kareem ^{156b}, E. Karentzos ⁵⁴, I. Karknias ¹⁵², O. Karkout ¹¹⁴, S.N. Karpov ³⁸, Z.M. Karpova ³⁸, V. Kartvelishvili ⁹¹,

A.N. Karyukhin ³⁷, E. Kasimi ¹⁵², J. Katzy ⁴⁸, S. Kaur ³⁴, K. Kawade ¹⁴⁰, T. Kawamoto ¹³⁵,
 E.F. Kay ³⁶, F.I. Kaya ¹⁵⁸, S. Kazakos ¹⁰⁷, V.F. Kazanin ³⁷, Y. Ke ¹⁴⁵, J.M. Keaveney ^{33a},
 R. Keeler ¹⁶⁵, G.V. Kehris ⁶¹, J.S. Keller ³⁴, A.S. Kelly ⁹⁶, J.J. Kempster ¹⁴⁶, K.E. Kennedy ⁴¹,
 P.D. Kennedy ¹⁰⁰, O. Kepka ¹³¹, B.P. Kerridge ¹⁶⁷, S. Kersten ¹⁷¹, B.P. Kerševan ⁹³,
 S. Keshri ⁶⁶, L. Keszezhova ^{28a}, S. Ketabchi Haghighat ¹⁵⁵, M. Khandoga ¹²⁷, A. Khanov ¹²¹,
 A.G. Kharlamov ³⁷, T. Kharlamova ³⁷, E.E. Khoda ¹³⁸, T.J. Khoo ¹⁸, G. Khoriauli ¹⁶⁶,
 J. Khubua ^{149b}, Y.A.R. Khwaira ⁶⁶, M. Kiehn ³⁶, A. Kilgallon ¹²³, D.W. Kim ^{47a,47b},
 Y.K. Kim ³⁹, N. Kimura ⁹⁶, A. Kirchhoff ⁵⁵, C. Kirfel ²⁴, F. Kirfel ²⁴, J. Kirk ¹³⁴,
 A.E. Kiryunin ¹¹⁰, C. Kitsaki ¹⁰, O. Kivernyk ²⁴, M. Klassen ^{63a}, C. Klein ³⁴, L. Klein ¹⁶⁶,
 M.H. Klein ¹⁰⁶, M. Klein ⁹², S.B. Klein ⁵⁶, U. Klein ⁹², P. Klimek ³⁶, A. Klimentov ²⁹,
 T. Klioutchnikova ³⁶, P. Kluit ¹¹⁴, S. Kluth ¹¹⁰, E. Kneringer ⁷⁹, T.M. Knight ¹⁵⁵, A. Knue ⁵⁴,
 R. Kobayashi ⁸⁷, S.F. Koch ¹²⁶, M. Kocian ¹⁴³, P. Kodyš ¹³³, D.M. Koeck ¹²³, P.T. Koenig ²⁴,
 T. Koffas ³⁴, M. Kolb ¹³⁵, I. Koletsou ⁴, T. Komarek ¹²², K. Köneke ⁵⁴, A.X.Y. Kong ¹,
 T. Kono ¹¹⁸, N. Konstantinidis ⁹⁶, B. Konya ⁹⁸, R. Kopeliansky ⁶⁸, S. Koperny ^{85a}, K. Korcyl ⁸⁶,
 K. Kordas ^{152,e}, G. Koren ¹⁵¹, A. Korn ⁹⁶, S. Korn ⁵⁵, I. Korolkov ¹³, N. Korotkova ³⁷,
 B. Kortman ¹¹⁴, O. Kortner ¹¹⁰, S. Kortner ¹¹⁰, W.H. Kostecka ¹¹⁵, V.V. Kostyukhin ¹⁴¹,
 A. Kotsokechagia ¹³⁵, A. Kotwal ⁵¹, A. Koulouris ³⁶, A. Kourkoumeli-Charalampidi ^{73a,73b},
 C. Kourkoumelis ⁹, E. Kourlitis ⁶, O. Kovanda ¹⁴⁶, R. Kowalewski ¹⁶⁵, W. Kozanecki ¹³⁵,
 A.S. Kozhin ³⁷, V.A. Kramarenko ³⁷, G. Kramberger ⁹³, P. Kramer ¹⁰⁰, M.W. Krasny ¹²⁷,
 A. Krasznahorkay ³⁶, J.W. Kraus ¹⁷¹, J.A. Kremer ¹⁰⁰, T. Kresse ⁵⁰, J. Kretschmar ⁹²,
 K. Kreul ¹⁸, P. Krieger ¹⁵⁵, S. Krishnamurthy ¹⁰³, M. Krivos ¹³³, K. Krizka ²⁰,
 K. Kroeninger ⁴⁹, H. Kroha ¹¹⁰, J. Kroll ¹³¹, J. Kroll ¹²⁸, K.S. Krowpman ¹⁰⁷, U. Kruchonak ³⁸,
 H. Krüger ²⁴, N. Krumnack ⁸¹, M.C. Kruse ⁵¹, J.A. Krzysiak ⁸⁶, O. Kuchinskaja ³⁷, S. Kuday ^{3a},
 S. Kuehn ³⁶, R. Kuesters ⁵⁴, T. Kuhl ⁴⁸, V. Kukhtin ³⁸, Y. Kulchitsky ^{37,a}, S. Kuleshov ^{137d,137b},
 M. Kumar ^{33g}, N. Kumari ¹⁰², A. Kupco ¹³¹, T. Kupfer ⁴⁹, A. Kupich ³⁷, O. Kuprash ⁵⁴,
 H. Kurashige ⁸⁴, L.L. Kurchaninov ^{156a}, O. Kurdysh ⁶⁶, Y.A. Kurochkin ³⁷, A. Kurova ³⁷,
 M. Kuze ¹⁵⁴, A.K. Kvam ¹⁰³, J. Kvita ¹²², T. Kwan ¹⁰⁴, N.G. Kyriacou ¹⁰⁶, L.A.O. Laatu ¹⁰²,
 C. Lacasta ¹⁶³, F. Lacava ^{75a,75b}, H. Lacker ¹⁸, D. Lacour ¹²⁷, N.N. Lad ⁹⁶, E. Ladygin ³⁸,
 B. Laforge ¹²⁷, T. Lagouri ^{137e}, S. Lai ⁵⁵, I.K. Lakomic ^{85a}, N. Lalloue ⁶⁰, J.E. Lambert ¹⁶⁵,
 S. Lammers ⁶⁸, W. Lampl ⁷, C. Lampoudis ^{152,e}, A.N. Lancaster ¹¹⁵, E. Lançon ²⁹,
 U. Landgraf ⁵⁴, M.P.J. Landon ⁹⁴, V.S. Lang ⁵⁴, R.J. Langenberg ¹⁰³, O.K.B. Langrekken ¹²⁵,
 A.J. Lankford ¹⁶⁰, F. Lanni ³⁶, K. Lantzsch ²⁴, A. Lanza ^{73a}, A. Lapertosa ^{57b,57a},
 J.F. Laporte ¹³⁵, T. Lari ^{71a}, F. Lasagni Manghi ^{23b}, M. Lassnig ³⁶, V. Latonova ¹³¹,
 A. Laudrain ¹⁰⁰, A. Laurier ¹⁵⁰, S.D. Lawlor ⁹⁵, Z. Lawrence ¹⁰¹, M. Lazzaroni ^{71a,71b}, B. Le ¹⁰¹,
 E.M. Le Boulicaut ⁵¹, B. Leban ⁹³, A. Lebedev ⁸¹, M. LeBlanc ³⁶, F. Ledroit-Guillon ⁶⁰,
 A.C.A. Lee ⁹⁶, S.C. Lee ¹⁴⁸, S. Lee ^{47a,47b}, T.F. Lee ⁹², L.L. Leeuw ^{33c}, H.P. Lefebvre ⁹⁵,
 M. Lefebvre ¹⁶⁵, C. Leggett ^{17a}, G. Lehmann Miotto ³⁶, M. Leigh ⁵⁶, W.A. Leight ¹⁰³,
 W. Leinonen ¹¹³, A. Leisos ^{152,s}, M.A.L. Leite ^{82c}, C.E. Leitgeb ⁴⁸, R. Leitner ¹³³,
 K.J.C. Leney ⁴⁴, T. Lenz ²⁴, S. Leone ^{74a}, C. Leonidopoulos ⁵², A. Leopold ¹⁴⁴, C. Leroy ¹⁰⁸,
 R. Les ¹⁰⁷, C.G. Lester ³², M. Levchenko ³⁷, J. Levêque ⁴, D. Levin ¹⁰⁶, L.J. Levinson ¹⁶⁹,
 M.P. Lewicki ⁸⁶, D.J. Lewis ⁴, A. Li ⁵, B. Li ^{62b}, C. Li ^{62a}, C-Q. Li ^{62c}, H. Li ^{62a}, H. Li ^{62b},
 H. Li ^{14c}, H. Li ^{62b}, K. Li ¹³⁸, L. Li ^{62c}, M. Li ^{14a,14e}, Q.Y. Li ^{62a}, S. Li ^{14a,14e}, S. Li ^{62d,62c,d},
 T. Li ⁵, X. Li ¹⁰⁴, Z. Li ¹²⁶, Z. Li ¹⁰⁴, Z. Li ⁹², Z. Li ^{14a,14e}, Z. Liang ^{14a}, M. Liberatore ⁴⁸,
 B. Liberti ^{76a}, K. Lie ^{64c}, J. Lieber Marin ^{82b}, H. Lien ⁶⁸, K. Lin ¹⁰⁷, R.E. Lindley ⁷,
 J.H. Lindon ², A. Lins ⁴⁸, E. Lipeles ¹²⁸, A. Lipniacka ¹⁶, A. Lister ¹⁶⁴, J.D. Little ⁴,
 B. Liu ^{14a}, B.X. Liu ¹⁴², D. Liu ^{62d,62c}, J.B. Liu ^{62a}, J.K.K. Liu ³², K. Liu ^{62d,62c}, M. Liu ^{62a},
 M.Y. Liu ^{62a}, P. Liu ^{14a}, Q. Liu ^{62d,138,62c}, X. Liu ^{62a}, Y. Liu ^{14d,14e}, Y.L. Liu ¹⁰⁶, Y.W. Liu ^{62a},

J. Llorente Merino ¹⁴², S.L. Lloyd ⁹⁴, E.M. Lobodzinska ⁴⁸, P. Loch ⁷, S. Loffredo ^{76a,76b},
 T. Lohse ¹⁸, K. Lohwasser ¹³⁹, E. Loiacono ⁴⁸, M. Lokajicek ^{131,*}, J.D. Lomas ²⁰,
 J.D. Long ¹⁶², I. Longarini ¹⁶⁰, L. Longo ^{70a,70b}, R. Longo ¹⁶², I. Lopez Paz ⁶⁷,
 A. Lopez Solis ⁴⁸, J. Lorenz ¹⁰⁹, N. Lorenzo Martinez ⁴, A.M. Lory ¹⁰⁹,
 G. Löschke Centeno ¹⁴⁶, O. Loseva ³⁷, X. Lou ^{47a,47b}, X. Lou ^{14a,14e}, A. Lounis ⁶⁶, J. Love ⁶,
 P.A. Love ⁹¹, G. Lu ^{14a,14e}, M. Lu ⁸⁰, S. Lu ¹²⁸, Y.J. Lu ⁶⁵, H.J. Lubatti ¹³⁸, C. Luci ^{75a,75b},
 F.L. Lucio Alves ^{14c}, A. Lucotte ⁶⁰, F. Luehring ⁶⁸, I. Luise ¹⁴⁵, O. Lukianchuk ⁶⁶,
 O. Lundberg ¹⁴⁴, B. Lund-Jensen ¹⁴⁴, N.A. Luongo ¹²³, M.S. Lutz ¹⁵¹, D. Lynn ²⁹, H. Lyons ⁹²,
 R. Lysak ¹³¹, E. Lytken ⁹⁸, V. Lyubushkin ³⁸, T. Lyubushkina ³⁸, M.M. Lyukova ¹⁴⁵, H. Ma ²⁹,
 L.L. Ma ^{62b}, Y. Ma ¹²¹, D.M. Mac Donell ¹⁶⁵, G. Maccarrone ⁵³, J.C. MacDonald ¹⁰⁰,
 R. Madar ⁴⁰, W.F. Mader ⁵⁰, J. Maeda ⁸⁴, T. Maeno ²⁹, M. Maerker ⁵⁰, H. Maguire ¹³⁹,
 V. Maiboroda ¹³⁵, A. Maio ^{130a,130b,130d}, K. Maj ^{85a}, O. Majersky ⁴⁸, S. Majewski ¹²³,
 N. Makovec ⁶⁶, V. Maksimovic ¹⁵, B. Malaescu ¹²⁷, Pa. Malecki ⁸⁶, V.P. Maleev ³⁷,
 F. Malek ⁶⁰, M. Mali ⁹³, D. Malito ⁹⁵, U. Mallik ⁸⁰, S. Maltezos ¹⁰, S. Malyukov ³⁸, J. Mamuzic ¹³,
 G. Mancini ⁵³, G. Manco ^{73a,73b}, J.P. Mandalia ⁹⁴, I. Mandić ⁹³,
 L. Manhaes de Andrade Filho ^{82a}, I.M. Maniatis ¹⁶⁹, J. Manjarres Ramos ^{102,ab}, D.C. Mankad ¹⁶⁹,
 A. Mann ¹⁰⁹, B. Mansoulie ¹³⁵, S. Manzoni ³⁶, A. Marantis ^{152,s}, G. Marchiori ⁵,
 M. Marcisovsky ¹³¹, C. Marcon ^{71a,71b}, M. Marinescu ²⁰, M. Marjanovic ¹²⁰, E.J. Marshall ⁹¹,
 Z. Marshall ^{17a}, S. Marti-Garcia ¹⁶³, T.A. Martin ¹⁶⁷, V.J. Martin ⁵², B. Martin dit Latour ¹⁶,
 L. Martinelli ^{75a,75b}, M. Martinez ^{13,t}, P. Martinez Agullo ¹⁶³, V.I. Martinez Outschoorn ¹⁰³,
 P. Martinez Suarez ¹³, S. Martin-Haugh ¹³⁴, V.S. Martoiu ^{27b}, A.C. Martyniuk ⁹⁶, A. Marzin ³⁶,
 D. Mascione ^{78a,78b}, L. Masetti ¹⁰⁰, T. Mashimo ¹⁵³, J. Masik ¹⁰¹, A.L. Maslennikov ³⁷,
 L. Massa ^{23b}, P. Massarotti ^{72a,72b}, P. Mastrandrea ^{74a,74b}, A. Mastroberardino ^{43b,43a},
 T. Masubuchi ¹⁵³, T. Mathisen ¹⁶¹, J. Matousek ¹³³, N. Matsuzawa ¹⁵³, J. Maurer ^{27b}, B. Maček ⁹³,
 D.A. Maximov ³⁷, R. Mazini ¹⁴⁸, I. Maznas ¹⁵², M. Mazza ¹⁰⁷, S.M. Mazza ¹³⁶,
 E. Mazzeo ^{71a,71b}, C. Mc Ginn ²⁹, J.P. Mc Gowan ¹⁰⁴, S.P. Mc Kee ¹⁰⁶, E.F. McDonald ¹⁰⁵,
 A.E. McDougall ¹¹⁴, J.A. Mcfayden ¹⁴⁶, R.P. McGovern ¹²⁸, G. Mchedlidze ^{149b},
 R.P. Mckenzie ^{33g}, T.C. Mclachlan ⁴⁸, D.J. Mclaughlin ⁹⁶, K.D. McLean ¹⁶⁵, S.J. McMahon ¹³⁴,
 P.C. McNamara ¹⁰⁵, C.M. Mcpartland ⁹², R.A. McPherson ^{165,x}, S. Mehlhase ¹⁰⁹, A. Mehta ⁹²,
 D. Melini ¹⁵⁰, B.R. Mellado Garcia ^{33g}, A.H. Melo ⁵⁵, F. Meloni ⁴⁸,
 A.M. Mendes Jacques Da Costa ¹⁰¹, H.Y. Meng ¹⁵⁵, L. Meng ⁹¹, S. Menke ¹¹⁰, M. Mentink ³⁶,
 E. Meoni ^{43b,43a}, C. Merlassino ¹²⁶, L. Merola ^{72a,72b}, C. Meroni ^{71a,71b}, G. Merz ¹⁰⁶,
 O. Meshkov ³⁷, J. Metcalfe ⁶, A.S. Mete ⁶, C. Meyer ⁶⁸, J-P. Meyer ¹³⁵, R.P. Middleton ¹³⁴,
 L. Mijović ⁵², G. Mikenberg ¹⁶⁹, M. Mikestikova ¹³¹, M. Mikuž ⁹³, H. Mildner ¹⁰⁰, A. Milic ³⁶,
 C.D. Milke ⁴⁴, D.W. Miller ³⁹, L.S. Miller ³⁴, A. Milov ¹⁶⁹, D.A. Milstead ^{47a,47b}, T. Min ^{14c},
 A.A. Minaenko ³⁷, I.A. Minashvili ^{149b}, L. Mince ⁵⁹, A.I. Mincer ¹¹⁷, B. Mindur ^{85a},
 M. Mineev ³⁸, Y. Mino ⁸⁷, L.M. Mir ¹³, M. Miralles Lopez ¹⁶³, M. Mironova ^{17a}, A. Mishima ¹⁵³,
 M.C. Missio ¹¹³, T. Mitani ¹⁶⁸, A. Mitra ¹⁶⁷, V.A. Mitsou ¹⁶³, O. Miu ¹⁵⁵, P.S. Miyagawa ⁹⁴,
 Y. Miyazaki ⁸⁹, A. Mizukami ⁸³, T. Mkrtychyan ^{63a}, M. Mlinarevic ⁹⁶, T. Mlinarevic ⁹⁶,
 M. Mlynarikova ³⁶, S. Mobius ¹⁹, K. Mochizuki ¹⁰⁸, P. Moder ⁴⁸, P. Mogg ¹⁰⁹,
 A.F. Mohammed ^{14a,14e}, S. Mohapatra ⁴¹, G. Mokgatitwane ^{33g}, L. Moleri ¹⁶⁹, B. Mondal ¹⁴¹,
 S. Mondal ¹³², K. Mönig ⁴⁸, E. Monnier ¹⁰², L. Monsonis Romero ¹⁶³, J. Montejó Berlingen ^{13,83},
 M. Montella ¹¹⁹, F. Montekali ^{77a,77b}, F. Monticelli ⁹⁰, S. Monzani ^{69a,69c}, N. Morange ⁶⁶,
 A.L. Moreira De Carvalho ^{130a}, M. Moreno Llácer ¹⁶³, C. Moreno Martinez ⁵⁶, P. Morettini ^{57b},
 S. Morgenstern ³⁶, M. Morii ⁶¹, M. Morinaga ¹⁵³, A.K. Morley ³⁶, F. Morodei ^{75a,75b},
 L. Morvaj ³⁶, P. Moschovakos ³⁶, B. Moser ³⁶, M. Mosidze ^{149b}, T. Moskalets ⁵⁴,
 P. Moskvitina ¹¹³, J. Moss ^{31,m}, E.J.W. Moyses ¹⁰³, O. Mtintsilana ^{33g}, S. Muanza ¹⁰²,

J. Mueller ¹²⁹, D. Muenstermann ⁹¹, R. Müller ¹⁹, G.A. Mullier ¹⁶¹, A.J. Mullin³², J.J. Mullin¹²⁸, D.P. Mungo ¹⁵⁵, D. Munoz Perez ¹⁶³, F.J. Munoz Sanchez ¹⁰¹, M. Murin ¹⁰¹, W.J. Murray ^{167,134}, A. Murrone ^{71a,71b}, J.M. Muse ¹²⁰, M. Muškinja ^{17a}, C. Mwewa ²⁹, A.G. Myagkov ^{37,a}, A.J. Myers ⁸, A.A. Myers¹²⁹, G. Myers ⁶⁸, M. Myska ¹³², B.P. Nachman ^{17a}, O. Nackenhorst ⁴⁹, A. Nag ⁵⁰, K. Nagai ¹²⁶, K. Nagano ⁸³, J.L. Nagle ^{29,ai}, E. Nagy ¹⁰², A.M. Nairz ³⁶, Y. Nakahama ⁸³, K. Nakamura ⁸³, K. Nakkalil ⁵, H. Nanjo ¹²⁴, R. Narayan ⁴⁴, E.A. Narayanan ¹¹², I. Naryshkin ³⁷, M. Naseri ³⁴, S. Nasri ¹⁵⁹, C. Nass ²⁴, G. Navarro ^{22a}, J. Navarro-Gonzalez ¹⁶³, R. Nayak ¹⁵¹, A. Nayaz ¹⁸, P.Y. Nechaeva ³⁷, F. Nechansky ⁴⁸, L. Nedic ¹²⁶, T.J. Neep ²⁰, A. Negri ^{73a,73b}, M. Negrini ^{23b}, C. Nellist ¹¹⁴, C. Nelson ¹⁰⁴, K. Nelson ¹⁰⁶, S. Nemecek ¹³¹, M. Nessi ^{36,h}, M.S. Neubauer ¹⁶², F. Neuhaus ¹⁰⁰, J. Neundorf ⁴⁸, R. Newhouse ¹⁶⁴, P.R. Newman ²⁰, C.W. Ng ¹²⁹, Y.W.Y. Ng ⁴⁸, B. Ngair ^{35e}, H.D.N. Nguyen ¹⁰⁸, R.B. Nickerson ¹²⁶, R. Nicolaidou ¹³⁵, J. Nielsen ¹³⁶, M. Niemeyer ⁵⁵, J. Niermann ^{55,36}, N. Nikiforou ³⁶, V. Nikolaenko ^{37,a}, I. Nikolic-Audit ¹²⁷, K. Nikolopoulos ²⁰, P. Nilsson ²⁹, I. Ninca ⁴⁸, H.R. Nindhito ⁵⁶, G. Ninio ¹⁵¹, A. Nisati ^{75a}, N. Nishu ², R. Nisius ¹¹⁰, J-E. Nitschke ⁵⁰, E.K. Nkadimeng ^{33g}, S.J. Noacco Rosende ⁹⁰, T. Nobe ¹⁵³, D.L. Noel ³², T. Nommensen ¹⁴⁷, M.B. Norfolk ¹³⁹, R.R.B. Norisam ⁹⁶, B.J. Norman ³⁴, J. Novak ⁹³, T. Novak ⁴⁸, L. Novotny ¹³², R. Novotny ¹¹², L. Nozka ¹²², K. Ntekas ¹⁶⁰, N.M.J. Nunes De Moura Junior ^{82b}, E. Nurse⁹⁶, J. Ocariz ¹²⁷, A. Ochi ⁸⁴, I. Ochoa ^{130a}, S. Oerdeek ¹⁶¹, J.T. Offermann ³⁹, A. Ogrodnik ¹³³, A. Oh ¹⁰¹, C.C. Ohm ¹⁴⁴, H. Oide ⁸³, R. Oishi ¹⁵³, M.L. Ojeda ⁴⁸, Y. Okazaki ⁸⁷, M.W. O'Keefe⁹², Y. Okumura ¹⁵³, L.F. Oleiro Seabra ^{130a}, S.A. Olivares Pino ^{137d}, D. Oliveira Damazio ²⁹, D. Oliveira Goncalves ^{82a}, J.L. Oliver ¹⁶⁰, M.J.R. Olsson ¹⁶⁰, A. Olszewski ⁸⁶, Ö.O. Öncel ⁵⁴, D.C. O'Neil ¹⁴², A.P. O'Neill ¹⁹, A. Onofre ^{130a,130e}, P.U.E. Onyisi ¹¹, M.J. Oreglia ³⁹, G.E. Orellana ⁹⁰, D. Orestano ^{77a,77b}, N. Orlando ¹³, R.S. Orr ¹⁵⁵, V. O'Shea ⁵⁹, L.M. Osojnak ¹²⁸, R. Ospanov ^{62a}, G. Otero y Garzon ³⁰, H. Otono ⁸⁹, P.S. Ott ^{63a}, G.J. Ottino ^{17a}, M. Ouchrif ^{35d}, J. Ouellette ²⁹, F. Ould-Saada ¹²⁵, M. Owen ⁵⁹, R.E. Owen ¹³⁴, K.Y. Oyulmaz ^{21a}, V.E. Ozcan ^{21a}, N. Ozturk ⁸, S. Ozturk ^{21d}, H.A. Pacey ³², A. Pacheco Pages ¹³, C. Padilla Aranda ¹³, G. Padovano ^{75a,75b}, S. Pagan Griso ^{17a}, G. Palacino ⁶⁸, A. Palazzo ^{70a,70b}, S. Palestini ³⁶, J. Pan ¹⁷², T. Pan ^{64a}, D.K. Panchal ¹¹, C.E. Pandini ¹¹⁴, J.G. Panduro Vazquez ⁹⁵, H. Pang ^{14b}, P. Pani ⁴⁸, G. Panizzo ^{69a,69c}, L. Paolozzi ⁵⁶, C. Papadatos ¹⁰⁸, S. Parajuli ⁴⁴, A. Paramonov ⁶, C. Paraskevopoulos ¹⁰, D. Paredes Hernandez ^{64b}, T.H. Park ¹⁵⁵, M.A. Parker ³², F. Parodi ^{57b,57a}, E.W. Parrish ¹¹⁵, V.A. Parrish ⁵², J.A. Parsons ⁴¹, U. Parzefall ⁵⁴, B. Pascual Dias ¹⁰⁸, L. Pascual Dominguez ¹⁵¹, F. Pasquali ¹¹⁴, E. Pasqualucci ^{75a}, S. Passaggio ^{57b}, F. Pastore ⁹⁵, P. Pasuwan ^{47a,47b}, P. Patel ⁸⁶, U.M. Patel ⁵¹, J.R. Pater ¹⁰¹, T. Pauly ³⁶, J. Pearkes ¹⁴³, M. Pedersen ¹²⁵, R. Pedro ^{130a}, S.V. Peleganchuk ³⁷, O. Penc ³⁶, E.A. Pender ⁵², H. Peng ^{62a}, K.E. Pensi ¹⁰⁹, M. Penzin ³⁷, B.S. Peralva ^{82d}, A.P. Pereira Peixoto ⁶⁰, L. Pereira Sanchez ^{47a,47b}, D.V. Perepelitsa ^{29,ai}, E. Perez Codina ^{156a}, M. Perganti ¹⁰, L. Perini ^{71a,71b,*}, H. Pernegger ³⁶, A. Perrevoort ¹¹³, O. Perrin ⁴⁰, K. Peters ⁴⁸, R.F.Y. Peters ¹⁰¹, B.A. Petersen ³⁶, T.C. Petersen ⁴², E. Petit ¹⁰², V. Petousis ¹³², C. Petridou ^{152,e}, A. Petrukhin ¹⁴¹, M. Pettee ^{17a}, N.E. Pettersson ³⁶, A. Petukhov ³⁷, K. Petukhova ¹³³, A. Peyaud ¹³⁵, R. Pezoa ^{137f}, L. Pezzotti ³⁶, G. Pezzullo ¹⁷², T.M. Pham ¹⁷⁰, T. Pham ¹⁰⁵, P.W. Phillips ¹³⁴, G. Piacquadio ¹⁴⁵, E. Pianori ^{17a}, F. Piazza ^{71a,71b}, R. Piegai ³⁰, D. Pietreanu ^{27b}, A.D. Pilkington ¹⁰¹, M. Pinamonti ^{69a,69c}, J.L. Pinfeld ², B.C. Pinheiro Pereira ^{130a}, A.E. Pinto Pinoargote ¹³⁵, K.M. Piper ¹⁴⁶, A. Pirttikoski ⁵⁶, C. Pitman Donaldson⁹⁶, D.A. Pizzi ³⁴, L. Pizzimento ^{76a,76b}, A. Pizzini ¹¹⁴, M.-A. Pleier ²⁹, V. Plesanovs⁵⁴, V. Pleskot ¹³³, E. Plotnikova³⁸, G. Poddar ⁴, R. Poettgen ⁹⁸, L. Poggioli ¹²⁷, I. Pokharel ⁵⁵, S. Polacek ¹³³, G. Polesello ^{73a}, A. Poley ^{142,156a}, R. Polifka ¹³²,

A. Polini ^{23b}, C.S. Pollard ¹⁶⁷, Z.B. Pollock ¹¹⁹, V. Polychronakos ²⁹, E. Pompa Pacchi ^{75a,75b},
 D. Ponomarenko ¹¹³, L. Pontecorvo ³⁶, S. Popa ^{27a}, G.A. Popenciu ^{27d}, A. Poreba ³⁶,
 D.M. Portillo Quintero ^{156a}, S. Pospisil ¹³², M.A. Postill ¹³⁹, P. Postolache ^{27c}, K. Potamianos ¹⁶⁷,
 P.A. Potepa ^{85a}, I.N. Potrap ³⁸, C.J. Potter ³², H. Potti ¹, T. Poulsen ⁴⁸, J. Poveda ¹⁶³,
 M.E. Pozo Astigarraga ³⁶, A. Prades Ibanez ¹⁶³, J. Pretel ⁵⁴, D. Price ¹⁰¹, M. Primavera ^{70a},
 M.A. Principe Martin ⁹⁹, R. Privara ¹²², T. Procter ⁵⁹, M.L. Proffitt ¹³⁸, N. Proklova ¹²⁸,
 K. Prokofiev ^{64c}, G. Proto ¹¹⁰, S. Protopopescu ²⁹, J. Proudfoot ⁶, M. Przybycien ^{85a},
 W.W. Przygoda ^{85b}, J.E. Puddefoot ¹³⁹, D. Pudzha ³⁷, D. Pyatiizbyantseva ³⁷, J. Qian ¹⁰⁶,
 D. Qichen ¹⁰¹, Y. Qin ¹⁰¹, T. Qiu ⁵², A. Quadt ⁵⁵, M. Queitsch-Maitland ¹⁰¹, G. Quetant ⁵⁶,
 G. Rabanal Bolanos ⁶¹, D. Rafanoharana ⁵⁴, F. Ragusa ^{71a,71b}, J.L. Rainbolt ³⁹, J.A. Raine ⁵⁶,
 S. Rajagopalan ²⁹, E. Ramakoti ³⁷, K. Ran ^{48,14e}, N.P. Rapheeha ^{33g}, H. Rasheed ^{27b},
 V. Raskina ¹²⁷, D.F. Rassloff ^{63a}, S. Rave ¹⁰⁰, B. Ravina ⁵⁵, I. Ravinovich ¹⁶⁹, M. Raymond ³⁶,
 A.L. Read ¹²⁵, N.P. Readioff ¹³⁹, D.M. Rebuzzi ^{73a,73b}, G. Redlinger ²⁹, A.S. Reed ¹¹⁰,
 K. Reeves ²⁶, J.A. Reidelsturz ¹⁷¹, D. Reikher ¹⁵¹, A. Rej ¹⁴¹, C. Rembser ³⁶, A. Renardi ⁴⁸,
 M. Renda ^{27b}, M.B. Rendel ¹¹⁰, F. Renner ⁴⁸, A.G. Rennie ⁵⁹, S. Resconi ^{71a},
 M. Ressegotti ^{57b,57a}, S. Rettie ³⁶, J.G. Reyes Rivera ¹⁰⁷, B. Reynolds ¹¹⁹, E. Reynolds ^{17a},
 O.L. Rezanova ³⁷, P. Reznicek ¹³³, N. Ribaric ⁹¹, E. Ricci ^{78a,78b}, R. Richter ¹¹⁰,
 S. Richter ^{47a,47b}, E. Richter-Was ^{85b}, M. Ridel ¹²⁷, S. Ridouani ^{35d}, P. Rieck ¹¹⁷, P. Riedler ³⁶,
 M. Rijssenbeek ¹⁴⁵, A. Rimoldi ^{73a,73b}, M. Rimoldi ⁴⁸, L. Rinaldi ^{23b,23a}, T.T. Rinn ²⁹,
 M.P. Rinnagel ¹⁰⁹, G. Ripellino ¹⁶¹, I. Riu ¹³, P. Rivadeneira ⁴⁸, J.C. Rivera Vergara ¹⁶⁵,
 F. Rizatdinova ¹²¹, E. Rizvi ⁹⁴, B.A. Roberts ¹⁶⁷, B.R. Roberts ^{17a}, S.H. Robertson ^{104,x},
 M. Robin ⁴⁸, D. Robinson ³², C.M. Robles Gajardo ^{137f}, M. Robles Manzano ¹⁰⁰, A. Robson ⁵⁹,
 A. Rocchi ^{76a,76b}, C. Roda ^{74a,74b}, S. Rodriguez Bosca ^{63a}, Y. Rodriguez Garcia ^{22a},
 A. Rodriguez Rodriguez ⁵⁴, A.M. Rodríguez Vera ^{156b}, S. Roe ³⁶, J.T. Roemer ¹⁶⁰,
 A.R. Roepe-Gier ¹³⁶, J. Roggel ¹⁷¹, O. Røhne ¹²⁵, R.A. Rojas ¹⁰³, C.P.A. Roland ⁶⁸, J. Roloff ²⁹,
 A. Romaniouk ³⁷, E. Romano ^{73a,73b}, M. Romano ^{23b}, A.C. Romero Hernandez ¹⁶²,
 N. Rompotis ⁹², L. Roos ¹²⁷, S. Rosati ^{75a}, B.J. Rosser ³⁹, E. Rossi ¹²⁶, E. Rossi ^{72a,72b},
 L.P. Rossi ^{57b}, L. Rossini ⁴⁸, R. Rosten ¹¹⁹, M. Rotaru ^{27b}, B. Rottler ⁵⁴, C. Rougier ^{102,ab},
 D. Rousseau ⁶⁶, D. Rousso ³², A. Roy ¹⁶², S. Roy-Garand ¹⁵⁵, A. Rozanov ¹⁰², Y. Rozen ¹⁵⁰,
 X. Ruan ^{33g}, A. Rubio Jimenez ¹⁶³, A.J. Ruby ⁹², V.H. Ruelas Rivera ¹⁸, T.A. Ruggeri ¹,
 A. Ruggiero ¹²⁶, A. Ruiz-Martinez ¹⁶³, A. Rummler ³⁶, Z. Rurikova ⁵⁴, N.A. Rusakovich ³⁸,
 H.L. Russell ¹⁶⁵, G. Russo ^{75a,75b}, J.P. Rutherford ⁷, S. Rutherford Colmenares ³², K. Rybacki ⁹¹,
 M. Rybar ¹³³, E.B. Rye ¹²⁵, A. Ryzhov ⁴⁴, J.A. Sabater Iglesias ⁵⁶, P. Sabatini ¹⁶³,
 L. Sabetta ^{75a,75b}, H.F-W. Sadrozinski ¹³⁶, F. Safai Tehrani ^{75a}, B. Safarzadeh Samani ¹⁴⁶,
 M. Safdari ¹⁴³, S. Saha ¹⁶⁵, M. Sahinsoy ¹¹⁰, M. Saimpert ¹³⁵, M. Saito ¹⁵³, T. Saito ¹⁵³,
 D. Salamani ³⁶, A. Salnikov ¹⁴³, J. Salt ¹⁶³, A. Salvador Salas ¹³, D. Salvatore ^{43b,43a},
 F. Salvatore ¹⁴⁶, A. Salzburger ³⁶, D. Sammel ⁵⁴, D. Sampsonidis ^{152,e}, D. Sampsonidou ¹²³,
 J. Sánchez ¹⁶³, A. Sanchez Pineda ⁴, V. Sanchez Sebastian ¹⁶³, H. Sandaker ¹²⁵, C.O. Sander ⁴⁸,
 J.A. Sandesara ¹⁰³, M. Sandhoff ¹⁷¹, C. Sandoval ^{22b}, D.P.C. Sankey ¹³⁴, T. Sano ⁸⁷,
 A. Sansoni ⁵³, L. Santi ^{75a,75b}, C. Santoni ⁴⁰, H. Santos ^{130a,130b}, S.N. Santpur ^{17a}, A. Santra ¹⁶⁹,
 K.A. Saoucha ¹³⁹, J.G. Saraiva ^{130a,130d}, J. Sardain ⁷, O. Sasaki ⁸³, K. Sato ¹⁵⁷, C. Sauer ^{63b},
 F. Sauerburger ⁵⁴, E. Sauvan ⁴, P. Savard ^{155,ag}, R. Sawada ¹⁵³, C. Sawyer ¹³⁴, L. Sawyer ⁹⁷,
 I. Sayago Galvan ¹⁶³, C. Sbarra ^{23b}, A. Sbrizzi ^{23b,23a}, T. Scanlon ⁹⁶, J. Schaarschmidt ¹³⁸,
 P. Schacht ¹¹⁰, D. Schaefer ³⁹, U. Schäfer ¹⁰⁰, A.C. Schaffer ^{66,44}, D. Schaile ¹⁰⁹,
 R.D. Schamberger ¹⁴⁵, C. Scharf ¹⁸, M.M. Schefer ¹⁹, V.A. Schegelsky ³⁷, D. Scheirich ¹³³,
 F. Schenck ¹⁸, M. Schernau ¹⁶⁰, C. Scheulen ⁵⁵, C. Schiavi ^{57b,57a}, E.J. Schioppa ^{70a,70b},
 M. Schioppa ^{43b,43a}, B. Schlag ^{143,o}, K.E. Schleicher ⁵⁴, S. Schlenker ³⁶, J. Schmeing ¹⁷¹,

M.A. Schmidt [ID171](#), K. Schmieden [ID100](#), C. Schmitt [ID100](#), S. Schmitt [ID48](#), L. Schoeffel [ID135](#),
A. Schoening [ID63b](#), P.G. Scholer [ID54](#), E. Schopf [ID126](#), M. Schott [ID100](#), J. Schovancova [ID36](#),
S. Schramm [ID56](#), F. Schroeder [ID171](#), T. Schroer [ID56](#), H-C. Schultz-Coulon [ID63a](#), M. Schumacher [ID54](#),
B.A. Schumm [ID136](#), Ph. Schune [ID135](#), A.J. Schuy [ID138](#), H.R. Schwartz [ID136](#), A. Schwartzman [ID143](#),
T.A. Schwarz [ID106](#), Ph. Schwemling [ID135](#), R. Schwienhorst [ID107](#), A. Sciandra [ID136](#), G. Sciolla [ID26](#),
F. Scuri [ID74a](#), C.D. Sebastiani [ID92](#), K. Sedlaczek [ID115](#), P. Seema [ID18](#), S.C. Seidel [ID112](#), A. Seiden [ID136](#),
B.D. Seidlitz [ID41](#), C. Seitz [ID48](#), J.M. Seixas [ID82b](#), G. Sekhniaidze [ID72a](#), S.J. Sekula [ID44](#), L. Selem [ID60](#),
N. Semprini-Cesari [ID23b,23a](#), D. Sengupta [ID56](#), V. Senthilkumar [ID163](#), L. Serin [ID66](#), L. Serkin [ID69a,69b](#),
M. Sessa [ID76a,76b](#), H. Severini [ID120](#), F. Sforza [ID57b,57a](#), A. Sfyrly [ID56](#), E. Shabalina [ID55](#), R. Shaheen [ID144](#),
J.D. Shahinian [ID128](#), D. Shaked Renous [ID169](#), L.Y. Shan [ID14a](#), M. Shapiro [ID17a](#), A. Sharma [ID36](#),
A.S. Sharma [ID164](#), P. Sharma [ID80](#), S. Sharma [ID48](#), P.B. Shatalov [ID37](#), K. Shaw [ID146](#), S.M. Shaw [ID101](#),
A. Shcherbakova [ID37](#), Q. Shen [ID62c,5](#), P. Sherwood [ID96](#), L. Shi [ID96](#), X. Shi [ID14a](#), C.O. Shimmin [ID172](#),
Y. Shimogama [ID168](#), J.D. Shinner [ID95](#), I.P.J. Shipsey [ID126](#), S. Shirabe [ID56,h](#), M. Shiyakova [ID38,v](#),
J. Shlomi [ID169](#), M.J. Shochet [ID39](#), J. Shojaii [ID105](#), D.R. Shope [ID125](#), S. Shrestha [ID119,aj](#), E.M. Shrif [ID33g](#),
M.J. Shroff [ID165](#), P. Sicho [ID131](#), A.M. Sickles [ID162](#), E. Sideras Haddad [ID33g](#), A. Sidoti [ID23b](#),
F. Siegert [ID50](#), Dj. Sijacki [ID15](#), R. Sikora [ID85a](#), F. Sili [ID90](#), J.M. Silva [ID20](#), M.V. Silva Oliveira [ID29](#),
S.B. Silverstein [ID47a](#), S. Simion [ID66](#), R. Simoniello [ID36](#), E.L. Simpson [ID59](#), H. Simpson [ID146](#),
L.R. Simpson [ID106](#), N.D. Simpson [ID98](#), S. Simsek [ID21d](#), S. Sindhu [ID55](#), P. Sinervo [ID155](#), S. Singh [ID155](#),
S. Sinha [ID48](#), S. Sinha [ID101](#), M. Sioli [ID23b,23a](#), I. Siral [ID36](#), E. Sitnikova [ID48](#), S.Yu. Sivoklov [ID37,*](#),
J. Sjölin [ID47a,47b](#), A. Skaf [ID55](#), E. Skorda [ID98](#), P. Skubic [ID120](#), M. Slawinska [ID86](#), V. Smakhtin [ID169](#),
B.H. Smart [ID134](#), J. Smiesko [ID36](#), S.Yu. Smirnov [ID37](#), Y. Smirnov [ID37](#), L.N. Smirnova [ID37,a](#),
O. Smirnova [ID98](#), A.C. Smith [ID41](#), E.A. Smith [ID39](#), H.A. Smith [ID126](#), J.L. Smith [ID92](#), R. Smith [ID143](#),
M. Smizanska [ID91](#), K. Smolek [ID132](#), A.A. Snesarev [ID37](#), S.R. Snider [ID155](#), H.L. Snoek [ID114](#),
S. Snyder [ID29](#), R. Sobie [ID165,x](#), A. Soffer [ID151](#), C.A. Solans Sanchez [ID36](#), E.Yu. Soldatov [ID37](#),
U. Soldevila [ID163](#), A.A. Solodkov [ID37](#), S. Solomon [ID26](#), A. Soloshenko [ID38](#), K. Solovieva [ID54](#),
O.V. Solovyanov [ID40](#), V. Solovyev [ID37](#), P. Sommer [ID36](#), A. Sonay [ID13](#), W.Y. Song [ID156b](#),
J.M. Sonneveld [ID114](#), A. Sopczak [ID132](#), A.L. Soppio [ID96](#), F. Sopkova [ID28b](#), V. Sothilingam [ID63a](#),
S. Sottocornola [ID68](#), R. Soualah [ID116b](#), Z. Soumami [ID35e](#), D. South [ID48](#), S. Spagnolo [ID70a,70b](#),
M. Spalla [ID110](#), D. Sperlich [ID54](#), G. Spigo [ID36](#), M. Spina [ID146](#), S. Spinali [ID91](#), D.P. Spiteri [ID59](#),
M. Spousta [ID133](#), E.J. Staats [ID34](#), A. Stabile [ID71a,71b](#), R. Stamen [ID63a](#), M. Stamenkovic [ID114](#),
A. Stampeki [ID20](#), M. Standke [ID24](#), E. Stanecka [ID86](#), M.V. Stange [ID50](#), B. Stanislaus [ID17a](#),
M.M. Stanitzki [ID48](#), B. Stapf [ID48](#), E.A. Starchenko [ID37](#), G.H. Stark [ID136](#), J. Stark [ID102,ab](#),
D.M. Starke [ID156b](#), P. Staroba [ID131](#), P. Starovoitov [ID63a](#), S. Stärz [ID104](#), R. Staszewski [ID86](#),
G. Stavropoulos [ID46](#), J. Steentoft [ID161](#), P. Steinberg [ID29](#), B. Stelzer [ID142,156a](#), H.J. Stelzer [ID129](#),
O. Stelzer-Chilton [ID156a](#), H. Stenzel [ID58](#), T.J. Stevenson [ID146](#), G.A. Stewart [ID36](#), J.R. Stewart [ID121](#),
M.C. Stockton [ID36](#), G. Stoica [ID27b](#), M. Stolarski [ID130a](#), S. Stonjek [ID110](#), A. Straessner [ID50](#),
J. Strandberg [ID144](#), S. Strandberg [ID47a,47b](#), M. Strauss [ID120](#), T. Strebler [ID102](#), P. Strizenc [ID28b](#),
R. Ströhmer [ID166](#), D.M. Strom [ID123](#), L.R. Strom [ID48](#), R. Stroynowski [ID44](#), A. Strubig [ID47a,47b](#),
S.A. Stucci [ID29](#), B. Stugu [ID16](#), J. Stupak [ID120](#), N.A. Styles [ID48](#), D. Su [ID143](#), S. Su [ID62a](#), W. Su [ID62d](#),
X. Su [ID62a,66](#), K. Sugizaki [ID153](#), V.V. Sulini [ID37](#), M.J. Sullivan [ID92](#), D.M.S. Sultan [ID78a,78b](#),
L. Sultaniyeva [ID37](#), S. Sultansoy [ID3b](#), T. Sumida [ID87](#), S. Sun [ID106](#), S. Sun [ID170](#),
O. Sunneborn Gudnadottir [ID161](#), M.R. Sutton [ID146](#), H. Suzuki [ID157](#), M. Svatos [ID131](#),
M. Swiatlowski [ID156a](#), T. Swirski [ID166](#), I. Sykora [ID28a](#), M. Sykora [ID133](#), T. Sykora [ID133](#), D. Ta [ID100](#),
K. Tackmann [ID48,u](#), A. Taffard [ID160](#), R. Tafirout [ID156a](#), J.S. Tafoya Vargas [ID66](#), R. Takashima [ID88](#),
E.P. Takeva [ID52](#), Y. Takubo [ID83](#), M. Talby [ID102](#), A.A. Talyshev [ID37](#), K.C. Tam [ID64b](#), N.M. Tamir [ID151](#),
A. Tanaka [ID153](#), J. Tanaka [ID153](#), R. Tanaka [ID66](#), M. Tanasini [ID57b,57a](#), Z. Tao [ID164](#), S. Tapia Araya [ID137f](#),
S. Tapprogge [ID100](#), A. Tarek Abouelfadl Mohamed [ID107](#), S. Tarem [ID150](#), K. Tariq [ID62b](#), G. Tarna [ID102,27b](#),

G.F. Tartarelli [ID71a](#), P. Tas [ID133](#), M. Tasevsky [ID131](#), E. Tassi [ID43b,43a](#), A.C. Tate [ID162](#), G. Tateno [ID153](#), Y. Tayalati [ID35e,w](#), G.N. Taylor [ID105](#), W. Taylor [ID156b](#), H. Teagle⁹², A.S. Tee [ID170](#), R. Teixeira De Lima [ID143](#), P. Teixeira-Dias [ID95](#), J.J. Teoh [ID155](#), K. Terashi [ID153](#), J. Terron [ID99](#), S. Terzo [ID13](#), M. Testa [ID53](#), R.J. Teuscher [ID155,x](#), A. Thaler [ID79](#), O. Theiner [ID56](#), N. Themistokleous [ID52](#), T. Thevenaux-Pelzer [ID102](#), O. Thielmann [ID171](#), D.W. Thomas⁹⁵, J.P. Thomas [ID20](#), E.A. Thompson [ID17a](#), P.D. Thompson [ID20](#), E. Thomson [ID128](#), Y. Tian [ID55](#), V. Tikhomirov [ID37,a](#), Yu.A. Tikhonov [ID37](#), S. Timoshenko³⁷, D. Timoshyn [ID133](#), E.X.L. Ting [ID1](#), P. Tipton [ID172](#), S.H. Tlou [ID33g](#), A. Tnourji [ID40](#), K. Todome [ID23b,23a](#), S. Todorova-Nova [ID133](#), S. Todt⁵⁰, M. Togawa [ID83](#), J. Tojo [ID89](#), S. Tokár [ID28a](#), K. Tokushuku [ID83](#), O. Toldaiev [ID68](#), R. Tombs [ID32](#), M. Tomoto [ID83,111](#), L. Tompkins [ID143,o](#), K.W. Topolnicki [ID85b](#), E. Torrence [ID123](#), H. Torres [ID102,ab](#), E. Torró Pastor [ID163](#), M. Toscani [ID30](#), C. Tosciri [ID39](#), M. Tost [ID11](#), D.R. Tovey [ID139](#), A. Traeet¹⁶, I.S. Trandafir [ID27b](#), T. Trefzger [ID166](#), A. Tricoli [ID29](#), I.M. Trigger [ID156a](#), S. Trincaz-Duvoid [ID127](#), D.A. Trischuk [ID26](#), B. Trocmé [ID60](#), C. Troncon [ID71a](#), L. Truong [ID33c](#), M. Trzebinski [ID86](#), A. Trzupke [ID86](#), F. Tsai [ID145](#), M. Tsai [ID106](#), A. Tsiamis [ID152,e](#), P.V. Tsiarehka³⁷, S. Tsigaridas [ID156a](#), A. Tsirigotis [ID152,s](#), V. Tsiskaridze [ID155](#), E.G. Tskhadadze [ID149a](#), M. Tsopoulou [ID152,e](#), Y. Tsujikawa [ID87](#), I.I. Tsukerman [ID37](#), V. Tsulaia [ID17a](#), S. Tsuno [ID83](#), O. Tsur¹⁵⁰, K. Tsurii [ID118](#), D. Tsybychev [ID145](#), Y. Tu [ID64b](#), A. Tudorache [ID27b](#), V. Tudorache [ID27b](#), A.N. Tuna [ID36](#), S. Turchikhin [ID38](#), I. Turk Cakir [ID3a](#), R. Turra [ID71a](#), T. Turtuvshin [ID38,y](#), P.M. Tuts [ID41](#), S. Tzamarias [ID152,e](#), P. Tzani [ID10](#), E. Tzovara [ID100](#), K. Uchida¹⁵³, F. Ukegawa [ID157](#), P.A. Ulloa Poblete [ID137c,137b](#), E.N. Umaka [ID29](#), G. Unal [ID36](#), M. Unal [ID11](#), A. Undrus [ID29](#), G. Unel [ID160](#), J. Urban [ID28b](#), P. Urquijo [ID105](#), G. Usai [ID8](#), R. Ushioda [ID154](#), M. Usman [ID108](#), Z. Uysal [ID21b](#), L. Vacavant [ID102](#), V. Vacek [ID132](#), B. Vachon [ID104](#), K.O.H. Vadla [ID125](#), T. Vafeiadis [ID36](#), A. Vaitkus [ID96](#), C. Valderanis [ID109](#), E. Valdes Santurio [ID47a,47b](#), M. Valente [ID156a](#), S. Valentinetti [ID23b,23a](#), A. Valero [ID163](#), E. Valiente Moreno [ID163](#), A. Vallier [ID102,ab](#), J.A. Valls Ferrer [ID163](#), D.R. Van Arneman [ID114](#), T.R. Van Daalen [ID138](#), A. Van Der Graaf [ID49](#), P. Van Gemmeren [ID6](#), M. Van Rijnbach [ID125,36](#), S. Van Stroud [ID96](#), I. Van Vulpen [ID114](#), M. Vanadia [ID76a,76b](#), W. Vandelli [ID36](#), M. Vandenbroucke [ID135](#), E.R. Vandewall [ID121](#), D. Vannicola [ID151](#), L. Vannoli [ID57b,57a](#), R. Vari [ID75a](#), E.W. Varnes [ID7](#), C. Varni [ID17a](#), T. Varol [ID148](#), D. Varouchas [ID66](#), L. Varriale [ID163](#), K.E. Varvell [ID147](#), M.E. Vasile [ID27b](#), L. Vaslin⁴⁰, G.A. Vasquez [ID165](#), F. Vazeille [ID40](#), T. Vazquez Schroeder [ID36](#), J. Veatch [ID31](#), V. Vecchio [ID101](#), M.J. Veen [ID103](#), I. Veliscek [ID126](#), L.M. Veloce [ID155](#), F. Veloso [ID130a,130c](#), S. Veneziano [ID75a](#), A. Ventura [ID70a,70b](#), A. Verbytskyi [ID110](#), M. Verducci [ID74a,74b](#), C. Vergis [ID24](#), M. Verissimo De Araujo [ID82b](#), W. Verkerke [ID114](#), J.C. Vermeulen [ID114](#), C. Vernieri [ID143](#), P.J. Verschuuren [ID95](#), M. Vessella [ID103](#), M.C. Vetterli [ID142,ag](#), A. Vgenopoulos [ID152,e](#), N. Viaux Maira [ID137f](#), T. Vickey [ID139](#), O.E. Vickey Boeriu [ID139](#), G.H.A. Viehhauser [ID126](#), L. Vighani [ID63b](#), M. Villa [ID23b,23a](#), M. Villaplana Perez [ID163](#), E.M. Villhauer⁵², E. Vilucchi [ID53](#), M.G. Vinciter [ID34](#), G.S. Virdee [ID20](#), A. Vishwakarma [ID52](#), A. Visibile¹¹⁴, C. Vittori [ID36](#), I. Vivarelli [ID146](#), V. Vladimirov¹⁶⁷, E. Voevodina [ID110](#), F. Vogel [ID109](#), P. Vokac [ID132](#), J. Von Ahnen [ID48](#), E. Von Toerne [ID24](#), B. Vormwald [ID36](#), V. Vorobel [ID133](#), K. Vorobev [ID37](#), M. Vos [ID163](#), K. Voss [ID141](#), J.H. Vossebeld [ID92](#), M. Vozak [ID114](#), L. Vozdecky [ID94](#), N. Vranjes [ID15](#), M. Vranjes Milosavljevic [ID15](#), M. Vreeswijk [ID114](#), R. Vuillermet [ID36](#), O. Vujanovic [ID100](#), I. Vukotic [ID39](#), S. Wada [ID157](#), C. Wagner¹⁰³, J.M. Wagner [ID17a](#), W. Wagner [ID171](#), S. Wahdan [ID171](#), H. Wahlberg [ID90](#), R. Wakasa [ID157](#), M. Wakida [ID111](#), J. Walder [ID134](#), R. Walker [ID109](#), W. Walkowiak [ID141](#), A. Wall [ID128](#), T. Wamorkar [ID6](#), A.Z. Wang [ID170](#), C. Wang [ID100](#), C. Wang [ID62c](#), H. Wang [ID17a](#), J. Wang [ID64a](#), R.-J. Wang [ID100](#), R. Wang [ID61](#), R. Wang [ID6](#), S.M. Wang [ID148](#), S. Wang [ID62b](#), T. Wang [ID62a](#), W.T. Wang [ID80](#), W. Wang [ID14a](#), X. Wang [ID14c](#), X. Wang [ID162](#), X. Wang [ID62c](#), Y. Wang [ID62d](#), Y. Wang [ID14c](#), Z. Wang [ID106](#), Z. Wang [ID62d,51,62c](#), Z. Wang [ID106](#), A. Warburton [ID104](#), R.J. Ward [ID20](#), N. Warrack [ID59](#), A.T. Watson [ID20](#), H. Watson [ID59](#), M.F. Watson [ID20](#), E. Watton [ID59,134](#), G. Watts [ID138](#), B.M. Waugh [ID96](#), C. Weber [ID29](#), H.A. Weber [ID18](#), M.S. Weber [ID19](#), S.M. Weber [ID63a](#), C. Wei [ID62a](#), Y. Wei [ID126](#), A.R. Weidberg [ID126](#), E.J. Weik [ID117](#),

J. Weingarten ^{id}49, M. Weirich ^{id}100, C. Weiser ^{id}54, C.J. Wells ^{id}48, T. Wenaus ^{id}29, B. Wendland ^{id}49, T. Wengler ^{id}36, N.S. Wenke ^{id}110, N. Wermes ^{id}24, M. Wessels ^{id}63a, K. Whalen ^{id}123, A.M. Wharton ^{id}91, A.S. White ^{id}61, A. White ^{id}8, M.J. White ^{id}1, D. Whiteson ^{id}160, L. Wickremasinghe ^{id}124, W. Wiedenmann ^{id}170, C. Wiel ^{id}50, M. Wielers ^{id}134, C. Wiglesworth ^{id}42, D.J. Wilbern ^{id}120, H.G. Wilkens ^{id}36, D.M. Williams ^{id}41, H.H. Williams ^{id}128, S. Williams ^{id}32, S. Willocq ^{id}103, B.J. Wilson ^{id}101, P.J. Windischhofer ^{id}39, F.I. Winkel ^{id}30, F. Winklmeier ^{id}123, B.T. Winter ^{id}54, J.K. Winter ^{id}101, M. Wittgen ^{id}143, M. Wobisch ^{id}97, Z. Wolffs ^{id}114, R. Wölker ^{id}126, J. Wollrath ^{id}160, M.W. Wolter ^{id}86, H. Wolters ^{id}130a,130c, A.F. Wongel ^{id}48, S.D. Worm ^{id}48, B.K. Wosiek ^{id}86, K.W. Woźniak ^{id}86, S. Wozniewski ^{id}55, K. Wraight ^{id}59, C. Wu ^{id}20, J. Wu ^{id}14a,14e, M. Wu ^{id}64a, M. Wu ^{id}113, S.L. Wu ^{id}170, X. Wu ^{id}56, Y. Wu ^{id}62a, Z. Wu ^{id}135, J. Wuerzinger ^{id}110, T.R. Wyatt ^{id}101, B.M. Wynne ^{id}52, S. Xella ^{id}42, L. Xia ^{id}14c, M. Xia ^{id}14b, J. Xiang ^{id}64c, X. Xiao ^{id}106, M. Xie ^{id}62a, X. Xie ^{id}62a, S. Xin ^{id}14a,14e, J. Xiong ^{id}17a, D. Xu ^{id}14a, H. Xu ^{id}62a, L. Xu ^{id}62a, R. Xu ^{id}128, T. Xu ^{id}106, Y. Xu ^{id}14b, Z. Xu ^{id}52, Z. Xu ^{id}14a, B. Yabsley ^{id}147, S. Yacoub ^{id}33a, N. Yamaguchi ^{id}89, Y. Yamaguchi ^{id}154, E. Yamashita ^{id}153, H. Yamauchi ^{id}157, T. Yamazaki ^{id}17a, Y. Yamazaki ^{id}84, J. Yan ^{id}62c, S. Yan ^{id}126, Z. Yan ^{id}25, H.J. Yang ^{id}62c,62d, H.T. Yang ^{id}62a, S. Yang ^{id}62a, T. Yang ^{id}64c, X. Yang ^{id}62a, X. Yang ^{id}14a, Y. Yang ^{id}44, Y. Yang ^{id}62a, Z. Yang ^{id}62a, W-M. Yao ^{id}17a, Y.C. Yap ^{id}48, H. Ye ^{id}14c, H. Ye ^{id}55, J. Ye ^{id}44, S. Ye ^{id}29, X. Ye ^{id}62a, Y. Yeh ^{id}96, I. Yeletsikh ^{id}38, B.K. Yeo ^{id}17a, M.R. Yexley ^{id}96, P. Yin ^{id}41, K. Yorita ^{id}168, S. Younas ^{id}27b, C.J.S. Young ^{id}54, C. Young ^{id}143, Y. Yu ^{id}62a, M. Yuan ^{id}106, R. Yuan ^{id}62b,k, L. Yue ^{id}96, M. Zaazoua ^{id}62a, B. Zabinski ^{id}86, E. Zaid ^{id}52, T. Zakareishvili ^{id}149b, N. Zakharchuk ^{id}34, S. Zambito ^{id}56, J.A. Zamora Saa ^{id}137d,137b, J. Zang ^{id}153, D. Zanzi ^{id}54, O. Zaplatilek ^{id}132, C. Zeitnitz ^{id}171, H. Zeng ^{id}14a, J.C. Zeng ^{id}162, D.T. Zenger Jr ^{id}26, O. Zenin ^{id}37, T. Ženiš ^{id}28a, S. Zenz ^{id}94, S. Zerradi ^{id}35a, D. Zerwas ^{id}66, M. Zhai ^{id}14a,14e, B. Zhang ^{id}14c, D.F. Zhang ^{id}139, J. Zhang ^{id}62b, J. Zhang ^{id}6, K. Zhang ^{id}14a,14e, L. Zhang ^{id}14c, P. Zhang ^{id}14a,14e, R. Zhang ^{id}170, S. Zhang ^{id}106, T. Zhang ^{id}153, X. Zhang ^{id}62c, X. Zhang ^{id}62b, Y. Zhang ^{id}62c,5, Y. Zhang ^{id}96, Z. Zhang ^{id}17a, Z. Zhang ^{id}66, H. Zhao ^{id}138, P. Zhao ^{id}51, T. Zhao ^{id}62b, Y. Zhao ^{id}136, Z. Zhao ^{id}62a, A. Zhemchugov ^{id}38, K. Zheng ^{id}162, X. Zheng ^{id}62a, Z. Zheng ^{id}143, D. Zhong ^{id}162, B. Zhou ^{id}106, H. Zhou ^{id}7, N. Zhou ^{id}62c, Y. Zhou ^{id}7, C.G. Zhu ^{id}62b, J. Zhu ^{id}106, Y. Zhu ^{id}62c, Y. Zhu ^{id}62a, X. Zhuang ^{id}14a, K. Zhukov ^{id}37, V. Zhulanov ^{id}37, N.I. Zimine ^{id}38, J. Zinsser ^{id}63b, M. Ziolkowski ^{id}141, L. Živković ^{id}15, A. Zoccoli ^{id}23b,23a, K. Zoch ^{id}56, T.G. Zorbas ^{id}139, O. Zormpa ^{id}46, W. Zou ^{id}41, L. Zwalinski ^{id}36.

¹Department of Physics, University of Adelaide, Adelaide; Australia.

²Department of Physics, University of Alberta, Edmonton AB; Canada.

³(^a)Department of Physics, Ankara University, Ankara; (^b)Division of Physics, TOBB University of Economics and Technology, Ankara; Türkiye.

⁴LAPP, Université Savoie Mont Blanc, CNRS/IN2P3, Annecy; France.

⁵APC, Université Paris Cité, CNRS/IN2P3, Paris; France.

⁶High Energy Physics Division, Argonne National Laboratory, Argonne IL; United States of America.

⁷Department of Physics, University of Arizona, Tucson AZ; United States of America.

⁸Department of Physics, University of Texas at Arlington, Arlington TX; United States of America.

⁹Physics Department, National and Kapodistrian University of Athens, Athens; Greece.

¹⁰Physics Department, National Technical University of Athens, Zografou; Greece.

¹¹Department of Physics, University of Texas at Austin, Austin TX; United States of America.

¹²Institute of Physics, Azerbaijan Academy of Sciences, Baku; Azerbaijan.

¹³Institut de Física d'Altes Energies (IFAE), Barcelona Institute of Science and Technology, Barcelona; Spain.

¹⁴(^a)Institute of High Energy Physics, Chinese Academy of Sciences, Beijing; (^b)Physics Department,

Tsinghua University, Beijing;^(c)Department of Physics, Nanjing University, Nanjing;^(d)School of Science, Shenzhen Campus of Sun Yat-sen University;^(e)University of Chinese Academy of Science (UCAS), Beijing; China.

¹⁵Institute of Physics, University of Belgrade, Belgrade; Serbia.

¹⁶Department for Physics and Technology, University of Bergen, Bergen; Norway.

¹⁷^(a)Physics Division, Lawrence Berkeley National Laboratory, Berkeley CA;^(b)University of California, Berkeley CA; United States of America.

¹⁸Institut für Physik, Humboldt Universität zu Berlin, Berlin; Germany.

¹⁹Albert Einstein Center for Fundamental Physics and Laboratory for High Energy Physics, University of Bern, Bern; Switzerland.

²⁰School of Physics and Astronomy, University of Birmingham, Birmingham; United Kingdom.

²¹^(a)Department of Physics, Bogazici University, Istanbul;^(b)Department of Physics Engineering, Gaziantep University, Gaziantep;^(c)Department of Physics, Istanbul University, Istanbul;^(d)Istinye University, Sariyer, Istanbul; Türkiye.

²²^(a)Facultad de Ciencias y Centro de Investigaciones, Universidad Antonio Nariño, Bogotá;^(b)Departamento de Física, Universidad Nacional de Colombia, Bogotá; Colombia.

²³^(a)Dipartimento di Fisica e Astronomia A. Righi, Università di Bologna, Bologna;^(b)INFN Sezione di Bologna; Italy.

²⁴Physikalisches Institut, Universität Bonn, Bonn; Germany.

²⁵Department of Physics, Boston University, Boston MA; United States of America.

²⁶Department of Physics, Brandeis University, Waltham MA; United States of America.

²⁷^(a)Transilvania University of Brasov, Brasov;^(b)Horia Hulubei National Institute of Physics and Nuclear Engineering, Bucharest;^(c)Department of Physics, Alexandru Ioan Cuza University of Iasi, Iasi;^(d)National Institute for Research and Development of Isotopic and Molecular Technologies, Physics Department, Cluj-Napoca;^(e)University Politehnica Bucharest, Bucharest;^(f)West University in Timisoara, Timisoara;^(g)Faculty of Physics, University of Bucharest, Bucharest; Romania.

²⁸^(a)Faculty of Mathematics, Physics and Informatics, Comenius University, Bratislava;^(b)Department of Subnuclear Physics, Institute of Experimental Physics of the Slovak Academy of Sciences, Kosice; Slovak Republic.

²⁹Physics Department, Brookhaven National Laboratory, Upton NY; United States of America.

³⁰Universidad de Buenos Aires, Facultad de Ciencias Exactas y Naturales, Departamento de Física, y CONICET, Instituto de Física de Buenos Aires (IFIBA), Buenos Aires; Argentina.

³¹California State University, CA; United States of America.

³²Cavendish Laboratory, University of Cambridge, Cambridge; United Kingdom.

³³^(a)Department of Physics, University of Cape Town, Cape Town;^(b)iThemba Labs, Western Cape;^(c)Department of Mechanical Engineering Science, University of Johannesburg, Johannesburg;

^(d)National Institute of Physics, University of the Philippines Diliman (Philippines);^(e)University of South Africa, Department of Physics, Pretoria;^(f)University of Zululand, KwaDlangezwa;^(g)School of Physics, University of the Witwatersrand, Johannesburg; South Africa.

³⁴Department of Physics, Carleton University, Ottawa ON; Canada.

³⁵^(a)Faculté des Sciences Ain Chock, Réseau Universitaire de Physique des Hautes Energies - Université Hassan II, Casablanca;^(b)Faculté des Sciences, Université Ibn-Tofail, Kénitra;^(c)Faculté des Sciences Semlalia, Université Cadi Ayyad, LPHEA-Marrakech;^(d)LPMR, Faculté des Sciences, Université Mohamed Premier, Oujda;^(e)Faculté des sciences, Université Mohammed V, Rabat;^(f)Institute of Applied Physics, Mohammed VI Polytechnic University, Ben Guerir; Morocco.

³⁶CERN, Geneva; Switzerland.

³⁷Affiliated with an institute covered by a cooperation agreement with CERN.

- ³⁸Affiliated with an international laboratory covered by a cooperation agreement with CERN.
- ³⁹Enrico Fermi Institute, University of Chicago, Chicago IL; United States of America.
- ⁴⁰LPC, Université Clermont Auvergne, CNRS/IN2P3, Clermont-Ferrand; France.
- ⁴¹Nevis Laboratory, Columbia University, Irvington NY; United States of America.
- ⁴²Niels Bohr Institute, University of Copenhagen, Copenhagen; Denmark.
- ⁴³(^a)Dipartimento di Fisica, Università della Calabria, Rende; (^b)INFN Gruppo Collegato di Cosenza, Laboratori Nazionali di Frascati; Italy.
- ⁴⁴Physics Department, Southern Methodist University, Dallas TX; United States of America.
- ⁴⁵Physics Department, University of Texas at Dallas, Richardson TX; United States of America.
- ⁴⁶National Centre for Scientific Research "Demokritos", Agia Paraskevi; Greece.
- ⁴⁷(^a)Department of Physics, Stockholm University; (^b)Oskar Klein Centre, Stockholm; Sweden.
- ⁴⁸Deutsches Elektronen-Synchrotron DESY, Hamburg and Zeuthen; Germany.
- ⁴⁹Fakultät Physik, Technische Universität Dortmund, Dortmund; Germany.
- ⁵⁰Institut für Kern- und Teilchenphysik, Technische Universität Dresden, Dresden; Germany.
- ⁵¹Department of Physics, Duke University, Durham NC; United States of America.
- ⁵²SUPA - School of Physics and Astronomy, University of Edinburgh, Edinburgh; United Kingdom.
- ⁵³INFN e Laboratori Nazionali di Frascati, Frascati; Italy.
- ⁵⁴Physikalisches Institut, Albert-Ludwigs-Universität Freiburg, Freiburg; Germany.
- ⁵⁵II. Physikalisches Institut, Georg-August-Universität Göttingen, Göttingen; Germany.
- ⁵⁶Département de Physique Nucléaire et Corpusculaire, Université de Genève, Genève; Switzerland.
- ⁵⁷(^a)Dipartimento di Fisica, Università di Genova, Genova; (^b)INFN Sezione di Genova; Italy.
- ⁵⁸II. Physikalisches Institut, Justus-Liebig-Universität Giessen, Giessen; Germany.
- ⁵⁹SUPA - School of Physics and Astronomy, University of Glasgow, Glasgow; United Kingdom.
- ⁶⁰LPSC, Université Grenoble Alpes, CNRS/IN2P3, Grenoble INP, Grenoble; France.
- ⁶¹Laboratory for Particle Physics and Cosmology, Harvard University, Cambridge MA; United States of America.
- ⁶²(^a)Department of Modern Physics and State Key Laboratory of Particle Detection and Electronics, University of Science and Technology of China, Hefei; (^b)Institute of Frontier and Interdisciplinary Science and Key Laboratory of Particle Physics and Particle Irradiation (MOE), Shandong University, Qingdao; (^c)School of Physics and Astronomy, Shanghai Jiao Tong University, Key Laboratory for Particle Astrophysics and Cosmology (MOE), SKLPPC, Shanghai; (^d)Tsung-Dao Lee Institute, Shanghai; China.
- ⁶³(^a)Kirchhoff-Institut für Physik, Ruprecht-Karls-Universität Heidelberg, Heidelberg; (^b)Physikalisches Institut, Ruprecht-Karls-Universität Heidelberg, Heidelberg; Germany.
- ⁶⁴(^a)Department of Physics, Chinese University of Hong Kong, Shatin, N.T., Hong Kong; (^b)Department of Physics, University of Hong Kong, Hong Kong; (^c)Department of Physics and Institute for Advanced Study, Hong Kong University of Science and Technology, Clear Water Bay, Kowloon, Hong Kong; China.
- ⁶⁵Department of Physics, National Tsing Hua University, Hsinchu; Taiwan.
- ⁶⁶IJCLab, Université Paris-Saclay, CNRS/IN2P3, 91405, Orsay; France.
- ⁶⁷Centro Nacional de Microelectrónica (IMB-CNM-CSIC), Barcelona; Spain.
- ⁶⁸Department of Physics, Indiana University, Bloomington IN; United States of America.
- ⁶⁹(^a)INFN Gruppo Collegato di Udine, Sezione di Trieste, Udine; (^b)ICTP, Trieste; (^c)Dipartimento Politecnico di Ingegneria e Architettura, Università di Udine, Udine; Italy.
- ⁷⁰(^a)INFN Sezione di Lecce; (^b)Dipartimento di Matematica e Fisica, Università del Salento, Lecce; Italy.
- ⁷¹(^a)INFN Sezione di Milano; (^b)Dipartimento di Fisica, Università di Milano, Milano; Italy.
- ⁷²(^a)INFN Sezione di Napoli; (^b)Dipartimento di Fisica, Università di Napoli, Napoli; Italy.
- ⁷³(^a)INFN Sezione di Pavia; (^b)Dipartimento di Fisica, Università di Pavia, Pavia; Italy.
- ⁷⁴(^a)INFN Sezione di Pisa; (^b)Dipartimento di Fisica E. Fermi, Università di Pisa, Pisa; Italy.

- ^{75(a)}INFN Sezione di Roma; ^(b)Dipartimento di Fisica, Sapienza Università di Roma, Roma; Italy.
- ^{76(a)}INFN Sezione di Roma Tor Vergata; ^(b)Dipartimento di Fisica, Università di Roma Tor Vergata, Roma; Italy.
- ^{77(a)}INFN Sezione di Roma Tre; ^(b)Dipartimento di Matematica e Fisica, Università Roma Tre, Roma; Italy.
- ^{78(a)}INFN-TIFPA; ^(b)Università degli Studi di Trento, Trento; Italy.
- ⁷⁹Universität Innsbruck, Department of Astro and Particle Physics, Innsbruck; Austria.
- ⁸⁰University of Iowa, Iowa City IA; United States of America.
- ⁸¹Department of Physics and Astronomy, Iowa State University, Ames IA; United States of America.
- ^{82(a)}Departamento de Engenharia Elétrica, Universidade Federal de Juiz de Fora (UFJF), Juiz de Fora; ^(b)Universidade Federal do Rio De Janeiro COPPE/EE/IF, Rio de Janeiro; ^(c)Instituto de Física, Universidade de São Paulo, São Paulo; ^(d)Rio de Janeiro State University, Rio de Janeiro; Brazil.
- ⁸³KEK, High Energy Accelerator Research Organization, Tsukuba; Japan.
- ⁸⁴Graduate School of Science, Kobe University, Kobe; Japan.
- ^{85(a)}AGH University of Krakow, Faculty of Physics and Applied Computer Science, Krakow; ^(b)Marian Smoluchowski Institute of Physics, Jagiellonian University, Krakow; Poland.
- ⁸⁶Institute of Nuclear Physics Polish Academy of Sciences, Krakow; Poland.
- ⁸⁷Faculty of Science, Kyoto University, Kyoto; Japan.
- ⁸⁸Kyoto University of Education, Kyoto; Japan.
- ⁸⁹Research Center for Advanced Particle Physics and Department of Physics, Kyushu University, Fukuoka ; Japan.
- ⁹⁰Instituto de Física La Plata, Universidad Nacional de La Plata and CONICET, La Plata; Argentina.
- ⁹¹Physics Department, Lancaster University, Lancaster; United Kingdom.
- ⁹²Oliver Lodge Laboratory, University of Liverpool, Liverpool; United Kingdom.
- ⁹³Department of Experimental Particle Physics, Jožef Stefan Institute and Department of Physics, University of Ljubljana, Ljubljana; Slovenia.
- ⁹⁴School of Physics and Astronomy, Queen Mary University of London, London; United Kingdom.
- ⁹⁵Department of Physics, Royal Holloway University of London, Egham; United Kingdom.
- ⁹⁶Department of Physics and Astronomy, University College London, London; United Kingdom.
- ⁹⁷Louisiana Tech University, Ruston LA; United States of America.
- ⁹⁸Fysiska institutionen, Lunds universitet, Lund; Sweden.
- ⁹⁹Departamento de Física Teórica C-15 and CIAFF, Universidad Autónoma de Madrid, Madrid; Spain.
- ¹⁰⁰Institut für Physik, Universität Mainz, Mainz; Germany.
- ¹⁰¹School of Physics and Astronomy, University of Manchester, Manchester; United Kingdom.
- ¹⁰²CPPM, Aix-Marseille Université, CNRS/IN2P3, Marseille; France.
- ¹⁰³Department of Physics, University of Massachusetts, Amherst MA; United States of America.
- ¹⁰⁴Department of Physics, McGill University, Montreal QC; Canada.
- ¹⁰⁵School of Physics, University of Melbourne, Victoria; Australia.
- ¹⁰⁶Department of Physics, University of Michigan, Ann Arbor MI; United States of America.
- ¹⁰⁷Department of Physics and Astronomy, Michigan State University, East Lansing MI; United States of America.
- ¹⁰⁸Group of Particle Physics, University of Montreal, Montreal QC; Canada.
- ¹⁰⁹Fakultät für Physik, Ludwig-Maximilians-Universität München, München; Germany.
- ¹¹⁰Max-Planck-Institut für Physik (Werner-Heisenberg-Institut), München; Germany.
- ¹¹¹Graduate School of Science and Kobayashi-Maskawa Institute, Nagoya University, Nagoya; Japan.
- ¹¹²Department of Physics and Astronomy, University of New Mexico, Albuquerque NM; United States of America.

- ¹¹³Institute for Mathematics, Astrophysics and Particle Physics, Radboud University/Nikhef, Nijmegen; Netherlands.
- ¹¹⁴Nikhef National Institute for Subatomic Physics and University of Amsterdam, Amsterdam; Netherlands.
- ¹¹⁵Department of Physics, Northern Illinois University, DeKalb IL; United States of America.
- ¹¹⁶^(a)New York University Abu Dhabi, Abu Dhabi;^(b)University of Sharjah, Sharjah; United Arab Emirates.
- ¹¹⁷Department of Physics, New York University, New York NY; United States of America.
- ¹¹⁸Ochanomizu University, Otsuka, Bunkyo-ku, Tokyo; Japan.
- ¹¹⁹Ohio State University, Columbus OH; United States of America.
- ¹²⁰Homer L. Dodge Department of Physics and Astronomy, University of Oklahoma, Norman OK; United States of America.
- ¹²¹Department of Physics, Oklahoma State University, Stillwater OK; United States of America.
- ¹²²Palacký University, Joint Laboratory of Optics, Olomouc; Czech Republic.
- ¹²³Institute for Fundamental Science, University of Oregon, Eugene, OR; United States of America.
- ¹²⁴Graduate School of Science, Osaka University, Osaka; Japan.
- ¹²⁵Department of Physics, University of Oslo, Oslo; Norway.
- ¹²⁶Department of Physics, Oxford University, Oxford; United Kingdom.
- ¹²⁷LPNHE, Sorbonne Université, Université Paris Cité, CNRS/IN2P3, Paris; France.
- ¹²⁸Department of Physics, University of Pennsylvania, Philadelphia PA; United States of America.
- ¹²⁹Department of Physics and Astronomy, University of Pittsburgh, Pittsburgh PA; United States of America.
- ¹³⁰^(a)Laboratório de Instrumentação e Física Experimental de Partículas - LIP, Lisboa;^(b)Departamento de Física, Faculdade de Ciências, Universidade de Lisboa, Lisboa;^(c)Departamento de Física, Universidade de Coimbra, Coimbra;^(d)Centro de Física Nuclear da Universidade de Lisboa, Lisboa;^(e)Departamento de Física, Universidade do Minho, Braga;^(f)Departamento de Física Teórica y del Cosmos, Universidad de Granada, Granada (Spain);^(g)Departamento de Física, Instituto Superior Técnico, Universidade de Lisboa, Lisboa; Portugal.
- ¹³¹Institute of Physics of the Czech Academy of Sciences, Prague; Czech Republic.
- ¹³²Czech Technical University in Prague, Prague; Czech Republic.
- ¹³³Charles University, Faculty of Mathematics and Physics, Prague; Czech Republic.
- ¹³⁴Particle Physics Department, Rutherford Appleton Laboratory, Didcot; United Kingdom.
- ¹³⁵IRFU, CEA, Université Paris-Saclay, Gif-sur-Yvette; France.
- ¹³⁶Santa Cruz Institute for Particle Physics, University of California Santa Cruz, Santa Cruz CA; United States of America.
- ¹³⁷^(a)Departamento de Física, Pontificia Universidad Católica de Chile, Santiago;^(b)Millennium Institute for Subatomic physics at high energy frontier (SAPHIR), Santiago;^(c)Instituto de Investigación Multidisciplinario en Ciencia y Tecnología, y Departamento de Física, Universidad de La Serena;^(d)Universidad Andres Bello, Department of Physics, Santiago;^(e)Instituto de Alta Investigación, Universidad de Tarapacá, Arica;^(f)Departamento de Física, Universidad Técnica Federico Santa María, Valparaíso; Chile.
- ¹³⁸Department of Physics, University of Washington, Seattle WA; United States of America.
- ¹³⁹Department of Physics and Astronomy, University of Sheffield, Sheffield; United Kingdom.
- ¹⁴⁰Department of Physics, Shinshu University, Nagano; Japan.
- ¹⁴¹Department Physik, Universität Siegen, Siegen; Germany.
- ¹⁴²Department of Physics, Simon Fraser University, Burnaby BC; Canada.
- ¹⁴³SLAC National Accelerator Laboratory, Stanford CA; United States of America.

- ¹⁴⁴Department of Physics, Royal Institute of Technology, Stockholm; Sweden.
- ¹⁴⁵Departments of Physics and Astronomy, Stony Brook University, Stony Brook NY; United States of America.
- ¹⁴⁶Department of Physics and Astronomy, University of Sussex, Brighton; United Kingdom.
- ¹⁴⁷School of Physics, University of Sydney, Sydney; Australia.
- ¹⁴⁸Institute of Physics, Academia Sinica, Taipei; Taiwan.
- ¹⁴⁹^(a)E. Andronikashvili Institute of Physics, Iv. Javakhishvili Tbilisi State University, Tbilisi;^(b)High Energy Physics Institute, Tbilisi State University, Tbilisi;^(c)University of Georgia, Tbilisi; Georgia.
- ¹⁵⁰Department of Physics, Technion, Israel Institute of Technology, Haifa; Israel.
- ¹⁵¹Raymond and Beverly Sackler School of Physics and Astronomy, Tel Aviv University, Tel Aviv; Israel.
- ¹⁵²Department of Physics, Aristotle University of Thessaloniki, Thessaloniki; Greece.
- ¹⁵³International Center for Elementary Particle Physics and Department of Physics, University of Tokyo, Tokyo; Japan.
- ¹⁵⁴Department of Physics, Tokyo Institute of Technology, Tokyo; Japan.
- ¹⁵⁵Department of Physics, University of Toronto, Toronto ON; Canada.
- ¹⁵⁶^(a)TRIUMF, Vancouver BC;^(b)Department of Physics and Astronomy, York University, Toronto ON; Canada.
- ¹⁵⁷Division of Physics and Tomonaga Center for the History of the Universe, Faculty of Pure and Applied Sciences, University of Tsukuba, Tsukuba; Japan.
- ¹⁵⁸Department of Physics and Astronomy, Tufts University, Medford MA; United States of America.
- ¹⁵⁹United Arab Emirates University, Al Ain; United Arab Emirates.
- ¹⁶⁰Department of Physics and Astronomy, University of California Irvine, Irvine CA; United States of America.
- ¹⁶¹Department of Physics and Astronomy, University of Uppsala, Uppsala; Sweden.
- ¹⁶²Department of Physics, University of Illinois, Urbana IL; United States of America.
- ¹⁶³Instituto de Física Corpuscular (IFIC), Centro Mixto Universidad de Valencia - CSIC, Valencia; Spain.
- ¹⁶⁴Department of Physics, University of British Columbia, Vancouver BC; Canada.
- ¹⁶⁵Department of Physics and Astronomy, University of Victoria, Victoria BC; Canada.
- ¹⁶⁶Fakultät für Physik und Astronomie, Julius-Maximilians-Universität Würzburg, Würzburg; Germany.
- ¹⁶⁷Department of Physics, University of Warwick, Coventry; United Kingdom.
- ¹⁶⁸Waseda University, Tokyo; Japan.
- ¹⁶⁹Department of Particle Physics and Astrophysics, Weizmann Institute of Science, Rehovot; Israel.
- ¹⁷⁰Department of Physics, University of Wisconsin, Madison WI; United States of America.
- ¹⁷¹Fakultät für Mathematik und Naturwissenschaften, Fachgruppe Physik, Bergische Universität Wuppertal, Wuppertal; Germany.
- ¹⁷²Department of Physics, Yale University, New Haven CT; United States of America.
- ^a Also Affiliated with an institute covered by a cooperation agreement with CERN.
- ^b Also at An-Najah National University, Nablus; Palestine.
- ^c Also at Borough of Manhattan Community College, City University of New York, New York NY; United States of America.
- ^d Also at Center for High Energy Physics, Peking University; China.
- ^e Also at Center for Interdisciplinary Research and Innovation (CIRI-AUTH), Thessaloniki; Greece.
- ^f Also at Centro Studi e Ricerche Enrico Fermi; Italy.
- ^g Also at CERN, Geneva; Switzerland.
- ^h Also at Département de Physique Nucléaire et Corpusculaire, Université de Genève, Genève; Switzerland.
- ⁱ Also at Departament de Física de la Universitat Autònoma de Barcelona, Barcelona; Spain.

- j* Also at Department of Financial and Management Engineering, University of the Aegean, Chios; Greece.
- k* Also at Department of Physics and Astronomy, Michigan State University, East Lansing MI; United States of America.
- l* Also at Department of Physics, Ben Gurion University of the Negev, Beer Sheva; Israel.
- m* Also at Department of Physics, California State University, Sacramento; United States of America.
- n* Also at Department of Physics, King's College London, London; United Kingdom.
- o* Also at Department of Physics, Stanford University, Stanford CA; United States of America.
- p* Also at Department of Physics, University of Fribourg, Fribourg; Switzerland.
- q* Also at Department of Physics, University of Thessaly; Greece.
- r* Also at Department of Physics, Westmont College, Santa Barbara; United States of America.
- s* Also at Hellenic Open University, Patras; Greece.
- t* Also at Institucio Catalana de Recerca i Estudis Avancats, ICREA, Barcelona; Spain.
- u* Also at Institut für Experimentalphysik, Universität Hamburg, Hamburg; Germany.
- v* Also at Institute for Nuclear Research and Nuclear Energy (INRNE) of the Bulgarian Academy of Sciences, Sofia; Bulgaria.
- w* Also at Institute of Applied Physics, Mohammed VI Polytechnic University, Ben Guerir; Morocco.
- x* Also at Institute of Particle Physics (IPP); Canada.
- y* Also at Institute of Physics and Technology, Ulaanbaatar; Mongolia.
- z* Also at Institute of Physics, Azerbaijan Academy of Sciences, Baku; Azerbaijan.
- aa* Also at Institute of Theoretical Physics, Ilia State University, Tbilisi; Georgia.
- ab* Also at L2IT, Université de Toulouse, CNRS/IN2P3, UPS, Toulouse; France.
- ac* Also at Lawrence Livermore National Laboratory, Livermore; United States of America.
- ad* Also at National Institute of Physics, University of the Philippines Diliman (Philippines); Philippines.
- ae* Also at Technical University of Munich, Munich; Germany.
- af* Also at The Collaborative Innovation Center of Quantum Matter (CICQM), Beijing; China.
- ag* Also at TRIUMF, Vancouver BC; Canada.
- ah* Also at Università di Napoli Parthenope, Napoli; Italy.
- ai* Also at University of Colorado Boulder, Department of Physics, Colorado; United States of America.
- aj* Also at Washington College, Chestertown, MD; United States of America.
- ak* Also at Yeditepe University, Physics Department, Istanbul; Türkiye.
- * Deceased